THERMOELASTIC ANALYSIS OF HEAT GENERATING MULTI-LAYERED COMPOSITE CYLINDERS AND TUBES

A MASTER'S THESIS

in

Manufacturing Engineering

Atılım University

by

MURAT YILDIRIM

APRIL 2012

THERMOELASTIC ANALYSIS OF HEAT GENERATING MULTI-LAYERED COMPOSITE CYLINDERS AND TUBES

A THESIS SUBMITTED TO

THE GRADUATE SCHOOL OF NATURAL AND APPLIED SCIENCES

OF

ATILIM UNIVERSITY

BY

MURAT YILDIRIM

IN PARTIAL FULFILLMENT OF THE REQUIREMENTS FOR THE DEGREE OF

MASTER OF SCIENCE

IN

THE DEPARTMENT OF MANUFACTURING ENGINEERING

APRIL 2012

Approval of the Graduate School of Natural and Applied Sciences, Atılım University.

_____

Prof. Dr. İbrahim Akman

Director

I certify that this thesis satisfies all the requirements as a thesis for the degree of Master of Science.

_____

Prof. Dr. Bilgin Kaftanoğlu

Head of Department

This is to certify that we have read the thesis "Thermoelastic Analysis of Heat Generating Multi-Layered Composite Cylinders and Tubes" submitted by Murat Yıldırım and that in our opinion it is fully adequate, in scope and quality, as a thesis for the degree of Master of Science.

_____

Asst. Prof. Dr. A Hakan Argeşo

Supervisor

Examining Committee Members

Assoc. Prof. Dr. Tolga Akış
Civil Eng. Dept., Atılım University _____

Asst. Prof. Dr. İzzet Özdemir
Manufacturing Eng. Dept., Atılım University _____

Asst. Prof. Dr. A. Hakan Argeşo
Manufacturing Eng. Dept., Atılım University _____

Date: April 18, 2012

I declare and guarantee that all data, knowledge and information in this document has been obtained, processed and presented in accordance with academic rules and ethical conduct. Based on these rules and conduct, I have fully cited and referenced all material and results that are not original to this work.

Murat Yıldırım

Signature:

ABSTRACT

THERMOELASTIC ANALYSIS OF HEAT GENERATING MULTI-LAYERED COMPOSITE CYLINDERS AND TUBES

Yıldırım, Murat

M.S., Manufacturing Engineering Department

Supervisor: Asst. Prof. Dr. A. Hakan Argeşo

April 2012, 88 pages

A computational method is developed for the thermoelastic analysis of internally heat generating multi-layered composite cylinders and tubes having temperature dependent physical properties. The composite assembly is considered to be infinitely long and have axially constrained ends. In the formulations, small deformation theory is used. The layers that form the composite assembly are isotropic and have uniform heat generation. The thermal and mechanical problems are uncoupled and axisymmetric. The thermal problem is steady state and the mechanical problem is a plane strain problem. The computational model is based shooting algorithm. Both the thermal and mechanical problems are solved with the use of shooting algorithm. The computational model is first verified through the use of some benchmark problems that have analytical solutions in which the physical properties are considered to be temperature independent. The computational method is then used to solve some composite cylinder/tube assemblies that have temperature dependent physical properties.

Keywords: Thermoelasticity, Composite, Shooting algorithm, Heat generating, Temperature dependent properties

ÖZ

ISI ÜRETEN ÇOK KATMANLI KOMPOZİT SİLİNDİR VE TÜPLERİN TERMOELASTİK ANALİZİ

Yıldırım, Murat

Yüksek Lisans, İmalat Mühendisliği Bölümü

Tez Yöneticisi: Yrd. Doç. Dr. A. Hakan Argeşo

Nisan 2012, 88 sayfa

Isıya bağımlı malzeme özelliklerine sahip içten ısı üreten çok katmanlı kompozit silindir ve tüplerin termoelastik analizi için bir sayısal hesaplama yöntemi geliştirilmiştir. Kompozit sistemin sonsuz uzunlukta ve uçlarının sabitlenmiş olduğu kabul edilmiştir. Formülasyonlarda, küçük şekil değiştirme teorisi kullanılmıştır. Kompozit yapıyı oluşturan katmanlar izotrop ve sabit ısı üretimine sahiptir. Termal ve mekanik problemler girişimsiz ve eksenel simekriktir. Termal problem kararlı ve mekanik problem düzlem gerinme problemidir. Hesaplamalı yöntem atış algoritmasına dayanmaktadır. Hem thermal hem mekanik problemler atış algoritması ile çözülmüştür. Hesaplamalı yöntem ilk olarak analitik çözümü bilinen ve fiziksel özellikleri ısıya bağlı olmayan bazı test problemleri ile doğrulanmıştır. Hesaplamalı yöntem daha sonra, fiziksel özellikleri ısıya bağlı olan kompozit silindir/tüp sistemlerinin çözümünde kullanılmıştır.

Anahtar Kelimeler: Termoelastisite, Kompozit, Atış algoritması, Isı üreten, Isıya bağlı özellikler

To My Parents

ACKNOWLEDGMENTS

I express sincere appreciation to my supervisor Asst. Prof. Dr. A. Hakan Argeşo for his guidance and insight throughout the research. He provided me with direction, technical support and became more of a mentor and friend, than a professor. It was through his persistence, understanding and kindness that I completed my master's degree. I doubt that I will ever be able to convey my appreciation fully, but I owe him my eternal gratitude. I would also like to thank my family for the support they provided me with all through my life and this study.

TABLE OF CONTENTS

LIST OF TABLES

TABLE

LIST OF FIGURES

FIGURE

CHAPTER 1

INTRODUCTION

The analysis of thermally induced stresses and deformations induced by internal heat generating axisymmetric/cylindrical structures such as cylinders, tubes, disks, and spherical shells is of great importance in engineering applications. The theoretical basis for the thermomechanical analysis of these structures can be found in textbooks such as Boley and Weiner [1], Nowacki [2], Timoshenko and Goodier [3], Noda, Hetnarski and Tanigawa [4].

One basic problem, that falls into above category is the infinitely long cylinders/tubes in which the thermal stresses and deformations are induced by symmetrical internal energy generation. This problem can be treated under plane strain assumption. In literature there are various works that studied the thermoelastic, thermoplastic and thermoelastoplastic stress states for the aforementioned problem under different boundary and loadings conditions. Among these, the works of Guven and Altay [5,6], Orcan [7,8], Gulgec and Orcan [9], Orcan and Gulgec [10,11], Orcan and Eraslan [12], Eraslan and Orcan [13,14], Eraslan and Argeso [15-17], Argeso and Eraslan [18,19] can be cited. In these works, the cylinders/tubes have been considered to be made from one specific type of material.

The same problem has also been studied for the case of two-layered composite tubes such as in the articles of Eraslan [20] , Eraslan, Sener and Argeso [21].

As it is known, the physical properties of engineering materials vary considerably with temperature. The thermomechanical analysis of structures by taking into account of this fact gives more dependable solutions. On the other hand, the mathematical and computational modelling of these problems require some additional efforts. Moreover, for some materials, it is not easy to find or to perform experiments for the neccessary data. However, for some critical structures, there can be a need to consider the temperature dependency of the physical properties in the

analysis. In the valuable work of Noda [22], the thermoelastic equations for temperature dependent properties have been described. This study is also important in the sense that, it outlines the works done in this regard until 1986.

The effect of temperature dependency of physical properties for the case of infinitely long internally heat generating cylinders/tubes has been studied in the articles such as Orcan and Gulgec [10] , Gulgec and Orcan [11] , Orcan and Eraslan [12], Eraslan and Orcan [13], Eraslan and Argeso [16,17], Argeso and Eraslan [18,19] and in the references cited therein.

The main objective of this study is to develop a computational method for the analysis of infinitely long heat generating multi-layered composite cylinders/tubes having temperature dependent physical properties. The computational method is based on nonlinear shooting algorithm. This technique has been successfully used by Eraslan and Argeso [15,16,17] and by Argeso and Eraslan [18,19] for the numerical evaluation of thermoelastic and thermoelastoplastic stress and deformation states for the problems involving heat generating infinitely long cylinders and tubes. In all these studies, the cylinders/tubes have been considered to be made from a single specific material, i.e., single layered structures have been considered. In this work, the nonlinear shooting algorithm is extended to be able to solve the multi-layered composite structure that is considered within the scope of this thesis. The second objective of this study is to compare the behaviors of the problem of interest having temperature dependent and independent physical properties. It should be noted that, the main motivation of this work comes from the studies of Argeso and Eraslan [18,19].

The following assumptions are made in the formulations: Deformations are small (small deformation theory is used). The infinitely long composite cylinder/tube system has axially constraint ends (fixed ends). There is a perfect bonding between the layers of the composite assembly. Each layer is made from an isotropic linear elastic material whose physical properties are temperature dependent. Each layer has a specified internal uniform heat generation. The thermal problem is steady state. Thermal and mechanical problems are uncoupled. For both types of assemblies the outer surface is kept at constant reference temperature and free of tractions. In case of composite tubes, the inner surface is insulated and free of tractions. It should be

clear that, both the thermal and mechanical problems are axisymmetric. Moreover the mechanical problem is a plane strain problem.

The analysis of the problem is performed in two phases. The computational method is first applied to thermal problem to determine of the distributions of temperature and its gradient (thermal variables). The results of the first phase (distributions of thermal variables) are stored so that they can be used in the analysis of mechanical problem. In the second phase, this time the computational method is used to solve the mechanical problem.

The study is organized as follows: In Chapter 2, first the field equations of thermoelasticity are briefly presented by referring to Cartesian coordinate system, then by referring to cylindrical coordinate system. In Chapter 3, the definition, modeling and formulation of the thermal and the mechanical problems within the scope of this thesis are discussed. The closed form solutions in case of temperature independent physical properties for thermal and mechanical problems are briefly reviewed also in this chapter. In Chapter 4, the details of our proposed computational method based on nonlinear shooting algorithm are given. First, the nonlinear shooting algorithm developed for the thermal problem is explained, then, the algorithm is described for the mechanical problem. In Chapter 5, first, the physical properties that are used in the study are introduced. Their variations with temperature are given. Next, three benchmark problems are solved to verify our computational method. In these problems, the physical properties are considered to be temperature independent. The closed form solutions of these benchmark problems are then compared with those obtained from the proposed computational method. In the final part of Chapter 5, the first three problems are reconsidered but this time we take into account of temperature dependency of physical properties. Finally, in Chapter 6, some conclusions are given.

CHAPTER 2

FIELD EQUATIONS OF THERMOELASTICITY

2.1 Field Equations in Terms of Cartesian Coordinates

In this section the field equations for an isotropic linear thermoelastic material are briefly reviewed under the assumption of small deformations. The thermoelastic medium is referred to x_1, x_2, x_3 rectangular coordinate system. The field equations are presented using indicial notation. The indices appearing in the equations have a range from 1 to 3 for three dimensional (3D) and from 1 to 2 for two dimensional (2D) analyses. It should be noted that, repeated index implies summation over its range. The partial derivative with respect to time ($\partial / \partial t$) is denoted by the dot "$\bullet$".

Stress equations of motion for a thermoelastic material are given by

$$\frac{\partial \sigma_{ji}}{\partial x_j} + f_i = \rho \ddot{u}_i \tag{2.1}$$

where u_i's and f_i's are the displacement and body force components, respectively, $\sigma_{ij} (= \sigma_{ji})$ is the stress tensor, and ρ is the mass density.

The strains and displacements are related by the geometric relations, that is,

$$\varepsilon_{ij} = \frac{1}{2}\left(\frac{\partial u_i}{\partial x_j} + \frac{\partial u_j}{\partial x_i} \right) \tag{2.2}$$

where $\varepsilon_{ij} \left(= \varepsilon_{ji} \right)$ is the strain tensor.

The constitutive equations for a linear isotropic thermoelastic medium are given by

$$\sigma_{ij} = 2\mu \varepsilon_{ij} + \lambda \delta_{ij} \varepsilon_{kk} - \beta \delta_{ij} T \tag{2.3}$$

where δ_{ij} is the Kronecher's delta , μ and λ are the shear and Lame' s moduli , respectively, $\varepsilon_{kk} = \varepsilon_{11} + \varepsilon_{22} + \varepsilon_{33}$ is the dilatation , $T = T_1 - T_0$ is the temperature deviation with T_1 and T_0 being the temperatures at the current and initial states , respectively and β is the thermoelastic constant . We note that, β is related to thermal expansion coefficient α by

$$\beta = (2\mu + 3\lambda)\alpha \tag{2.4}$$

The thermal expansion coefficient α is the length change per unit length when the temperature is increased by unity.

Shear modulus μ and Lame's constant λ are related to elasticity modulus E and Poisson's ratio υ by

$$E = \frac{\mu(2\mu + 3\lambda)}{(\lambda + \mu)} \quad ; \quad \upsilon = \frac{\lambda}{2(\lambda + \mu)} \tag{2.5}$$

The following relations also hold between E, υ, μ, λ, α and β:

$$\mu = \frac{E}{2(1+\upsilon)} \quad ; \quad \lambda = \frac{\upsilon E}{(1+\upsilon)(1-2\upsilon)} = \frac{2\upsilon\mu}{1-2\upsilon} \quad ; \quad \beta = \frac{E\alpha}{1-2\upsilon} \tag{2.6}$$

Constitutive equations given in Eq. (2.3) for a linear thermoelastic material can be written in alternative forms using above relations presented in Eqs. (2.4), (2.5) and (2.6). In fact, a linear isotropic thermoelastic material contains two independent elastic coefficients and one independent thermal coefficient. This means that, the pairs (E,υ), (E,μ), (E,λ), (υ,μ), (υ,λ) or (λ,μ) can be used for elastic coefficients and α or β can be used for thermal coefficients in the equations of thermoelasticity.

Equation (2.3) relates stresses to strains. If this equation is inverted for strains, we have

$$\varepsilon_{ij} = \frac{1+\upsilon}{E}\sigma_{ij} - \frac{\upsilon}{E}\delta_{ij}\sigma_{kk} + \delta_{ij}\alpha T \tag{2.7}$$

which is the equation that relates strains to stresses.

The energy equation for an isotropic linear thermoelastic material is given by

$$C_v\dot{T} = -T_0\beta\dot{\varepsilon}_{ii} + Q + \frac{\partial}{\partial x_i}\left(k\frac{\partial T}{\partial x_i}\right) \tag{2.8}$$

where C_v is the specific heat at constant deformation measured per unit volume of thermoelastic material, $\dot{\varepsilon}_{ii}\left(=\dot{\varepsilon}_{11}+\dot{\varepsilon}_{22}+\dot{\varepsilon}_{33}\right)$ is the time rate of dilatation, Q is the heat generation defined per unit volume of thermoelastic material in unit time and k is the coefficient of heat conduction.

The field equations of isotropic linear thermoelastic material are summarized in Table 2.1 and number of unknowns in these equations is indicated for 3D and 2D problems.

Table 2.1: Field equations of linear thermoelasticity

Name of the equation	**Equation**	**Number of equations for 3D problems**	**Number of equations for 2D problems**
Stress equations of motion	$\frac{\partial \sigma_{ji}}{\partial x_j}+f_i=\rho\ddot{u}_i$	3	2
Geometric relations	$\varepsilon_{ij}=\frac{1}{2}\left(\frac{\partial u_i}{\partial x_j}+\frac{\partial u_j}{\partial x_i}\right)$	6	3
Constitutive equations	$\sigma_{ij}=2\mu\varepsilon_{ij}+\lambda\delta_{ij}\varepsilon_{kk}-\beta\delta_{ij}T$	6	3
Energy equation	$C_V\dot{T}=-T_0\beta\dot{\varepsilon}_{ii}+Q+\frac{\partial}{\partial x_i}\left(k\frac{\partial T}{\partial x_i}\right)$	1	1

Table 2.2: The unknown field variables in the field equations of isotropic linear thermoelasticity.

	NUMBER OF UNKNOWNS	
Field variable	**3D problems**	**2D problems**
σ_{ij}	6	3
u_i	3	2
ε_{ij}	6	3
T	1	1
Total	16	9

From Table 2.1 it is seen that, we have total number of 16 equations for 3D and 9 equations for 2D problems. The unknown field variables in these equations are

shown in Table 2.2. As seen from the last row of Table 2.2, the total number of unknown field variables is 16 and 9 for 3D and 2D problems, respectively, which are the same with that of total number of equations.

2.1.1 Initial and Boundary Conditions

Field equations of a thermoelastic material (See Table 2.1) involve partial differential equations (PDE's). The solutions of these PDE's require taking integrations and this gives unknown integration constants. These integration constants are determined by using initial and boundary conditions, which are the prescribed conditions for each thermoelastic problem uniquely.

For the initial conditions (IC's), displacements (u_i), velocity ($\dot{u}_i$) and temperature (T) distributions must be specified at the initial time ($t=0$) for the thermoelastic body. This means for a thermoelastic problem, at the initial time $t=0$, u_i, $\dot{u}_i$ and T must be known at every point in the domain that defines the body.

In order to discuss boundary conditions (BC's) more clearly, we refer to Figure 2.1, which shows a thermoelastic body

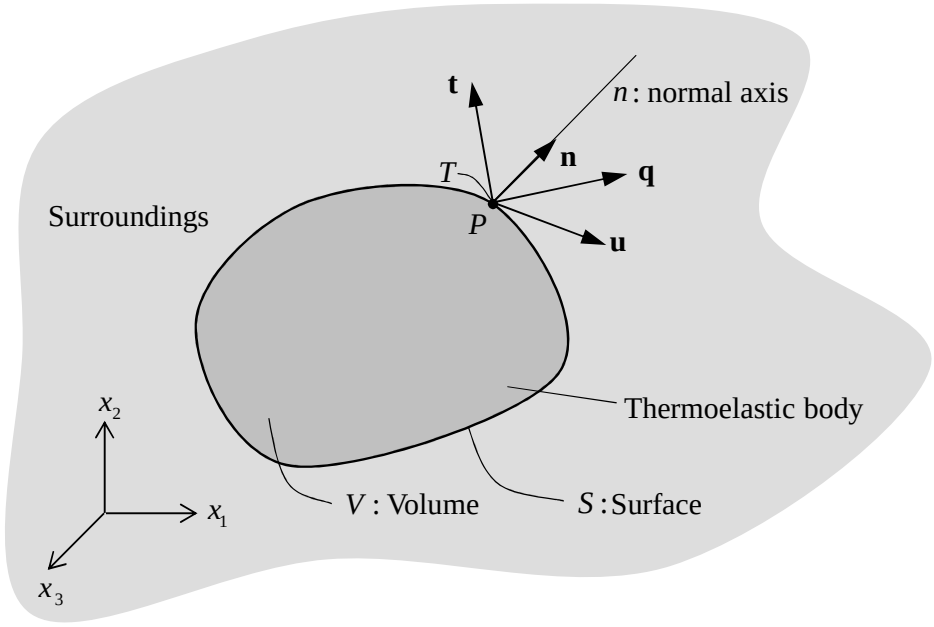

Figure 2.1: A thermoelastic body.

For the BC's, one member or combination from each of the following pairs

$$(u_1,t_1),\ (u_2,t_2),\ (u_3,t_3) \tag{2.9}$$

and

$$(T,q_n) \tag{2.10}$$

have to be specified at every point on the surface S of the thermoelastic body. Here, t_i's are the components of traction vector $\mathbf{t}$, that are related to the stresses by

$$t_i = \sigma_{ij} n_j \tag{2.11}$$

where n_j's being the components of outer unit normal vector $\mathbf{n}$ of the boundary point considered. q_n is the amount of heat flowing per unit area in unit time and it is related to components of heat flux vector $\mathbf{q} = (q_i)$ by

$$q_n = n_i q_i \tag{2.12}$$

where by the Fourier's law of heat conduction

$$q_i = -k \frac{\partial T}{\partial x_i} \tag{2.13}$$

In Figure 1, P denotes an arbitrary point on the surface S of the thermoelastic body. The displacement, traction, heat flux vectors and the temperature at point P are shown in the figure. It should be noted that, the BC's specified using the pairs given in Eq. (2.9) are known as mechanical BC's. On the other hand, the BC specified by using the pair given in Eq. (2.10) is called thermal BC.

Next, we discuss three types of thermal BC's that are commonly used in thermoelastic problems. Throughout this discussion it is assumed that the initial temperature T_0 is uniform spacewise and T_0 is the same for the body and its surroundings. Referring to Figure 1, if

1) the temperature of point P is changed by amount T^*, then,

$$T = T^* \text{ at point } P \tag{2.14}$$

in which the temperature of the surface is prescribed by a certain value.

2) there is no heat flux at point P, i.e., point P is insulated , then,

$$q_n = 0 \text{ at point } P \tag{2.15}$$

or with the use of Eq. (2.13)

$$q_n = -k n_i \frac{\partial T}{\partial x_i} = -k \frac{\partial T}{\partial n} = 0 \text{ at point } P \tag{2.16}$$

where $(\partial / \partial n)$ denotes directional derivative along normal axis n. This type thermal BC is called insulated BC.

3) the temperature of surrounding medium of the body at point P is changed by amount T^*, then

$$q_n = h\left(T - T^*\right) \quad \text{at point } P \tag{2.17}$$

or with the use of Eq. (2.13)

$$n_i \frac{\partial T}{\partial x_i} = \frac{\partial T}{\partial n} = Z\left(T - T^*\right) \quad \text{at point } P \tag{2.18}$$

where $Z = h/k$ with h being heat transfer coefficient. This type of thermal BC is called convective BC.

2.1.2 Interface Conditions

Here, we consider a thermoelastic body that is composed of multiply connected domains in which each domain has its own material characteristics. It is assumed that, there is a perfect bonding between the interfaces of the domains. If the problem involves a thermoelastic body as described above, then the field equations are written for each domain and integrated. As mentioned before the results contain integration constants. But for the problem at hand, the initial and boundary conditions are not enough to determine these integration constants. To determine these constants some additional conditions are needed. These additional conditions are written at every point that constitutes the interfaces of the connected domains and they are called interface conditions (IFC's).

For the discussions, we consider a thermoelastic body which is composed of two connected domains as shown in Figure 2.2.

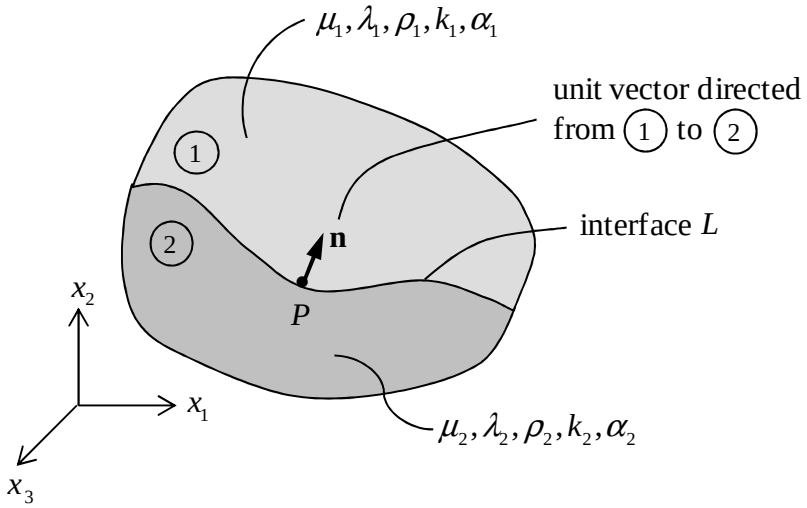

Figure 2.2: A composite thermoelastic body.

In the figure, the domains having different material properties are identified by 1 and 2. P is an arbitrary point on the interface L between domains 1 and 2, $\mathbf{n} = (n_i)$ is the unit normal vector directed from 1 and 2 defined at point P. The IFC's at point P are then given by:

1) $(u_i)_1 = (u_i)_2$ at point P (2.19)

which states the continuity of displacements on L.

2) $(t_i)_1 = (t_i)_2$ at point P (2.20)

or, with the use of Eq. (2.11),

$$\left(\sigma_{ij} n_j\right)_1 = \left(\sigma_{ij} n_j\right)_2 \text{ at point } P \tag{2.21}$$

which comes from equilibrium of forces on L.

3) $\left(T\right)_1 = \left(T\right)_2$ at point P (2.22)

which states the continuity of temperature on L.

4) $(q_n)_1 = (q_n)_2$ at point P (2.23)

or, with the use of Eq. (2.16),

$$k_1\left(\frac{\partial T}{\partial n}\right)_1 = k_2\left(\frac{\partial T}{\partial n}\right)_2 \text{ at point } P \tag{2.24}$$

which comes from the equilibrium of total heat flux on L.

It should be noted that, conditions given in Eqs. (2.19) and (2.21) are called mechanical IFC's, while conditions given in Eqs. (2.22) and (2.24) are called thermal IFC's.

2.2 Field Equations in Terms of Cylindrical Coordinates

The thermoelastic problem considered in this study is going to be formulated by referring to cylindrical coordinate system (CSS), which is an orthogonal curvilinear coordinate system. Therefore, in this section a brief review of CSS is given and also the field equations of thermoelasticity are presented by referring to CSS. We also present the relations of the field quantities between Cartesian and CSS coordinate systems.

Figure 2.3 shows both the CSS and the x_i Cartesian coordinate system having the same origin.

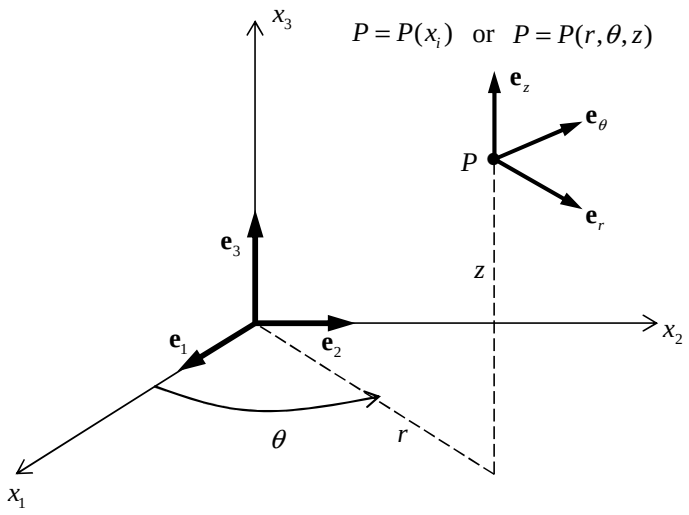

Figure 2.3: Cartesian and cylindrical coordinate systems **.**

The location of any point P in space can be identified either by specifying a triple set of x_1, x_2, x_3 values if Cartesian system is used, or by specifying a triple set of r, θ, z values if CSS is used. The relations between these two systems are given by

$$x_1 = r\cos\theta, \quad x_2 = r\sin\theta, \quad x_3 = z \tag{2.25}$$

with

$$r = \sqrt{x_1^{\,2} + x_2^{\,2}} \;; \qquad \theta = \tan^{-1}\left(\frac{x_1}{x_2}\right) \tag{2.26}$$

In Figure 2.3, the base vectors of Cartesian system and CSS are denoted respectively by $\mathbf{e}_i$ $(i = 1-3)$ and $\mathbf{e}_r$, $\mathbf{e}_\theta$, $\mathbf{e}_z$. The base vectors of two systems are related by

$$\begin{aligned} \mathbf{e}_r &= \cos\theta\,\mathbf{e}_1 + \sin\theta\,\mathbf{e}_2 \\ \mathbf{e}_\theta &= -\sin\theta\,\mathbf{e}_1 + \cos\theta\,\mathbf{e}_2 \\ \mathbf{e}_z &= \mathbf{e}_3 \end{aligned} \tag{2.27}$$

Defining a direction cosine matrix $\mathbf{A} = (a_{ij})$ with $(i, j = 1-3)$ between these orthogonal coordinate systems as

$$\mathbf{A} = \begin{bmatrix} \cos\theta & \sin\theta & 0 \\ -\sin\theta & \cos\theta & 0 \\ 0 & 0 & 1 \end{bmatrix} \tag{2.28}$$

Eqns. (2.27) can be written using indicial notation:

$$\mathbf{e}_r = a_{1i}\mathbf{e}_i$$

$$\mathbf{e}_\theta = a_{2i}\mathbf{e}_i \qquad (2.29)$$

$$\mathbf{e}_z = a_{3i}\mathbf{e}_i$$

for $i = 1-3$. It should be noted that, matrix $\mathbf{A}$ is orthogonal that is $\mathbf{A}^{-1} = \mathbf{A}^T$ and also $\det(\mathbf{A}) = 1$.

In order to express field equations of thermoelasticity in CSS, the partial derivatives $\partial / \partial x_i$ $(i = 1-3)$ must be expressed in terms of r, θ, z. From Eqs. (2.25), using chain rule, one can write

$$\begin{aligned}
\frac{\partial}{\partial x_1} &= \frac{\partial r}{\partial x_1}\frac{\partial}{\partial r} + \frac{\partial \theta}{\partial x_1}\frac{\partial}{\partial \theta} + \frac{\partial z}{\partial x_1}\frac{\partial}{\partial z} \\
\frac{\partial}{\partial x_2} &= \frac{\partial r}{\partial x_2}\frac{\partial}{\partial r} + \frac{\partial \theta}{\partial x_2}\frac{\partial}{\partial \theta} + \frac{\partial z}{\partial x_2}\frac{\partial}{\partial z} \\
\frac{\partial}{\partial x_3} &= \frac{\partial r}{\partial x_3}\frac{\partial}{\partial r} + \frac{\partial \theta}{\partial x_3}\frac{\partial}{\partial \theta} + \frac{\partial z}{\partial x_3}\frac{\partial}{\partial z}
\end{aligned} \qquad (2.30)$$

The derivatives of r, θ and z with respect to x_i are evaluated as

$$\begin{aligned}
&\frac{\partial r}{\partial x_1} = \frac{x_1}{r}\ ,\ \frac{\partial r}{\partial x_2} = \frac{x_2}{r}\ ,\ \frac{\partial r}{\partial x_3} = 0 \\
&\frac{\partial \theta}{\partial x_1} = -\frac{x_2}{r^2}\ ,\ \frac{\partial \theta}{\partial x_2} = \frac{x_1}{r^2}\ ,\ \frac{\partial \theta}{\partial x_3} = 0 \\
&\frac{\partial z}{\partial x_1} = 0\ ,\ \frac{\partial z}{\partial x_2} = 0\ ,\ \frac{\partial z}{\partial x_3} = 1
\end{aligned} \qquad (2.31)$$

Inserting Eqs. (2.31) into Eqs. (2.30) we have,

$$\begin{aligned}
\frac{\partial}{\partial x_1} &= \cos\theta\frac{\partial}{\partial r} - \frac{\sin\theta}{r}\frac{\partial}{\partial \theta} \\
\frac{\partial}{\partial x_2} &= \sin\theta\frac{\partial}{\partial r} + \frac{\cos\theta}{r}\frac{\partial}{\partial \theta} \\
\frac{\partial}{\partial x_3} &= \frac{\partial}{\partial z}
\end{aligned} \qquad (2.32)$$

2.2.1 Displacement and Body Force Components, Stress and Strain Tensors in CSS

The components of displacement vector u_i in Cartesian system and in CSS, that is, (u_r, u_θ, u_z), are related by

$$\mathbf{u} = \mathbf{A}^T \mathbf{u}' \tag{2.33}$$

where $\mathbf{u} = [u_1, u_2, u_3]^T$ and $\mathbf{u}' = [u_r, u_\theta, u_z]^T$ gives

$$\begin{aligned} u_r &= u_1 \cos\theta + u_2 \sin\theta \\ u_\theta &= -u_1 \sin\theta + u_2 \cos\theta \\ u_z &= u_3 \end{aligned} \tag{2.34}$$

Similarly for the body force components, we can easily obtain

$$\begin{aligned} f_r &= f_1 \cos\theta + f_2 \sin\theta \\ f_\theta &= -f_1 \sin\theta + f_2 \cos\theta \\ f_z &= u_z \end{aligned} \tag{2.35}$$

The form of stress tensor $\boldsymbol{\sigma}'$ in CSS is given by

$$\boldsymbol{\sigma}' = \begin{bmatrix} \sigma_{rr} & \sigma_{r\theta} & \sigma_{rz} \\ \sigma_{r\theta} & \sigma_{\theta\theta} & \sigma_{\theta z} \\ \sigma_{rz} & \sigma_{\theta z} & \sigma_{zz} \end{bmatrix} \tag{2.36}$$

The components of $\boldsymbol{\sigma} = (\sigma_{ij})$ in Cartesian system and in CSS ($\boldsymbol{\sigma}'$) are related with the stress transformation equations that can be written in matrix form as

$$\boldsymbol{\sigma}' = \mathbf{A}\,\boldsymbol{\sigma}\,\mathbf{A}^T \tag{2.37}$$

from which we have

$$\begin{aligned} \sigma_{rr} &= \sigma_{11}\cos^2\theta + \sigma_{22}\sin^2\theta + \sigma_{12}\sin 2\theta \\ \sigma_{\theta\theta} &= \sigma_{11}\sin^2\theta + \sigma_{22}\sin^2\theta - \sigma_{12}\sin 2\theta \\ \sigma_{zz} &= \sigma_{33} \\ \sigma_{r\theta} &= \sigma_{12}\cos 2\theta + \frac{(\sigma_{22} - \sigma_{11})}{2}\sin 2\theta \\ \sigma_{rz} &= \sigma_{13}\cos\theta + \sigma_{23}\sin\theta \\ \sigma_{\theta z} &= \sigma_{23}\cos\theta - \sigma_{13}\sin\theta \end{aligned} \tag{2.38}$$

The components of stress tensor in CSS is shown for an infinitely small element in Figure 2.4.

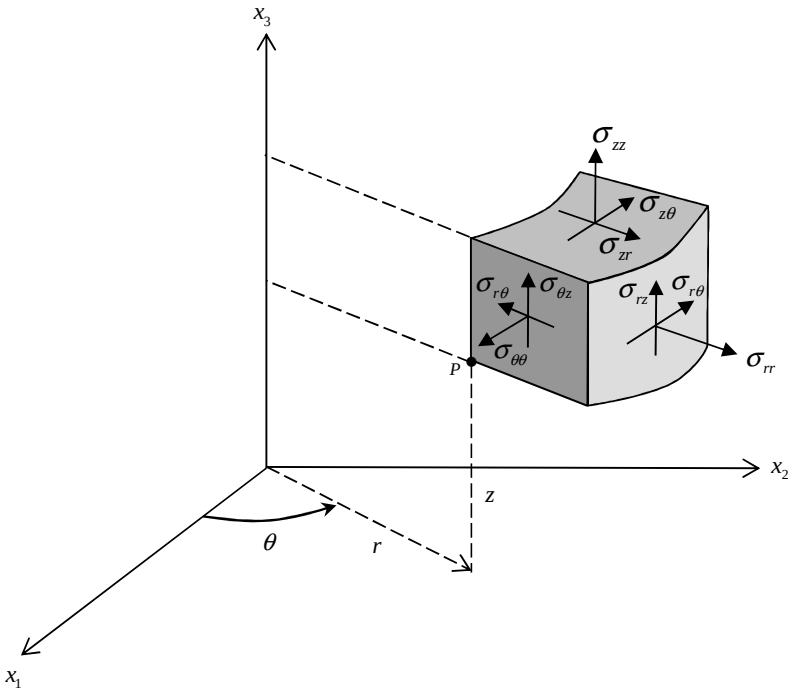

Figure 2.4: A small element showing stress components in CSS.

Similarly from the strain transformation equations, the strain components in Cartesian system and in CSS are related with

$$\varepsilon_{rr} = \varepsilon_{11}\cos^2\theta + \varepsilon_{22}\sin^2\theta + \varepsilon_{12}\sin 2\theta$$

$$\varepsilon_{\theta\theta} = \varepsilon_{11}\sin^2\theta + \varepsilon_{22}\sin^2\theta - \varepsilon_{12}\sin 2\theta$$

$$\varepsilon_{zz} = \varepsilon_{33} \tag{2.39}$$

$$\varepsilon_{r\theta} = \varepsilon_{12}\cos 2\theta + \frac{(\varepsilon_{22} - \varepsilon_{11})}{2}\sin 2\theta$$

$$\varepsilon_{rz} = \varepsilon_{13}\cos\theta + \varepsilon_{23}\sin\theta$$

$$\varepsilon_{\theta z} = \varepsilon_{23}\cos\theta - \varepsilon_{13}\sin\theta$$

2.2.2 Stress Equations of Motion, Strain Displacement Relations, Constitutive Equations, Energy Equation in CSS

Through the use of relations between the Cartesian system and CSS (Eqs. (2.25) and (2.26)), the definition of direction cosine matrix (Eq. (2.28)), the stress and strain transformation laws (Eqs. (2.38) and (2.39)), and the partial derivative relation given Eqs. (2.32), the field equations of a thermoelastic material in CSS become:

Stress equations of motion

$$\frac{\partial \sigma_{rr}}{\partial r}+\frac{1}{r}\frac{\partial \sigma_{\theta r}}{\partial \theta}+\frac{\partial \sigma_{zr}}{\partial z}+\frac{\sigma_{rr}-\sigma_{\theta\theta}}{r}+f_r=\rho \ddot{u}_r$$

$$\frac{\partial \sigma_{r\theta}}{\partial r}+\frac{1}{r}\frac{\partial \sigma_{\theta\theta}}{\partial \theta}+\frac{\partial \sigma_{z\theta}}{\partial z}+\frac{2\sigma_{r\theta}}{r}+f_\theta=\rho \ddot{u}_\theta \qquad (2.40)$$

$$\frac{\partial \sigma_{rz}}{\partial r}+\frac{1}{r}\frac{\partial \sigma_{\theta z}}{\partial \theta}+\frac{\partial \sigma_{zz}}{\partial z}+\frac{\sigma_{rz}}{r}+f_z=\rho \ddot{u}_z$$

Strain-displacement relations

$$\varepsilon_{rr}=\frac{\partial u_r}{\partial r} \quad ; \quad \varepsilon_{\theta\theta}=\frac{u_r}{r}+\frac{1}{r}\frac{\partial u_\theta}{\partial \theta} \quad ; \quad \varepsilon_{zz}=\frac{\partial u_z}{\partial z}$$

$$\varepsilon_{r\theta}=\frac{1}{2}\left(\frac{1}{r}\frac{\partial u_r}{\partial \theta}+\frac{\partial u_\theta}{\partial r}-\frac{u_\theta}{r}\right) \qquad (2.41)$$

$$\varepsilon_{rz}=\frac{1}{2}\left(\frac{\partial u_r}{\partial z}+\frac{\partial u_z}{\partial r}\right)$$

$$\varepsilon_{\theta z}=\frac{1}{2}\left(\frac{\partial u_\theta}{\partial z}+\frac{1}{r}\frac{\partial u_z}{\partial \theta}\right)$$

Constitutive equations

For an isotropic material

a) Stress-Strain relations

$$\sigma_{rr}=2\mu\varepsilon_{rr}+\lambda\left(\varepsilon_{rr}+\varepsilon_{\theta\theta}+\varepsilon_{zz}\right)-\beta T$$

$$\sigma_{\theta\theta}=2\mu\varepsilon_{\theta\theta}+\lambda\left(\varepsilon_{rr}+\varepsilon_{\theta\theta}+\varepsilon_{zz}\right)-\beta T \qquad (2.42)$$

$$\sigma_{zz}=2\mu\varepsilon_{zz}+\lambda\left(\varepsilon_{rr}+\varepsilon_{\theta\theta}+\varepsilon_{zz}\right)-\beta T$$

$$\sigma_{r\theta}=2\mu\varepsilon_{r\theta} \quad ; \quad \sigma_{rz}=2\mu\varepsilon_{rz} \quad ; \quad \sigma_{\theta z}=2\mu\varepsilon_{\theta z}$$

b) Strain-Stress relations

$$\varepsilon_{rr}=\frac{1}{E}\left[\sigma_{rr}-\nu\left(\sigma_{\theta\theta}+\sigma_{zz}\right)\right]+\alpha T$$

$$\varepsilon_{\theta\theta}=\frac{1}{E}\left[\sigma_{\theta\theta}-\nu\left(\sigma_{rr}+\sigma_{zz}\right)\right]+\alpha T \qquad (2.43)$$

$$\varepsilon_{zz}=\frac{1}{E}\left[\sigma_{zz}-\nu\left(\sigma_{rr}+\sigma_{zz}\right)\right]+\alpha T$$

$$\varepsilon_{r\theta}=\frac{\sigma_{r\theta}}{2\mu} \quad ; \quad \varepsilon_{rz}=\frac{\sigma_{rz}}{2\mu} \quad ; \quad \varepsilon_{\theta z}=\frac{\sigma_{\theta z}}{2\mu}$$

Energy equation

$$\begin{aligned} C_v\dot{T} &= -T_0\beta\left(\dot{\varepsilon}_{rr}+\dot{\varepsilon}_{\theta\theta}+\dot{\varepsilon}_{zz}\right)+Q \\ &+\frac{\partial}{\partial r}\left(k\frac{\partial T}{\partial r}\right)+\frac{1}{r}k\frac{\partial T}{\partial r}+\frac{1}{r^2}\frac{\partial}{\partial\theta}\left(k\frac{\partial T}{\partial\theta}\right)+\frac{\partial}{\partial z}\left(k\frac{\partial T}{\partial z}\right) \end{aligned} \tag{2.44}$$

2.2.3 Initial, Boundary and Interface Conditions in CSS

Initial conditions (IC's)

At every point inside the body displacements (u_r,u_θ,u_z), velocities $(\dot{u}_r,\dot{u}_\theta,\dot{u}_z)$ and temperature T must be known at initial time $t=0$.

Boundary conditions (BC's)

One member or combination from each of the following pairs (u_r,t_r), (u_θ,t_θ), (u_z,t_z) and (T,q_n) have to be specified at every point on the surface S of thermoelastic body. Here the components of traction vector $\mathbf{t}=(t_r,t_\theta,t_z)$ in CSS are related to stresses with

$$\begin{aligned} t_r &= \sigma_{rr}n_r+\sigma_{r\theta}n_\theta+\sigma_{rz}n_z \\ t_\theta &= \sigma_{r\theta}n_r+\sigma_{\theta\theta}n_\theta+\sigma_{\theta z}n_z \\ t_z &= \sigma_{rz}n_r+\sigma_{\theta z}n_\theta+\sigma_{zz}n_z \end{aligned} \tag{2.45}$$

where n_r, n_θ and n_z are components of outer unit normal $\mathbf{n}$ in CSS of the boundary point considered. q_n is the amount of heat flowing per unit area in unit time and it is related to temperature T by

$$q_n=-k\left(n_r\frac{\partial T}{\partial r}+n_\theta\frac{1}{r}\frac{\partial T}{\partial\theta}+n_z\frac{\partial T}{\partial z}\right)=-k\frac{\partial T}{\partial n} \tag{2.46}$$

Interface Conditions (IFC's)

In order to write *IFC's*, we refer to Figure 2.2 again that shows two different domains identified by 1 and 2. Recalling that, P is an arbitrary point on the

interface L between domains 1 and 2, $\mathbf{n} = (n_r, n_\theta, n_z)$ is the unit normal vector directed from 1 and 2 defined at point P. The IFC's at point P are then given by:

1) $(u_r)_1 = (u_r)_2$, $(u_\theta)_1 = (u_\theta)_2$, $(u_z)_1 = (u_z)_2$ at point P (2.47)

which states continuity of displacements on L.

2) $(t_r)_1 = (t_r)_2$, $(t_\theta)_1 = (t_\theta)_2$, $(t_z)_1 = (t_z)_2$ at point P (2.48)

or, with the use of Eq. (2.45),

$$\begin{aligned}
&\left(\sigma_{rr}n_r + \sigma_{r\theta}n_\theta + \sigma_{rz}n_z\right)_1 = \left(\sigma_{rr}n_r + \sigma_{r\theta}n_\theta + \sigma_{rz}n_z\right)_2 \\
&\left(\sigma_{r\theta}n_r + \sigma_{\theta\theta}n_\theta + \sigma_{\theta z}n_z\right)_1 = \left(\sigma_{r\theta}n_r + \sigma_{\theta\theta}n_\theta + \sigma_{\theta z}n_z\right)_2 \\
&\left(\sigma_{rz}n_r + \sigma_{\theta z}n_\theta + \sigma_{zz}n_z\right)_1 = \left(\sigma_{rz}n_r + \sigma_{\theta z}n_\theta + \sigma_{zz}n_z\right)_2
\end{aligned} \tag{2.49}$$

at point P which comes from equilibrium of forces on L.

3) $(T)_1 = (T)_2$ at point P (2.50)

which states the continuity of temperature on L.

4) $(q_n)_1 = (q_n)_2$ at point P (2.51)

or, with the use of Eq. (2.46),

$$k_1\left(\frac{\partial T}{\partial n}\right)_1 = k_2\left(\frac{\partial T}{\partial n}\right)_2 \text{ at point } P \tag{2.52}$$

which comes from the equilibrium of total heat flux on L.

CHAPTER 3

DEFINITION OF THE PROBLEM

In this study, thermally induced axisymmetric elastic deformations of infinitely long heat generating composite cylinders and tubes are examined. The geometry of the assemblies are shown, respectively, for cylinders and tubes in Figures 3.1 and 3.2. The layers are assumed to be perfectly bonded with each other and it is also assumed that the system have axially constraint ends (fixed ends).

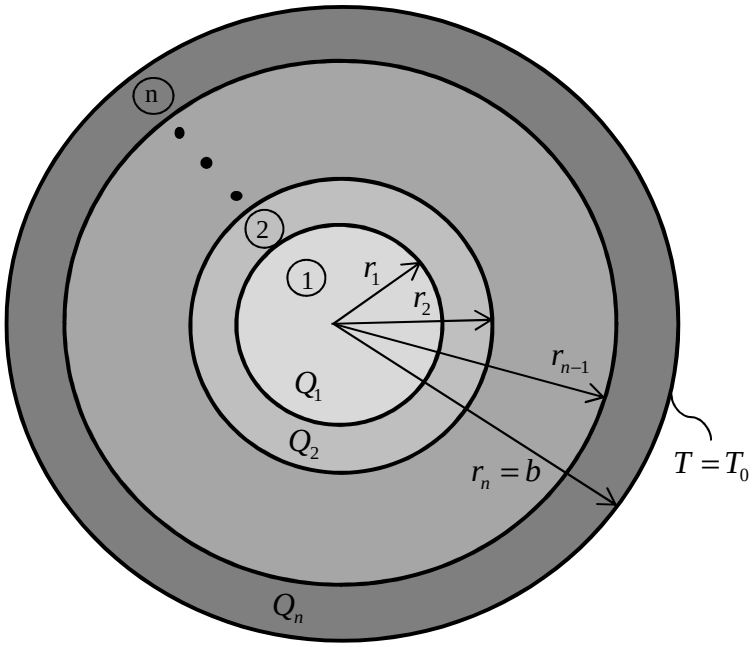

Figure 3.1: Composite cylinder.

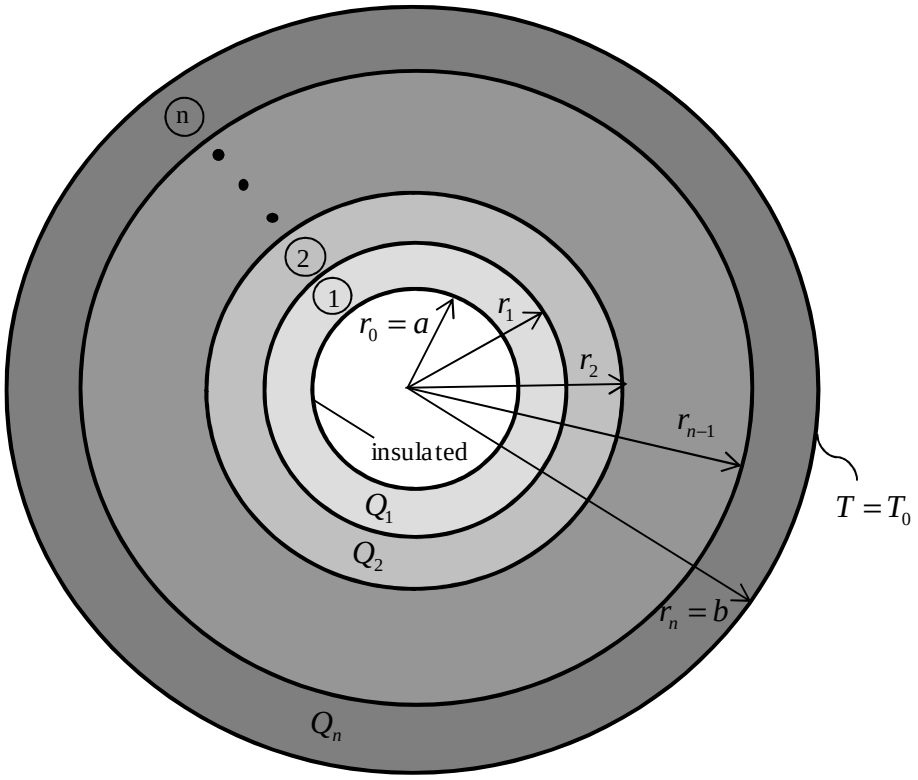

Figure 3.2: Composite tube.

Each layer is made up of an isotropic material whose physical properties are temperature dependent. It is assumed that each layer has different levels of uniform heat generation. For an n-layered system, the radial coordinate r of the interface between *i*' th and (*i+1*)' th layer is denoted by r_i $(i = 1,.....n-1)$. In the case of cylinders the inner radius is $r_0 = 0$. The outer radius for both systems is $r_n = b$. The uniform heat generation of the *i*'th layer is Q_i.

For both types of assemblies the outer surface is assumed to be kept at constant reference temperature T_0 and free of tractions. In case of composite tubes the inner surface is assumed to be insulated and free of tractions. The thermal problem is steady state and uncoupled from the mechanical one. The mechanical problem is a plane strain problem. Both thermal and mechanical problems are axisymmetric.

Next, we will present the governing equations of thermal and mechanical problems by referring to cylindrical coordinate system (CSS). In the formulations small deformation theory is used. As we state before, all the physical properties of

the materials vary with temperature. In other words, physical properties are functions of temperature T, that is,

$$E = E(T); \quad \nu = \nu(T); \quad k = k(T); \quad \alpha = \alpha(T); \quad \sigma_U = \sigma_U(T) \tag{3.1}$$

Here E is the elastic modulus, ν is the Poisson's ratio, k is the thermal conductivity, α is the thermal expansion coefficient and σ_U is the uniaxial yield limit.

3.1 Thermal Problem

Since the problem is steady state and axisymmetric, the energy equation for *i*'th layer of composite system can be written as (in view of Eq. (2.44))

$$\frac{d}{dr}\left(k_i \frac{dT^i}{dr}\right) + \frac{k_i}{r}\frac{dT^i}{dr} + Q_i = 0 \tag{3.2}$$

Here, $k_i = k_i(T)$ is thermal conductivity of the *i*'th layer, T^i is the temperature distrubution in the *i*'th layer and Q_i is the uniform heat generation in the *i*'th layer. Noting that the temperature distrubution is a function of position, $T = T(r)$, the thermal conductivity can be expressed as a function of r also, that is, $k = k(T(r)) = k(r)$. Eq. (3.2) can be written in an alternative form as

$$k_i \frac{d^2T^i}{dr^2} + \left(\frac{k_i}{r} + \frac{dk_i}{dr}\right)\frac{dT^i}{dr} + Q_i = 0 \tag{3.3}$$

In the above equation, the derivative of k_i with respect to radial coordinate is evaluated by using the chain rule, that is,

$$\frac{dk_i}{dr} = \frac{dk_i}{dT^i}\frac{dT^i}{dr} \tag{3.4}$$

By considering reference temperature $T_0 = 0$, the boundary conditions (BC's) associated with thermal problem in the case of composite cylinders are given by

$$\left.\frac{dT^1}{dr}\right|_{r=0} = 0 \quad \text{and} \quad T^n(b) = 0 \tag{3.5}$$

whereas in the case of composite tubes, they become

$$\left.\frac{dT^1}{dr}\right|_{r=a} = 0 \quad \text{and} \quad T^n(b) = 0 \tag{3.6}$$

For the interface conditions (IFC's), we have

$$T^i(r_i) = T^{i+1}(r_i) \qquad (i = 1, 2 \ldots n-1) \tag{3.7}$$

and

$$q_n^i(r_i) = q_n^{i+1}(r_i) \qquad (i = 1, 2 \ldots n-1) \tag{3.8}$$

In view of Eq. (2.46), Eq. (3.8) can also be written as

$$k_i(r_i)\frac{dT^i}{dr}\bigg|_{r=r_i} = k_{i+1}(r_i)\frac{dT^{i+1}}{dr}\bigg|_{r=r_i} \qquad (i = 1, 2 \ldots n-1) \tag{3.9}$$

Here, $k_i(r_i)$ denotes the value of the thermal conductivity at the temperature value $T = T^i(r_i)$, that is, $k_i(r_i) = k_i(T^i(r_i))$. Similary, $k_{i+1}(r_i) = k_{i+1}(T^i(r_i))$.

In summary, the thermal problem of the composite system is governed by (a) the 2nd order ODE's presented in Eq. (3.3) for $i = 1-n$, (b) the BC's and IFC's presented in Eqs. (3.5), (3.6), (3.7) and (3.9). Alltogether, these equations and conditions define the boundary value problem (BVP) of the thermal problem under consideration.

3.2 Mechanical Problem

As we state before, the mechanical problem is a plane strain and axisymmetric problem. Under these assumptions, the only nonzero strain components are ε_r and ε_θ. We note that, $\varepsilon_z = 0$ since the ends of the composite system are assumed to be fixed. On the other hand, the only nonzero stress components are σ_r, σ_θ and σ_z.

By using the notation that we introduce in the previous section, the strain displacement relations for the *i*'th layer of the composite system reads

$$\varepsilon_r^i = \frac{du^i}{dr} \tag{3.10}$$

$$\varepsilon_\theta^i = \frac{u^i}{r} \tag{3.11}$$

Here, u^i is the radial displacement of the *i*'th layer (The only nonzero displacement component). The compatibility relation is obtained by inserting $u^i = r\varepsilon_\theta^i$ (from Eq. (3.11)) into Eq. (3.10) as

$$\frac{d}{dr}\left[r\varepsilon_\theta^i\right] - \varepsilon_r^i = 0 \tag{3.12}$$

The equation of equilibrium in radial direction of the *i*'th layer is given by

$$\frac{d\sigma_r^i}{dr}+\frac{\sigma_r^i-\sigma_\theta^i}{r}=0 \tag{3.13}$$

The equations of generalized Hooke's law which relates strains to stresses of the *i*'th layer are:

$$\varepsilon_r^i=\frac{1}{E_i}\left[\sigma_r^i-\nu_i\left(\sigma_\theta^i+\sigma_z^i\right)\right]+G^i \tag{3.14}$$

$$\varepsilon_\theta^i=\frac{1}{E_i}\left[\sigma_\theta^i-\nu_i\left(\sigma_r^i+\sigma_z^i\right)\right]+G^i \tag{3.15}$$

$$\varepsilon_z^i=\frac{1}{E_i}\left[\sigma_z^i-\nu_i\left(\sigma_r^i+\sigma_\theta^i\right)\right]+G^i=0 \tag{3.16}$$

with the function G^i given by

$$G^i=G^i(T^i)=\int_{T_0}^{T^i}\alpha_i dT^i \tag{3.17}$$

The equations presented above form the basis of our formulation. Here, T_0 stands for the reference temperature. $E_i=E_i(T^i)$, $\nu_i=\nu_i(T^i)$ and $\alpha_i=\alpha_i(T^i)$ represent, respectively, elasticity modulus, Poisson's ratio and thermal expansion coefficient of the *i*'th layer. We also note that, since temperature is a function of radial coordinate ($T^i=T^i(r)$), the above parameters and function G^i can be represented as: $E_i=E_i(T^i(r))=E_i(r)$, $\nu_i=\nu_i(T^i(r))=\nu_i(r)$, $\alpha_i=\alpha_i(T^i(r))=\alpha_i(r)$ and $G^i=G^i(T^i(r))=G^i(r)$.

Since we assume $\varepsilon_z^i=0$, the axial stress σ_z^i can be determined from Eq. (3.16) as

$$\sigma_z^i=\nu_i\left(\sigma_r^i+\sigma_\theta^i\right)-E_iG^i \tag{3.18}$$

At this point, we introduce a stress function in terms of radial stress as

$$Y^i(r)=r\sigma_r^i \tag{3.19}$$

Inserting Eq. (3.19) into equation of equlibrium (Eq. (3.13)), we obtain

$$\sigma_\theta^i=\frac{dY^i}{dr} \tag{3.20}$$

The strain components can be expressed in terms of stress function by first eliminating axial stress σ_z^i from Eqs. (3.14) and (3.15), and then using Eqs. (3.19) and (3.20) in the resulting expression. The results are

$$\varepsilon_r^i = \frac{1}{E_i}\left[\frac{\left(1-\nu_i^2\right)}{r}Y^i - \nu_i\left(1+\nu_i\right)\frac{dY^i}{dr}\right] + \left(1+\nu_i\right)G^i \tag{3.21}$$

$$\varepsilon_\theta^i = -\frac{1}{E_i}\left[\frac{\nu_i\left(1+\nu_i\right)}{r}Y^i - \left(1-\nu_i^2\right)\frac{dY^i}{dr}\right] + \left(1+\nu_i\right)G^i \tag{3.22}$$

The thermoelastic equation is obtained by substituting Eqs. (3.21) and (3.22) into the compatibility relation given by Eq. (3.12). The result is

$$\begin{aligned}&\frac{d^2Y^i}{dr^2} + \left[\frac{1}{r} - \frac{1}{E_i}\frac{dE_i}{dr} - \frac{2\nu_i}{1-\nu_i^2}\frac{d\nu_i}{dr}\right]\frac{dY^i}{dr} \\ &-\left[\frac{1}{r} - \frac{\nu_i}{E_i\left(1-\nu_i\right)}\frac{dE_i}{dr} + \frac{1+2\nu_i}{1-\nu_i^2}\frac{d\nu_i}{dr}\right]\frac{Y^i}{r} \\ &\quad = -\frac{E_i}{1-\nu_i}\left\{\frac{1}{1+\nu_i}\frac{d\nu_i}{dr}G^i + \alpha_i\frac{dT^i}{dr}\right\}\end{aligned} \tag{3.23}$$

Equation (3.23) governs the mechanical problem for the *i*'th layer of the composite assembly. We note that, in Eq. (3.23), the derivatives of E_i and ν_i with respect to radial coordinate are evaluated by using the chain rule, that is,

$$\frac{dE_i}{dr} = \frac{dE_i}{dT^i}\frac{dT^i}{dr} \quad ; \quad \frac{d\nu_i}{dr} = \frac{d\nu_i}{dT^i}\frac{dT^i}{dr} \tag{3.24}$$

Next, we will introduce the boundary and interface conditions for the mechanical problem. In case of composite cylinders the BC's are

$$u^1(0) = 0 \quad \text{and} \quad \sigma_r^n(b) = 0 \tag{3.25}$$

whereas for composite tubes they become

$$\sigma_r^1(a) = 0 \quad \text{and} \quad \sigma_r^n(b) = 0 \tag{3.26}$$

For the IFC's, we have

$$u^i(r_i) = u^{i+1}(r_i) \qquad (i = 1, 2 \ldots n-1) \tag{3.27}$$

and

$$\sigma_r^i(r_i) = \sigma_r^{i+1}(r_i) \qquad (i = 1, 2 \ldots n-1) \tag{3.28}$$

Since Eq. (3.23) are given in terms of stress function Y^i, the conditions given above must also be presented in terms Y^i. For composite cylinders, the first BC $u^1(0) = 0$ yields $Y^1(0) = 0$ from Eq. (3.11) and (3.22), while the second BC $\sigma_r^n(b) = 0$ gives $Y^n(b) = 0$ from Eq. (3.19). In the case of composite tubes, $\sigma_r^1(a) = 0$ and $\sigma_r^n(b) = 0$

gives $Y^1(a)=0$ and $Y^n(b)=0$. In summary these BC's in terms of stress function become:

$$Y^1(0)=0 \text{ and } Y^n(b)=0 \quad \text{for composite cylinders} \tag{3.29}$$

and

$$Y^1(a)=0 \text{ and } Y^n(b)=0 \quad \text{for composite tubes} \tag{3.30}$$

The second IFC given in Eq. (3.28) can easily be written in terms of stress function (from Eq. (3.19)) as

$$Y^i(r_i)=Y^{i+1}(r_i) \tag{3.31}$$

Using the above relation together with Eqs. (3.11), (3.22) and (3.27), the first IFC can be represented in terms of stress function as

$$H_1^i(r_i)Y^i(r_i)+H_2^i(r_i)\left.\frac{dY^i}{dr}\right|_{r=r_i}+H_3^i(r_i)$$
$$= \tag{3.32}$$
$$H_1^{i+1}(r_i)Y^i(r_i)+H_2^{i+1}(r_i)\left.\frac{dY^{i+1}}{dr}\right|_{r=r_i}+H_3^{i+1}(r_i)$$

where

$$H_1^i(r)=-\frac{\nu_i(r)\left(1+\nu_i(r)\right)}{E_i(r)} \tag{3.33}$$

$$H_2^i(r)=\frac{r\left(1-(\nu_i(r))^2\right)}{E_i(r)} \tag{3.34}$$

$$H_3^i(r)=r\left(1+\nu_i(r)\right)G^i(r) \tag{3.35}$$

In summary, the mechanical problem of the composite system is governed by a) the 2nd order ODE's presented in Eq. (3.23) for $i=1-n$, b) the BC's and IFC's presented in Eqs. (3.29), (3.30), (3.31) and (3.32). Altogether, these equations and conditions define the boundary value problem (BVP) of the mechanical problem under consideration.

3.3 Thermal and Mechanical Problems in Case of Temperature Independent Physical Properties and Their Closed Form Solutions

Here, we consider that the layers of the composite system have temperature independent physical properties. In that case, we have

$$dk_i/dT^i=0 \text{ or } dk_i/dr=0 \quad , \quad k_i=(k_0)_i \,,$$

$$dE_i / dT^i = 0 \text{ or } dE_i / dr = 0 \quad , \quad E_i = (E_0)_i \,, \tag{3.36}$$

$$d\nu_i / dT^i = 0 \text{ or } d\nu_i / dr = 0 \quad , \quad \nu_i = (\nu_0)_i \,,$$

$$d\alpha_i / dT^i = 0 \text{ or } d\alpha_i / dr = 0 \quad , \quad \alpha_i = (\alpha_0)_i \,,$$

where $(k_0)_i$, $(E_0)_i$, $(\nu_0)_i$ and $(\alpha_0)_i$ are the constant valued properties of the the *i*'th layer of the composite assembly. Making use of (3.36), the governing ODE's for the *i*'th layer of the composite assembly of the thermal and mechanical problems (Eqs (3.3) and (3.23)) , respectively, reduce to

$$(k_0)_i \frac{d^2T^i}{dr^2} + \frac{(k_0)_i}{r}\frac{dT^i}{dr} + Q_i = 0 \tag{3.37}$$

$$\frac{d^2Y^i}{dr^2} + \frac{1}{r}\frac{dY^i}{dr} - \frac{Y^i}{r^2} = -\frac{(E_0)_i(\alpha_0)_i}{1-(\nu_0)_i}\frac{dT^i}{dr} \tag{3.38}$$

We note that, the closed form solutions of thermal and mechanical problems under consideration can be easily determined and these solutions are also available in literature such as [4,15]. The derivations are performed by assuming reference temperature $T_0 = 0$. We will use these analytical solutions to verify our computational method that is proposed in this study. Therefore these analytical solutions are briefly presented next.

3.3.1 Closed Form Solution of Thermal Problem

The solution of Eq. (3.37) is

$$T^i(r) = C_{2i-1}\ln(r) + C_{2i} - \frac{Q_i r^2}{4(k_0)_i} \tag{3.39}$$

which gives the temperature distrubution in the *i*'th layer. Here C_{2i-1} and C_{2i} are the integration constants to be determined. The derivative of $T^i(r)$ with respect to radial coordinate r can easily be evaluated as

$$\frac{dT^i}{dr} = \frac{C_{2i-1}}{r} - \frac{Q_i r}{2(k_0)_i} \tag{3.40}$$

It should be noted that, for an n-layered composite system, we have a total number of $2n$ integration constants. These constants are determined with the use of boundary and interface conditions which are given in Eqs. (3.5) through (3.9).

In case of composite cylinders, the first BC in Eq. (3.5), that is $dT^1/dr\big|_{r=0}=0$, requires $C_1=0$ to have a finite value of temperature at the axis of the system. Writing IFC's given in Eqs. (3.7) and (3.9) for each interface in turn and also having the BC at outer surface (Eq. (3.5)), a total of $2n-1$ equations are obtained as shown below.

$$
\left.\begin{aligned}
&T^1(r_1)=T^2(r_1)\\
&(k_0)_1\left.\frac{dT^1}{dr}\right|_{r=r_1}=(k_0)_2\left.\frac{dT^2}{dr}\right|_{r=r_1}
\end{aligned}\right\}\ \text{IFC's for the } 1^{\text{st}} \text{ interface}
$$

$$
\left.\begin{aligned}
&T^2(r_2)=T^3(r_2)\\
&(k_0)_2\left.\frac{dT^2}{dr}\right|_{r=r_2}=(k_0)_3\left.\frac{dT^3}{dr}\right|_{r=r_2}
\end{aligned}\right\}\ \text{IFC's for the } 2^{\text{nd}} \text{ interface} \qquad (3.41)
$$

$$
\left.\begin{aligned}
&T^{n-1}(r_{n-1})=T^n(r_{n-1})\\
&(k_0)_{(n-1)}\left.\frac{dT^{n-1}}{dr}\right|_{r=r_{n-1}}=(k_0)_n\left.\frac{dT^n}{dr}\right|_{r=r_{n-1}}
\end{aligned}\right\}\ \text{IFC's for the } (n-1)^{\text{th}} \text{ interface}
$$

$$
T^n(r_n)=T^n(b)=0 \quad \rightarrow \text{BC at the outer surface}
$$

The use of Eqs. (3.39) and (3.40) in the above equations give us $2n-1$ equations having $2n-1$ unknowns $(C_2, C_3 \ldots\ldots\ldots C_{2n})$. After setting the numerical values of parameters, we can constitude a linear system of algebraic equations in which its solution determines the unknown integration constants.

In the case of tubes, the first BC in Eq. (3.6) is written first, then IFC's given in Eqs. given in Eqs. (3.7) and (3.9) for each interface are written in turn. Finally, the last BC given in Eq. (3.6) is written. This gives a total of $2n$ equations as shown below.

$$
(k_0)_1\left.\frac{dT^1}{dr}\right|_{r=a}=0 \quad \rightarrow \text{BC at the inner surface}
$$

$$
\left.
\begin{aligned}
&T^1(r_1) = T^2(r_1) \\
&(k_0)_1 \left.\frac{dT^1}{dr}\right|_{r=r_1} = (k_0)_2 \left.\frac{dT^2}{dr}\right|_{r=r_1}
\end{aligned}
\right\} \text{ IFC's for the } 1^{\text{st}} \text{ interface}
$$

$$
\left.
\begin{aligned}
&T^2(r_2) = T^3(r_2) \\
&(k_0)_2 \left.\frac{dT^2}{dr}\right|_{r=r_2} = (k_0)_3 \left.\frac{dT^3}{dr}\right|_{r=r_2}
\end{aligned}
\right\} \text{ IFC's for the } 2^{\text{nd}} \text{ interface} \qquad (3.42)
$$

$$
\begin{aligned}
&\vdots \qquad\qquad\qquad\qquad \vdots \\
&\vdots \qquad\qquad\qquad\qquad \vdots \\
&\vdots \qquad\qquad\qquad\qquad \vdots
\end{aligned}
$$

$$
\left.
\begin{aligned}
&T^{(n-1)}(r_{n-1}) = T^n(r_{n-1}) \\
&(k_0)_{(n-1)} \left.\frac{dT^{(n-1)}}{dr}\right|_{r=r_{n-1}} = (k_0)_n \left.\frac{dT^n}{dr}\right|_{r=r_{n-1}}
\end{aligned}
\right\} \text{ IFC's for the } (n-1)^{\text{th}} \text{ interface}
$$

$$
T^n(r_n) = T^n(b) = 0 \qquad \rightarrow \text{ BC at the outer surface}
$$

The use of Eqs (3.39) and (3.40) in the above equations give us $2n$ equations having $2n$ unknowns $(C_1, C_2, ...C_{2n})$. After setting the numerical values of parameters, a system of algebraic equations can be formed in which its solution determines the integration constants.

3.3.2 Closed Form Solution of Mechanical Problem

The solution of Eq. (3.38) is

$$
Y^i = \frac{D_{2i-1}}{r} + D_{2i} r + \frac{(E_0)_i (\alpha_0)_i}{2\left(1-(\nu_0)_i\right)} r \left[\frac{Q_i r^2}{8(k_0)_i} - C_{2i-1}\left(\ln(r) - \frac{1}{2} \right) - C_{2i} \right] \qquad (3.43)
$$

which gives the variation of stress function with radial coordinate in the i'th layer of the composite system. Here, D_{2i-1} and D_{2i} are the integration constants. We recall that, C_{2i-1} and C_{2i} are the integration constants that belong to the thermal problem and it is assumed that these constant are already determined from the solution of thermal problem. The derivative of Y^i with respect to radial coordinate r can easily be evaluated as

$$
\frac{dY^i}{dr} = -\frac{D_{2i-1}}{r^2} + D_{2i} + \frac{(E_0)_i (\alpha_0)_i}{2\left(1-(\nu_0)_i\right)} \left[\frac{3Q_i r^2}{8(k_0)_i} - C_{2i-1}\left(\ln(r) + \frac{1}{2} \right) - C_{2i} \right] \qquad (3.44)
$$

The expressions for the field variables for the problem under consideration become

$$\sigma_r^i = \frac{Y^i}{r} \tag{3.45}$$

$$\sigma_\theta^i = \frac{dY^i}{dr} \tag{3.46}$$

$$\sigma_z^i = (\nu_0)_i (Y^i + \frac{dY^i}{dr}) - (E_0)_i (\alpha_0)_i T^i \tag{3.47}$$

$$\varepsilon_r^i = \frac{1+(\nu_0)_i}{(E_0)_i}\left[(1-(\nu_0)_i)\frac{Y^i}{r} - (\nu_0)_i \frac{dY^i}{dr}\right] + (\alpha_0)_i (1+(\nu_0)_i) T^i \tag{3.48}$$

$$\varepsilon_\theta^i = \frac{1+(\nu_0)_i}{(E_0)_i}\left[(1-(\nu_0)_i)\frac{dY^i}{dr} - (\nu_0)_i \frac{Y^i}{r}\right] + (\alpha_0)_i (1+(\nu_0)_i) T^i \tag{3.49}$$

$$u^i = r\varepsilon_\theta^i \tag{3.50}$$

The substitution of stress function and its derivative together with the temperature T^i into Eqs. (3.45) through (3.50) determines the distribution of field variables in the i'th layer composite system. On the other hand, the integration constants are still needed to be determined with the application of boundary and interface conditions of the mechanical problem. As in the thermal problem, there are a total number of $2n$ integration constants in the mechanical problem for an n - layered composite system.

For cylinders, the first BC is $Y^1(0) = 0$ from Eq. (3.29). Writing Eq. (3.43) for $i = 1$ at $r = 0$ (recall that $C_1 = 0$), we observe that, $Y^1(0) = 0$ if and only if D_1 is equal to zero. Otherwise, $Y^1(0)$ becomes indeterminate at the axis of the disk. Therefore the first BC requires $D_1 = 0$. Next, we write the IFC's of the mechanical problem given in Eqs. (3.31) and (3.32) for each interface in turn. The final condition BC $Y^n(b) = 0$ comes from Eq. (3.29). These give a total of $2n-1$ equations as shown below.

$$
\left.
\begin{aligned}
&Y^1(r_1) = Y^2(r_1) \\
&H_1^1(r_1)Y^1(r_1) + H_2^1(r_1)\left.\frac{dY^1}{dr}\right|_{r=r_1} + H_3^1(r_1) \\
&= \\
&H_1^2(r_1)Y^1(r_1) + H_2^2(r_1)\left.\frac{dY^2}{dr}\right|_{r=r_1} + H_3^2(r_1)
\end{aligned}
\right\} \text{ IFC's for the } 1^{st} \text{ interface}
$$

$$
\left.
\begin{aligned}
&Y^2(r_2) = Y^3(r_2) \\
&H_1^2(r_2)Y^2(r_2) + H_2^2(r_2)\left.\frac{dY^2}{dr}\right|_{r=r_2} + H_3^2(r_2) \\
&= \\
&H_1^3(r_2)Y^2(r_2) + H_2^3(r_2)\left.\frac{dY^3}{dr}\right|_{r=r_2} + H_3^3(r_2)
\end{aligned}
\right\} \text{ IFC's for the } 2^{nd} \text{ interface} \qquad (3.51)
$$

$$
\begin{matrix}
\vdots & \vdots \\
\vdots & \vdots \\
\vdots & \vdots
\end{matrix}
$$

$$
\left.
\begin{aligned}
&Y^2(r_{n-1}) = Y^3(r_{n-1}) \\
&H_1^{n-1}(r_{n-1})Y^{n-1}(r_{n-1}) + H_2^{n-1}(r_{n-1})\left.\frac{dY^{n-1}}{dr}\right|_{r=r_{n-1}} + H_3^{n-1}(r_{n-1}) \\
&= \\
&H_1^{n}(r_{n-1})Y^{n-1}(r_{n-1}) + H_2^{n}(r_{n-1})\left.\frac{dY^{n}}{dr}\right|_{r=r_{n-1}} + H_3^{n}(r_{n-1})
\end{aligned}
\right\} \begin{aligned} &\text{IFC's for the} \\ &(n-1)^{th} \text{ interface} \end{aligned}
$$

$$Y^n(b) = 0 \quad \rightarrow \text{ BC at the outer surface}$$

where

$$H_1^i(r) = -\frac{(\nu_0)_i\left(1+(\nu_0)_i\right)}{(E_0)_i} \qquad (3.52)$$

$$H_2^i(r) = \frac{r\left(1-(\nu_0)_i^2\right)}{(E_0)_i} \qquad (3.53)$$

$$H_3^i(r) = r\left(1+(\nu_0)_i\right)T^i(r) \qquad (3.54)$$

Inserting the stress function and its derivative from Eqs. (3.43) and (3.44) into the above equations yields $2n-1$ equations having $2n-1$ unknowns $(D_2.....D_{2n})$. As

discussed previously, from these equations a linear system of algebraic equations can be formed to determine the unknown integration constants.

For tubes, the BC $Y^1(a)=0$ given in Eq. (3.30) is written first, then the IFC's for each interface are written in turn. As a final condition, from Eq. (3.30) $Y^n(b)=0$ is written. This gives a total of $2n$ equations as shown below.

$Y^1(a)=0 \quad \rightarrow$ BC at the inner surface

$$\left.\begin{aligned} & Y^1(r_1)=Y^2(r_1) \\ & H_1^1(r_1)Y^1(r_1)+H_2^1(r_1)\left.\frac{dY^1}{dr}\right|_{r=r_1}+H_3^1(r_1) \\ & = \\ & H_1^2(r_1)Y^1(r_1)+H_2^2(r_1)\left.\frac{dY^2}{dr}\right|_{r=r_1}+H_3^2(r_1) \end{aligned}\right\} \text{ IFC's for the } 1^{\text{st}} \text{ interface}$$

$$\left.\begin{aligned} & Y^2(r_2)=Y^3(r_2) \\ & H_1^2(r_2)Y^2(r_2)+H_2^2(r_2)\left.\frac{dY^2}{dr}\right|_{r=r_2}+H_3^2(r_2) \\ & = \\ & H_1^3(r_2)Y^2(r_2)+H_2^3(r_2)\left.\frac{dY^3}{dr}\right|_{r=r_2}+H_3^3(r_2) \end{aligned}\right\} \text{ IFC's for the } 2^{\text{nd}} \text{ interface} \qquad (3.55)$$

$$\vdots \qquad\qquad \vdots$$

$$\left.\begin{aligned} & Y^2(r_{n-1})=Y^3(r_{n-1}) \\ & H_1^{n-1}(r_{n-1})Y^{n-1}(r_{n-1})+H_2^{n-1}(r_{n-1})\left.\frac{dY^{n-1}}{dr}\right|_{r=r_{n-1}}+H_3^{n-1}(r_{n-1}) \\ & = \\ & H_1^n(r_{n-1})Y^{n-1}(r_{n-1})+H_2^n(r_{n-1})\left.\frac{dY^n}{dr}\right|_{r=r_{n-1}}+H_3^n(r_{n-1}) \end{aligned}\right\} \begin{aligned} & \text{IFC's for the} \\ & (n-1)^{\text{th}} \text{ interface} \end{aligned}$$

$Y^n(b)=0 \quad \rightarrow$ BC at the outer surface

With the use of these conditions a $2n$ linear algebraic equations having $2n$ unknowns can be obtained where their solution determines the integration constants $(D_1, D_2 \ldots\ldots\ldots D_{2n})$.

CHAPTER 4

NUMERICAL SOLUTION OF THERMAL AND MECHANICAL PROBLEMS

In this chapter, a computational model is introduced for obtaining the numerical solution of thermoelastic composite cylinder / tube problem. The model is based on shooting algorithm. It should be recalled that, the thermal and mechanical problems are uncoupled. Therefore, the shooting algorithm is first applied to thermal problem to estimate the variation of the thermal variables inside the layers of the composite system. Then, by making use of these thermal variables, the shooting method is applied to mechanical problem to estimate the distribution of stresses, strains and radial displacement for each layer of the composite assembly. In the formulations n-layered composite system is considered. In the formulations, the reference temperature $T_0 = 0$.

4.1 Shooting Algorithm for Thermal Problem

The ODE that defines the thermal problem for the i'th layer of the composite system is rewritten here from Eq. (3.3), that is,

$$k_i \frac{d^2T^i}{dr^2} + \left(\frac{k_i}{r} + \frac{dk_i}{dT^i} \frac{dT^i}{dr} \right) \frac{dT^i}{dr} + Q_i = 0 \tag{4.1}$$

The BC's of the thermal problem are given by Eqs. (3.5) and (3.6)

$$\left. \frac{dT^1}{dr} \right|_{\substack{r=0 \\ (r=r_0)}} = 0 \text{ and } T^n(b) = T^n(r_n) = 0 \text{ for cylinders} \tag{4.2}$$

and

$$\left. \frac{dT^1}{dr} \right|_{\substack{r=a \\ (r=r_0)}} = 0 \text{ and } T^n(b) = T^n(r_n) = 0 \text{ for tubes} \tag{4.3}$$

whereas the IFC's are, (Eqs. (3.7) and (3.9))

$$T^i(r_i) = T^{i+1}(r_i) \tag{4.4}$$

$$k_i(r_i)\left.\frac{dT^i}{dr}\right|_{r=r_i} = k_{i+1}(r_i)\left.\frac{dT^{i+1}}{dr}\right|_{r=r_i} \tag{4.5}$$

for $i = 1, 2....., n-1$.

In order to apply shooting algorithm, the BVP given above will be first transformed to an n- number of system of initial value problems (IVP's). For this aim, two new variables, X_1^i and X_2^i are defined as

$$X_1^i = T^i \tag{4.6}$$

$$X_2^i = \frac{dT^i}{dr} \tag{4.7}$$

Using these variables, Eq. (4.1) is converted into system of first order ODE's that have the form

$$\begin{aligned} \frac{dX_1^i}{dr} &= X_2^i \\ \frac{dX_2^i}{dr} &= -\left[\frac{1}{r} + \frac{1}{k_i}\frac{dk_i}{dX_1^i}X_2^i\right]X_2^i - \frac{Q_i}{k_i} \end{aligned} \tag{4.8}$$

The solution of the above system requires two IC's which are denoted by

$$X_1^i = T^i(r_i) \qquad \text{first initial condition} \tag{4.9}$$

and

$$X_2^i = \left.\frac{dT^i}{dr}\right|_{r=r_i} \qquad \text{second initial condition} \tag{4.10}$$

for $i = 1, ..., n$. Equation (4.8) with the IC's given by Eqs. (4.9) and (4.10) define a system of IVP. If we can determine the IC's of the system given in Eq. (4.8) for each layer $(i = 1-n)$, then we have n number of system of IVP's where each one can be solved numerically. We note that, these system of IVP's should be solved consequtively starting from the first layer $(i = 1)$ to the last $(i = n)$, since the solution of the system of IVP for the $(i-1)^{\text{th}}$ layer provides IC 's of the i^{th} system of IVP. However, the first IC X_1^1 of the first layer is unknown. In order to determine X_1^1, an iterative computational algorithm (shooting algorithm) is established. The algorithm uses Newton's iterations to estimate X_1^1. In the following, the details of shooting algorithm for the solution of thermal problem is explained.

Consider the system of IVP for the first layer $(i=1)$. The BC $dT^1/dr\Big|_{r=0}=0$ for cylinders and $dT^1/dr\Big|_{r=a}=0$ for tubes both yields

$$X_2^1=0 \tag{4.11}$$

for the second IC. As stated before, the first IC X_1^1 is unknown. Therefore an estimate value Φ is given to X_1^1, that is

$$X_1^1=\Phi \tag{4.12}$$

The solution of the system IVP of the first layer subjected to these IC's determines the distribution of T^1 and dT^1/dr. Next, we consider the system of IVP for the second layer $(i=2)$. The IC's for this problem can be determined from the IFC's given for the first interface, that are,

$$T^1(r_1)=T^2(r_1) \tag{4.13}$$

$$k_1(r_1)\frac{dT^1}{dr}\bigg|_{r=r_1}=k_2(r_1)\frac{dT^2}{dr}\bigg|_{r=r_1} \tag{4.14}$$

Writing these conditions in terms of X_1^1 and X_2^1 and rearranging the results give

$$X_1^{\,2}(r_1)=X_1^1(r_1) \tag{4.15}$$

$$X_2^2(r_1)=\frac{k_1(r_1)}{k_2(r_2)}X_2^1(r_1) \tag{4.16}$$

Here, we recall that $X_1^1(r_1)$ and $X_2^1(r_1)$ are already determined from the solution of system of IVP of the first layer. Using the IC's given in Eqs. (4.15) and (4.16) the solution for the system of IVP for the second layer can be accomplished.

The above procedure is repeated to determine the solution of system of IVP from layer $i=3$ through $i=n$. Recall that, the BC that must be satisfied at the outer surface of the composite system is $T^n(b)=0$. In order to satisfy $T^n(b)=0$, Newton iterations are used. For this aim, a function $f=f(\Phi)$ is defined as

$$f(\Phi)=\left[X_1^n(b)\right]_{estimate=\Phi} \tag{4.17}$$

where the right side denotes the value of $X_1^n(b)$ which is obtained for estimate value Φ. Next, we solve the thermal problem two more times first by setting

$$X_1^1=\Phi+\Delta\Phi \tag{4.18}$$

that gives

$$f(\Phi+\Delta\Phi)=\left[X_1^n(b)\right]_{estimate=\Phi+\Delta\Phi} \tag{4.19}$$

and second by setting

$$X_1^1=\Phi-\Delta\Phi \tag{4.20}$$

that gives

$$f(\Phi-\Delta\Phi)=\left[X_1^n(b)\right]_{estimate=\Phi-\Delta\Phi} \tag{4.21}$$

where $\Delta\Phi$ is a small increment. Recall that, the formula of Newton's iterations is given by

$$\Phi^{k+1}=\Phi^k-\frac{f(\Phi^k)}{f'(\Phi^k)} \tag{4.22}$$

Here, Φ^k is the estimated value of X_1^1 in the k^{th} iteration cycle. $f'(\Phi^k)=df/dr\big|_{\Phi=\Phi^k}$ can be approximated with the use of central difference formula

$$f'(\Phi^k)=\frac{f(\Phi^k+\Delta\Phi)-f(\Phi^k-\Delta\Phi)}{2\Delta\Phi} \tag{4.23}$$

Rewriting Eq. (4.22) by making use of Eq. (4.23), we have

$$X_1^1=\Phi^{k+1}=\Phi^k-\frac{2(\Delta\Phi)f(\Phi^k)}{f(\Phi^k+\Delta\Phi)-f(\Phi-\Delta\Phi)} \tag{4.24}$$

The application of Eq. (4.24) requires the solution of thermal problem three times for each iteration cycle. The iterations are carried out until

$$\left|\Phi^{k+1}-\Phi^k\right|<\varepsilon_T \tag{4.25}$$

where ε_T represent the specified error tolerance.

4.2 Shooting Algorithm for Mechanical Problem

The ODE that defines the mechanical problem for the i^{th} layer of the composite system is given by Eq. (3.23), that is,

$$\begin{aligned}&\frac{d^2Y^i}{dr^2}+\left[\frac{1}{r}-\frac{1}{E_i}\frac{dE_i}{dr}-\frac{2\nu_i}{1-\nu_i^2}\frac{d\nu_i}{dr}\right]\frac{dY^i}{dr}\\&-\left[\frac{1}{r}-\frac{\nu_i}{E_i(1-\nu_i)}\frac{dE_i}{dr}+\frac{1+2\nu_i}{1-\nu_i^2}\frac{d\nu_i}{dr}\right]\frac{Y^i}{r}\\&\quad=-\frac{E_i}{1-\nu_i}\left\{\frac{1}{1+\nu_i}\frac{d\nu_i}{dr}G^i+\alpha_i\frac{dT^i}{dr}\right\}\end{aligned} \tag{4.26}$$

with

$$G^i = G^i(T^i) = \int_0^{T^i} \alpha_i dT^i \tag{4.27}$$

The BC's of the mechanical problem are given by Eqs. (3.29) and (3.30) as

$$Y^1(0) = 0 \text{ and } Y^n(b) = 0 \text{ for composite cylinders} \tag{4.28}$$

and

$$Y^1(a) = 0 \text{ and } Y^n(b) = 0 \text{ for composite tubes} \tag{4.29}$$

whereas for the IFC's we have (Eqs. (3.31) and (3.32))

$$Y^i(r_i) = Y^{i+1}(r_i) \tag{4.30}$$

and

$$H_1^i(r_i)Y^i(r_i) + H_2^i(r_i)\left.\frac{dY^i}{dr}\right|_{r=r_i} + H_3^i(r_i)$$

$$= \tag{4.31}$$

$$H_1^{i+1}(r_i)Y^i(r_i) + H_2^{i+1}(r_i)\left.\frac{dY^{i+1}}{dr}\right|_{r=r_i} + H_3^{i+1}(r_i)$$

with

$$H_1^i(r) = -\frac{\nu_i(r)\left(1+\nu_i(r)\right)}{E_i(r)} \tag{4.32}$$

$$H_2^i(r) = \frac{r\left(1-(\nu_i(r))^2\right)}{E_i(r)} \tag{4.33}$$

$$H_3^i(r) = r\left(1+\nu_i(r)\right)G^i(r) \tag{4.34}$$

for $i = 1, 2....., n-1$. Following a similar procedure as we did in thermal problem, this BVP will be transformed to a n- number of system of IVP. This is accomplished by defining two new variables, Z_1^i and Z_2^i as

$$Z_1^i = Y^i \tag{4.35}$$

$$Z_2^i = \frac{dY^i}{dr} \tag{4.36}$$

Using these variables, Eq. (4.26) is converted into a system of first order ODE's, that is,

$$\frac{dZ_1^i}{dr} = Z_2^i \tag{4.37}$$

$$\frac{dZ_2^i}{dr} = N_1 Z_2^i + N_2 \frac{Z_1^i}{r} + N_3 \tag{4.38}$$

where

$$N_1 = -\frac{1}{r} + \frac{1}{E_i}\frac{dE_i}{dr} + \frac{2\nu_i}{1-\nu_1^{\,2}}\frac{d\nu_i}{dr} \tag{4.39}$$

$$N_2 = \frac{1}{r} - \frac{\nu_i}{E_i(1-\nu_i)}\frac{dE_i}{dr} + \frac{1+2\nu_i}{1-\nu_i^{\,2}}\frac{d\nu_i}{dr} \tag{4.40}$$

$$N_3 = -\frac{E_i}{1-\nu_i}\left\{\frac{1}{1+\nu_i}\frac{d\nu_i}{dr}\int_0^{T^i}\alpha_i dT^i + \alpha_i\frac{dT^i}{dr}\right\} \tag{4.41}$$

Here, we recall that, the terms dE_i/dr and $d\nu_i/dr$ can be evaluated by using the chain rule as (see Eq. (3.24))

$$\frac{dE_i}{dr} = \frac{dE_i}{dZ_1^i}\frac{dZ_1^i}{dr} \text{ and } \frac{d\nu_i}{dr} = \frac{d\nu_i}{dZ_1^i}\frac{dZ_1^i}{dr} \tag{4.42}$$

The solution of the above system requires two IC's which are denoted by

$$Z_1^i = Y^i(r_i) \qquad \text{first initial condition} \tag{4.43}$$

and

$$Z_2^i = \left.\frac{dY^i}{dr}\right|_{r=r_i} \qquad \text{second initial condition} \tag{4.44}$$

for $i = 1, 2.....n$.

The IC's for each layer have to be determined to obtain the solutions of these n-number of system of IVP. As we explained previously, the solutions have to be carried out in a consequtive manner. However, the second IC Z_2^1 of the system of IVP for the first layer is unknown and to determine Z_2^1 we will again use shooting algorithm. The details of the algorithm for the mechanical problem will be discussed next.

Consider the system of IVP for the first layer ($i = 1$). The BC $Y^1(0) = 0$ for cylinders and $Y^1(a) = 0$ for tubes both yields

$$Z_1^1 = 0 \tag{4.45}$$

for the first IC (see Eq. (4.35)). The second IC Z_2^1 is unknown, therefore an estimate value Ψ is assigned to Z_2^1 as

$$Z_2^1 = \Psi \tag{4.46}$$

The solution of system of IVP for the first layer subjected to IC's given by Eqs. (4.45) and (4.46) determines the distribution of Y^1 and dY^1/dr. Next, we consider the system of IVP for the second layer $(i=2)$. The IC's for this problem can be determined from the IFC's given for the first interface, that are,

$$Y^1(r_1) = Y^2(r_1) \tag{4.47}$$

$$H_1^2(r_1)Y^1(r_1) + H_2^1(r_1)\left.\frac{dY^1}{dr}\right|_{r=r_1} + H_3^1(r_1)$$

$$= \tag{4.48}$$

$$H_1^2(r_1)Y^1(r_1) + H_2^2(r_1)\left.\frac{dY^2}{dr}\right|_{r=r_1} + H_3^2(r_1)$$

Writing these conditions in terms of Z_1^1 and Z_2^1 are rearranging the results give

$$Z_1^2(r_1) = Z_1^1(r_1) \tag{4.49}$$

$$Z_2^2(r_1) = \frac{1}{H_2^2(r_1)}\left\{\left[H_1^1(r_1) - H_1^2(r_1)\right]Z_1^1(r_1) + H_2^1(r_1)Z_2^1(r_1) + H_3^1(r_1) - H_3^2(r_1)\right\} \tag{4.50}$$

Here we recall that, $Z_1^1(r_1)$ and $Z_2^1(r_1)$ are already determined from the solution of system of IVP for the first layer. Using the IC's given in Eqs. (4.49) and (4.50), the solution for the system of IVP for the second layer can be accomplished.

The above procedure is repeated for the solution of system of IVP from layer $i=3$ through $i=n$. Recall that, the BC that must be satisfied at the outer surface of the composite system is $Y^n(b)=0$. As we did in the previous section, Newton iterations are performed for this purpose. A function $g = g(\Psi)$ is defined as

$$g(\Psi) = \left[Z_2^n(b)\right]_{estimate=\Psi} \tag{4.51}$$

where the right side denotes the value of $Z_2^n(b)$ which is obtained for estimate value Ψ. Solving the mechanical problem two more times first by setting

$$Z_2^1 = \Psi + \Delta\Psi \tag{4.52}$$

to give

$$g(\Psi + \Delta\Psi) = \left[Z_2^n(b)\right]_{estimate=\Psi+\Delta\Psi} \tag{4.53}$$

and second by setting

$$Z_2^1 = \Psi - \Delta\Psi \tag{4.54}$$

to give

$$g(\Psi - \Delta\Psi) = \left[Z_2^n(b) \right]_{estimate=\Psi-\Delta\Psi} \tag{4.55}$$

with $\Delta\Psi$ being a small increment. The formula of Newton's iterations method can be constructed as

$$(Z_2^1)^0 = \Psi^{k+1} = \Psi^k - \frac{2(\Delta\Psi)g(\Psi^k)}{g(\Psi^k + \Delta\Psi) - g(\Psi^k - \Delta\Psi)} \tag{4.56}$$

The application of Eq. (4.56) requires the solution of mechanical problem three times for each iteration cycle. The iterations are carried out until

$$\left| \Psi^{k+1} - \Psi^k \right| < \varepsilon_M \tag{4.57}$$

where ε_M represents the specified error tolerance.

4.3 Solution of Initial Value Problems

In the study, the numerical solution of system of IVP's for thermal and mechanical problems are obtained by using double presicion version of the state-of-the-art ordinary differential equation solver LSODE developed by Hindmarsh [23] and Brown and Hindmarsh [24].

The computational method is first applied to thermal problem and system of IVP's are solved using LSODE consecutively starting from the one corresponding to the first layer up to the one corresponding to the final layer. For each solution, LSODE is executed by choosing the stiff option turned on. The solution of each system of IVP provides the initial conditions of the next one. It should be noted that, the initial estimate value Φ given for the temperature (see Eq. (4.17)) at the axis the cylinder or at the inner radius of the tube greatly affects the accuracy and stability of the method. In the sample problems presented in Chapter 5, the specified error tolerance defined in Eq. (4.25) ε_T is chosen as 10^{-9}. The Newton iterations achieve the desired convergence in 3 to 10 iterations in problems having temperature independent properties whereas 3 to 50 iterations are needed for the problems having temperature dependent properties.

The results of the thermal problem (temperature and its gradient) are stored so that they can be used in the analysis of mechanical problem.

The computational method is finally applied to mechanical problem and system of IVP's are again solved using LSODE similary as explained in the thermal problem. In this case LSODE is executed by turning on the nonstiff option. In the sample problems presented in Chapter 5, the specified error tolerance defined in Eq. (4.57) ε_M is chosen as 10^{-9}. The Newton iterations achieve the desired convergence in 3 to 10 iterations in problems having both temperature independent and dependent properties.

CHAPTER 5

ASSESSMENT OF THE FORMULATION AND SAMPLE PROBLEMS

In this chapter, we consider some sample problems and analyze them using the computational method which uses shooting algorithm. We recall that, the definition of the thermoelastic heat generating composite cylinder/ tube problem that is considered within the scope of this thesis is given in Chapter 3 and computational method based on the shooting algorithm is discussed in Chapter 4.

In order to implement the proposed computational algorithm, we developed a computer program using FORTRAN 90 programming language.

For the verification of the computer program we first consider some benchmark problems whose closed form solutions exist. In these problems the physical properties of the selected materials are considered to be temperature independent. We recall that, these closed form solutions are briefly discussed in Section 3.3. The results of closed form solutions are evaluated using MATHEMATICA 7.0 and they are compared with those obtained from our computer program. Next, some problems with temperature dependent properties are considered.

5.1 Material Properties

In the example problems, two different materials are considered. The first one is a steel alloy UNS G41300 and the second one is an aluminum alloy UNS A93550. We note that the abbreviation "UNS" stands for "**U**nified **N**umbering **S**ystem for Metals and Alloys". The variations of physical properties with temperature for these two alloys are taken from Material Property Database[25] and they are given as follows:

UNS G41300

Thermal Expansion coefficient [1/^{o}C]:

For $-273.15^{\circ}C \le T \le 703.85^{\circ}C$

$$\alpha = 1.0599206523482848\times10^{-5} + 2.2723516478\times10^{-8}T - 2.370094\times10^{-11}T^2$$

Thermal Conductivity [W/(m ^{o}C)]:

For $-173.15^{\circ}C \le T < 99.85^{\circ}C$

$$k = 35.31225322775733 + 8.00414160477575\times10^{-3}T - 1.65649658595\times10^{-4}T^2 + 2.637029\times10^{-7}T^3$$

For $99.85^{\circ}C \le T \le 1199.85^{\circ}C$

$$k = 36.866873461078896 - 2.23034782934\times10^{-2}T + 8.615782\times10^{-6}T^2$$

Elasticity Modulus [GPa]:

For $-0.15^{\circ}C \le T < 776.85^{\circ}C$

$$E = 212.81411995016902 - 2.235395748\times10^{-2}T - 1.063196\times10^{-4}T^2$$

Poisson's Ratio:

For $-0.15^{\circ}C \le T < 779.85^{\circ}C$

$$\nu = 0.28780622069544737 + 5.2022465862756857\times10^{-5}T - 2.8354173801\times10^{-8}T^2 + 1.246582\times10^{-11}T^3$$

Uniaxial Yield Limit [MPa]:

For $-0.15^{\circ}C \le T < 537.85^{\circ}C$

$$\sigma_U = 518.9861958549853 - 2.6898899534063475\times10^{-1}T + 1.3533688071\times10^{-3}T^2 - 2.619722\times10^{-6}T^3$$

UNS A93550

Thermal Expansion coefficient [1/^{o}C]:

For $-0.15^{\circ}C \le T < 300^{\circ}C$

$$\alpha = 2.08778751995\times10^{-5} + 1.873273\times10^{-8}T$$

Thermal Conductivity [W/(m ^{o}C)]:

For $-0.15^{\circ}C \le T < 537.85^{\circ}C$

$$k = 137.43357167622128 + 1.1427869395\times10^{-1}T - 1.663835\times10^{-4}T^2$$

Elasticity Modulus [GPa]:

For $-273.15^{\circ}C \le T < 499.85^{\circ}C$

$$E = 70.83972778471862 - 3.501227309841928\times10^{-2}T + 6.153504541239795\times10^{-7}T^2 + 3.788598464\times10^{-8}T^3 - 3.545736\times10^{-10}T^4$$

Poisson's Ratio:

For $-273.15^{\circ}C \le T < 499.85^{\circ}C$

$$\nu = 0.3308563373280359 + 2.0906580661445568\times10^{-5}T - 6.340010832582345\times10^{-8}T^2 + 4.033925304086235\times10^{-11}T^3 + 8.54288720375\times10^{-13}T^4 + 3.170505\times10^{-16}T^5$$

Uniaxial Yield Limit [MPa]:

For $-28.15^{\circ}C \le T < 24.85^{\circ}C$

$$\sigma_U = 160.0$$

For $24.85^{\circ}C \le T < 149.85^{\circ}C$

$$\sigma_U = 160.30020743509633 + 2.873355265967277\times10^{-3}T - 4.4952925255\times10^{-4}T^2 - 6.132959\times10^{-6}T^3$$

For $149.85^{\circ}C \le T < 259.85^{\circ}C$

$$\sigma_U = -358.47557252930073 + 11.902469111358533T - 9.388632890356514\times10^{-2}T^2 + 2.882823166\times10^{-4}T^3 - 3.11259\times10^{-7}T^4$$

For $259.85^{\circ}C \le T < 369.85^{\circ}C$

$$\sigma_U = 176.55675868099885 - 8.0631389635\times10^{-1}T + 9.917355\times10^{-4}T^2$$

We note that, in the above variations the temperature T is given in terms of Celcius. Table 5.1 shows the values of physical properties at $T = 0^{\circ}$ for UNS G41300 and UNS A93550. These values are obtained by setting temperature $T = 0^{\circ}$ in the above equations, that is, $\alpha_0 = \alpha(0)$, $k_0 = k(0)$, $E_0 = E(0)$, $\nu_0 = \nu(0)$, $(\sigma_U)_0 = \sigma_U(0)$.

Table 5.1: Physical properties of UNS G41300 and UNS A93550 at $T = 0^{\circ}$

Property	UNS G41300	UNS A93550
α_0 [1/C]	$1.0599206523482848\times10^{-5}$	$2.08778751995\times10^{-5}$
k_0 [W/mC]	35.31225322775733	137.43357167622128
E_0 [GPa]	212.81411995016902	70.83972778471862
ν_0	0.28780622069544737	0.3308563373280359
$(\sigma_U)_0$ [MPa]	518.9861958549853	160.0

Figures 5.1 through 5.5 show the normalized variations of physical properties for the steel alloy UNS G41300 from $0^{\circ}C$ to $300^{\circ}C$. Similarly Figures 5.6 and 5.7 depict these variations for the aluminum alloy UNS A93550.

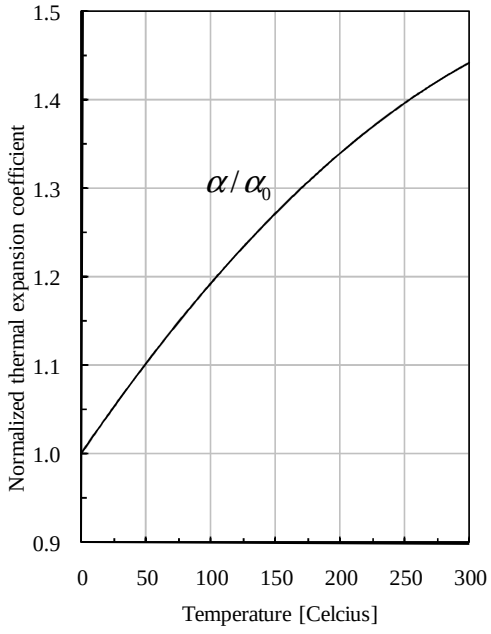

Figure 5.1: Variation of normalized thermal expansion coefficient (α/α_0) with temperature for UNS G41300.

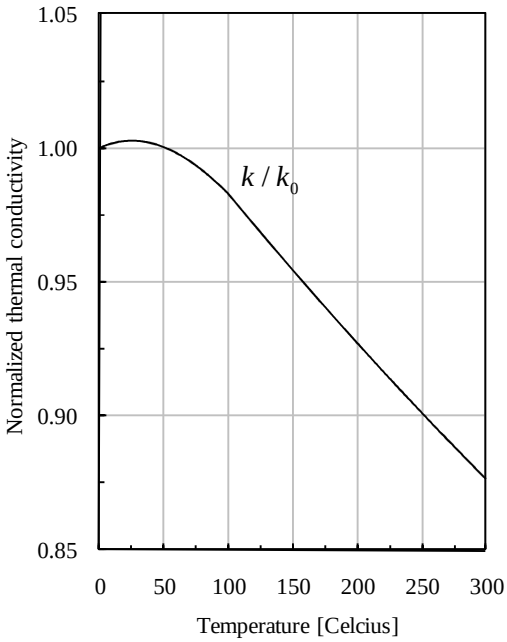

Figure 5.2: Variation of normalized thermal conductivity (k/k_0) with temperature for UNS G41300.

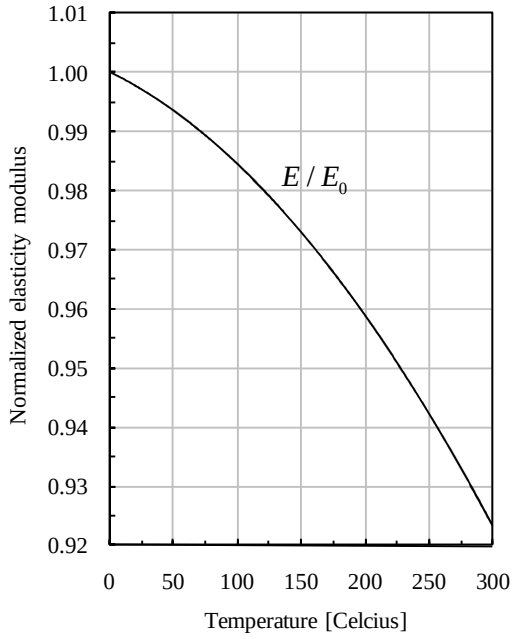

Figure 5.3: Variation of normalized elasticity modulus (E / E_0) with temperature for UNS G41300.

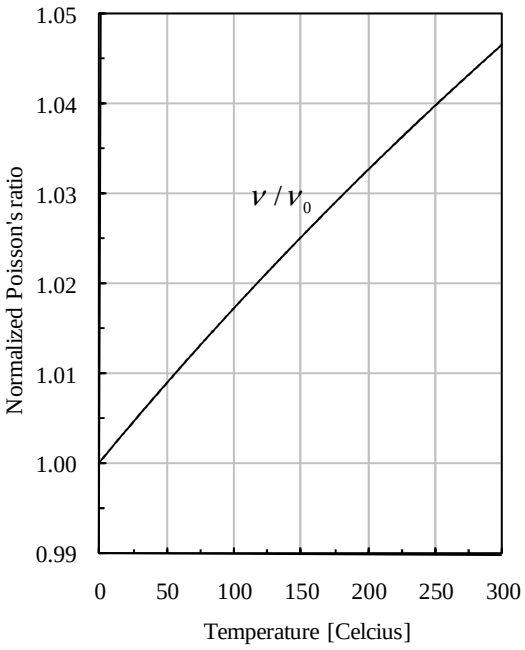

Figure 5.4: Variation of normalized Poisson's ratio (ν / ν_0) with temperature for UNS G41300.

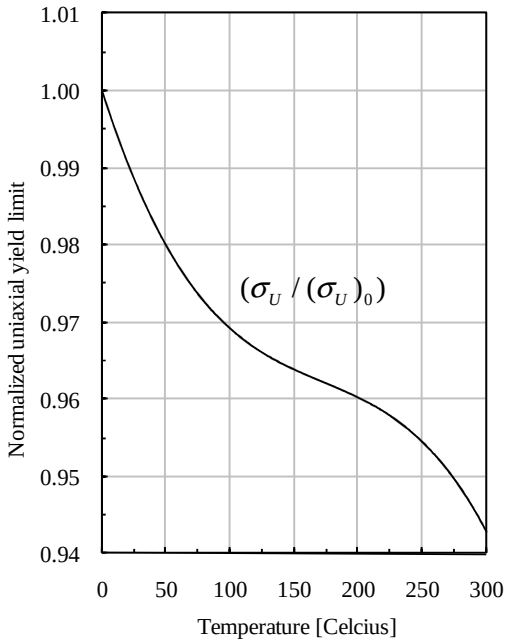

Figure 5.5: Variation of normalized uniaxial yield limit $(\sigma_U / (\sigma_U)_0)$ with temperature for UNS G41300.

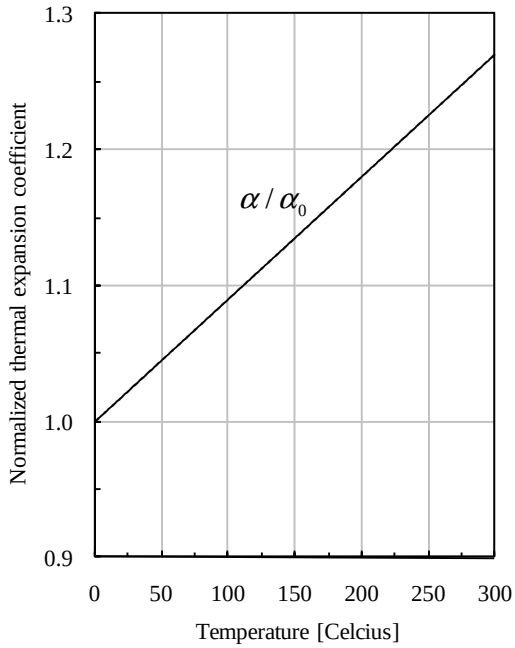

Figure 5.6: Variation of normalized thermal expansion coefficient (α / α_0) with temperature for UNS A93550.

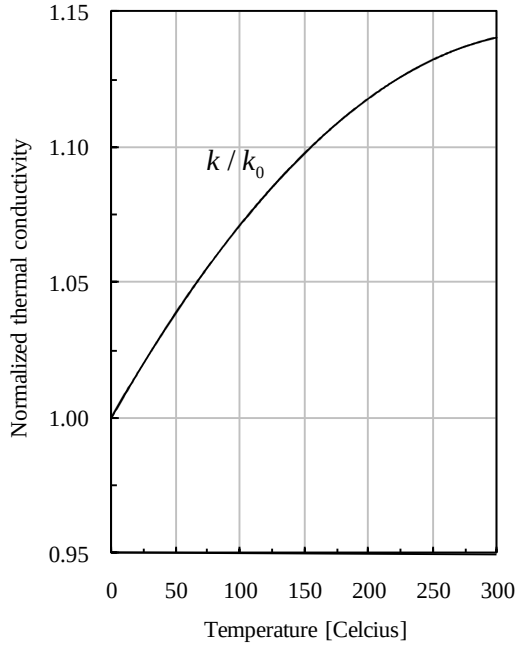

Figure 5.7: Variation of normalized thermal conductivity (k / k_0) with temperature for UNS A93550.

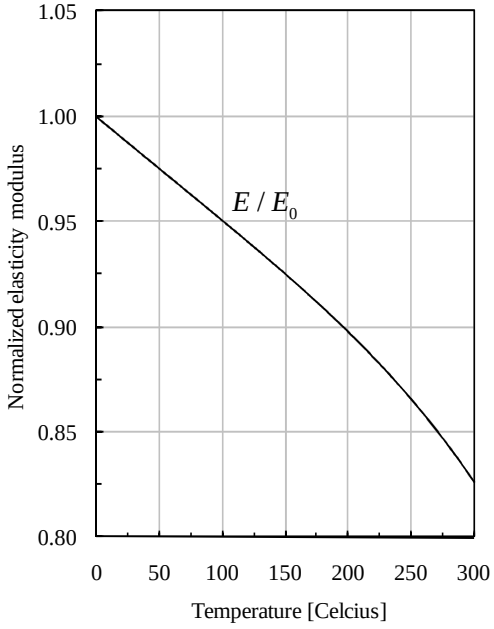

Figure 5.8: Variation of normalized elasticity modulus (E / E_0) with temperature for UNS A93550.

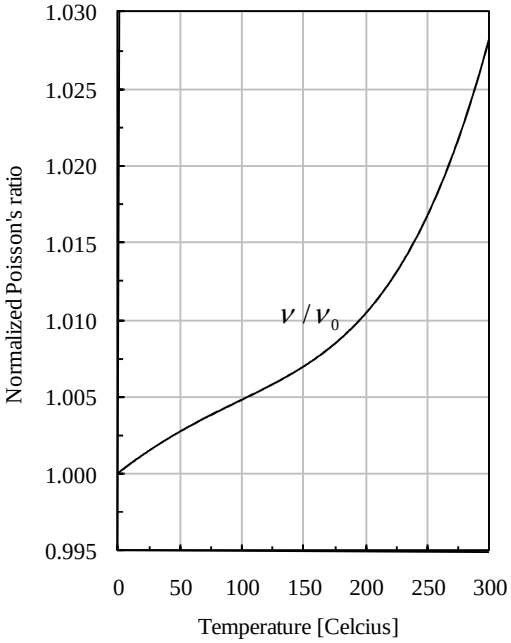

Figure 5.9: Variation of normalized Poisson's ratio (ν / ν_0) with temperature for UNS A93550.

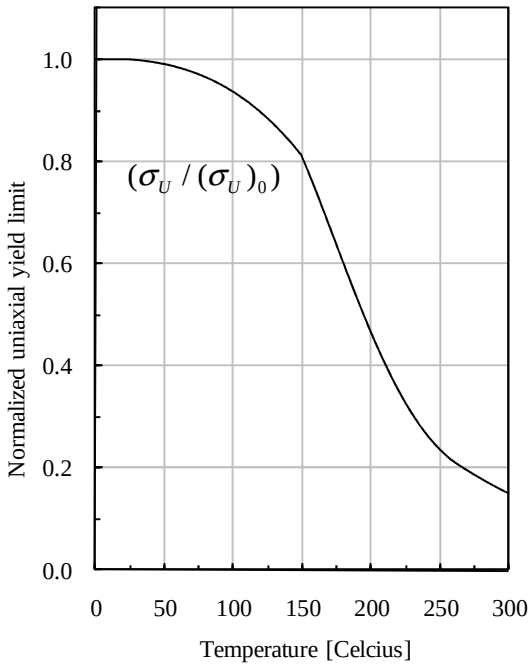

Figure 5.10: Variation of normalized uniaxial yield limit $(\sigma_U / (\sigma_U)_0)$ with temperature for UNS A93550.

In the examples presented below, the temperature problem is solved using dimensional variables whereas the solution of mechanical problem is performed by using the nondimensional and normalized variables shown in Table 5.2.

Table 5.2: Normalized and nondimensional variables used for the solution mechanical problem.

Nondimensional radial coordinate	$\bar{r} = r / b$
Nondimensional elasticity modulus	$\bar{E} = E(T) / E_R$
Nondimensional stress components	$\bar{\sigma}_j = \sigma_j / \sigma_{UR}$, $(j = r, \theta, z)$
Normalized strain	$\bar{\varepsilon}_j = \varepsilon_j E_R / \sigma_{UR}$, $(j = r, \theta, z)$
Nondimensional radial displacement	$\bar{u} = u E_R / b\sigma_{UR}$
Normalized thermal expansion coefficient	$\bar{\alpha} = \alpha(T) E_R / \sigma_{UR}$
Nondimensional heat load	$\bar{Q} = Q E_R \alpha_R b^2 / \sigma_{UR} k_R$

In Table 5.2, b is the outer radii of the composite/tube system; E_R, σ_{UR}, α_R and k_R , respectively, are the reference values of elasticity modulus, uniaxial yield limit, coefficient of thermal expansion and coefiicient of thermal conductivity.

5.2 Numerical Examples

In all the examples, the reference temperature is selected as $T_0 = 0$ and the reference values material parameters are set to corresponding values of UNS G41300 at $T = 0$, that is,

$$E_R = [E_0]_{\text{UNS G41300}} \;\; ; \;\; \sigma_{UR} = [(\sigma_U)_0]_{\text{UNS G41300}}$$

$$\alpha_R = [\alpha_0]_{\text{UNS G41300}} \;\; ; \;\; k_R = [k_0]_{\text{UNS G41300}}$$

It should be noted that, since thermoelastic analysis is considered in the study, our solutions are valid in the elastic range. As well known, yielding commences when the yield stress σ_Y is equal to uniaxial yield limit, i.e.

$$\sigma_Y = \sigma_U \tag{5.1}$$

Here, we note that uniaxial yield limit is a function of temperature, i.e, $\sigma_U = \sigma_U(T)$. Assuming that the materials considered here yields according to von Mises yield criterion, for the state of plane strain we have

$$\sigma_Y = \sqrt{\frac{1}{2}\left[(\sigma_r - \sigma_\theta)^2 + (\sigma_r - \sigma_z)^2 + (\sigma_\theta - \sigma_z)^2\right]} \tag{5.2}$$

Inserting Eq. (5.2) into Eq. (5.1) and dividing the result into the reference value of uniaxial yield stress (σ_{UR}) gives

$$\frac{\sigma_U}{\sigma_{UR}} = \sqrt{\frac{1}{2}\left[(\bar{\sigma}_r - \bar{\sigma}_\theta)^2 + (\bar{\sigma}_r - \bar{\sigma}_z)^2 + (\bar{\sigma}_\theta - \bar{\sigma}_z)^2\right]} \tag{5.3}$$

Rearranging Eq. (5.3) as

$$1 = \frac{1}{\bar{\sigma}_U}\sqrt{\frac{1}{2}\left[(\bar{\sigma}_r - \bar{\sigma}_\theta)^2 + (\bar{\sigma}_r - \bar{\sigma}_z)^2 + (\bar{\sigma}_\theta - \bar{\sigma}_z)^2\right]} \tag{5.4}$$

gives the yield condition in terms of nondimensional stresses. Note that $\bar{\sigma}_U = \sigma_U / \sigma_{UR}$ is the nondimensional uniaxial yield stress. In the computations, we define a nondimensional stress variable as

$$\Phi^i = \frac{1}{\bar{\sigma}_U^i}\sqrt{\frac{1}{2}\left[(\bar{\sigma}_r^i - \bar{\sigma}_\theta^i)^2 + (\bar{\sigma}_r^i - \bar{\sigma}_z^i)^2 + (\bar{\sigma}_\theta^i - \bar{\sigma}_z^i)^2\right]} \tag{5.5}$$

which its radial distribution is calculated for each layer of composite system (for $i = 1 - n$). Therefrom, the values of $\Phi^i < 1$ states that we are in elastic range, whereas as soon as $\Phi^i = 1$ the plastic deformation starts.

The first three examples are the benchmark problems that are solved to verify our computational method. In these problems, the physical properties are considered to be temperature independent and their values are taken from Table 5.1. The results of analytical solutions are obtained through the use of MATHEMATICA 7.0. In the next three examples, the examples presented as benchmark problems are reconsidered. But in these problems, we obtain the solutions by assuming that the physical properties of the materials change with temperature according to the variations given in the beginning of this chapter. In following discussions, the abbreviation "CP" is used for **C**onstant **P**roperty (or for *temperature independent physical properties*) while the abbreviation "VP" is used for **V**ariable **P**roperty (or for *temperature dependent physical properties*). We also note that, these abbreviations are also used as a subscript under some variables to denote whether the variable is obtained from the solution of composite cylinder/tube system having CP and VP.

5.2.1 Example 1: Two Layered Composite Cylinder Having Temperature Independent Physical Properties

In this problem, we consider a two layered composite cylinder where the inner core is assumed to be made from steel alloy UNS G41300 and the outer layer is made from aluminum alloy UNS A93550. Figure 5.11 shows the composite assembly. It is also assumed that, uniform heat is generated only in the inner core, that is, $Q^1 \neq 0$ and $Q^2 = 0$. The nondimensional values of radial coordinates of the interface between layers and the outer radius are, respectively, $\bar{r}_1 = 0.2$ and $\bar{r}_2 = 1.0$. Figure 5.12 and 5.13 show the variations of temperature and its gradient at the elastic limit heat load $\left[\bar{Q}^1_{el}\right]_{CP} = 63.37630781$, that is, at the heat load $\bar{Q}^1$ when the yielding starts. The corresponding stress and radial displacement-strain variations are depicted in Figures 5.14 and 5.15, respectively. In these figures, the results obtained from analytical and numerical solutions (NSM) are denoted, respectively, by diamonds and solid lines. In the analytical solutions, the values of integration constants

evaluated, respectively, for the thermal and mechanical problems are: $C_1 = 0$, $C_2 = 266.4168368$, $C_3 = -74.93272728$, $C_4 = 0$, and, $\bar{D}_1 = 0$, $\bar{D}_2 = 0.4408072713$, $\bar{D}_3 = 0.4464758095 \times 10^{-2}$, $\bar{D}_4 = 0.7531625621 \times 10^{-1}$. We also use red and blue colors in the plots in order to identify the results of the different layers easily. From Figure 5.14, it is seen that, the yielding starts at the axis of the cylinder ($\Phi_Y^1(0) = 1$) in the steel alloy.

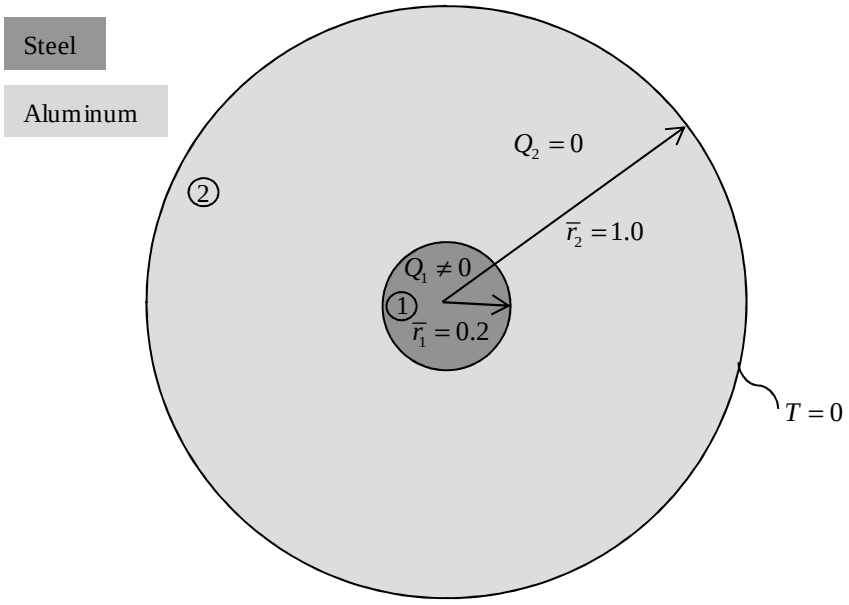

Figure 5.11: Two layered composite cylinder. First layer is made from UNS G41300 and second layer is made from UNS A93550. Uniform heat is generated in the first layer.

We also compare these results in Tables 5.3 through 5.5. Table 5.3 shows the values temperature and its gradient at some nondimensional radial distances. On the other hand, Table 5.4 and 5.5 compares the results of mechanical problem. In these tables, the digits of the values of any quantity which agree for both solutions are denoted by blue colors whereas the digits which do not agree are denoted by red colors.

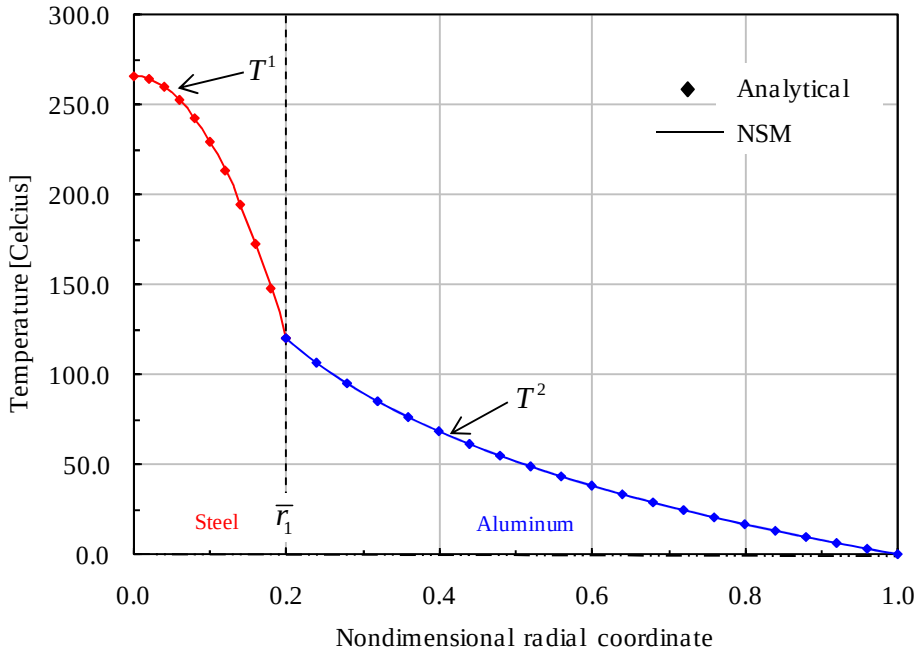

Figure 5.12: Variation of temperature with nondimensional radial coordinate in the two layered composite cylinder considered in Example 1.

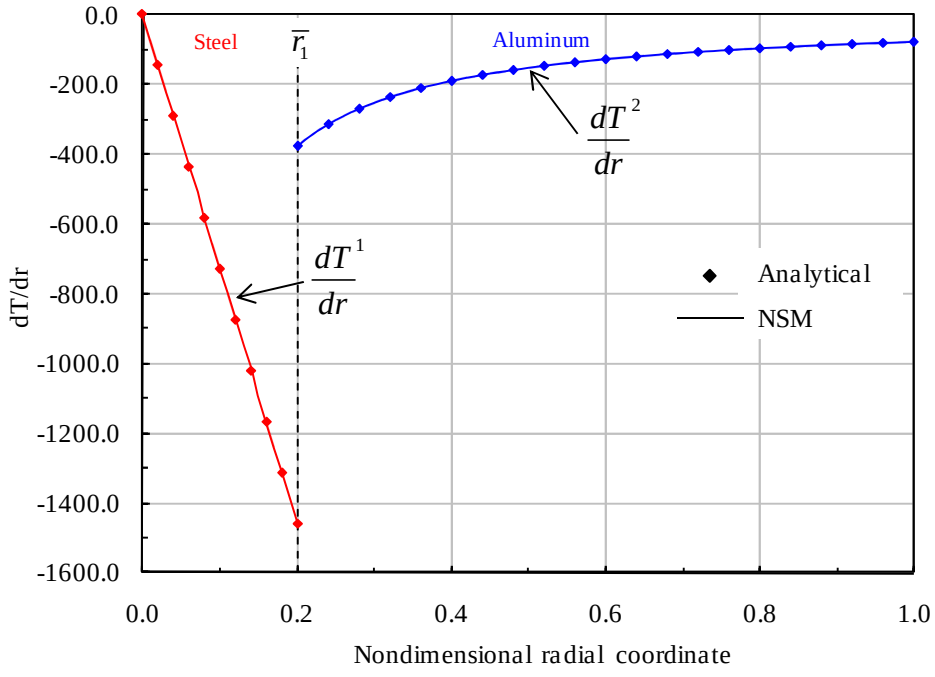

Figure 5.13: Variation of temperature gradient with nondimensional radial coordinate in the two layered composite cylinder considered in Example 1.

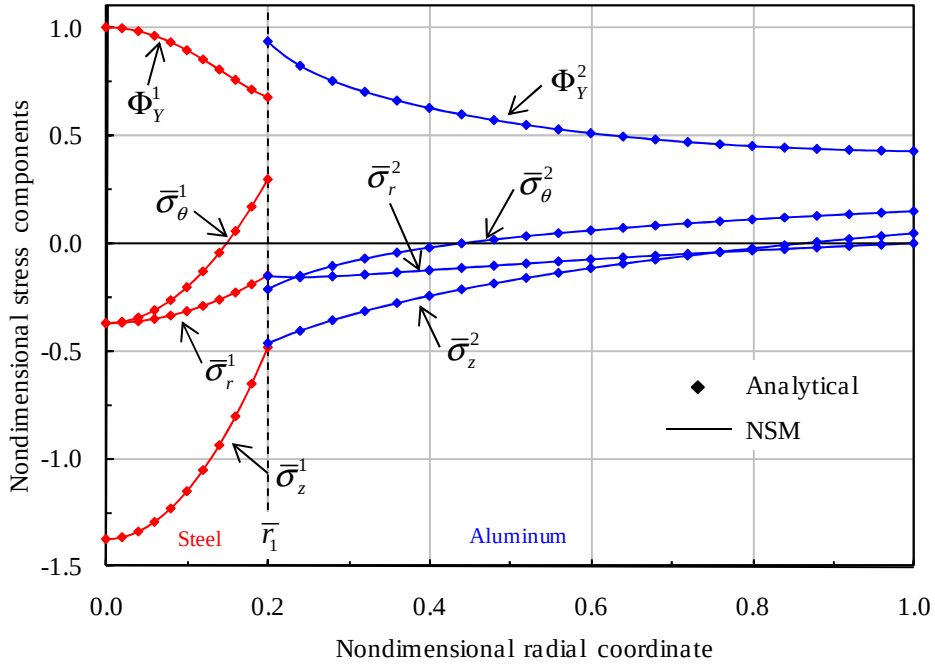

Figure 5.14: Variation of nondimensional stress components with nondimensional radial coordinate in the two layered composite cylinder considered in Example 1.

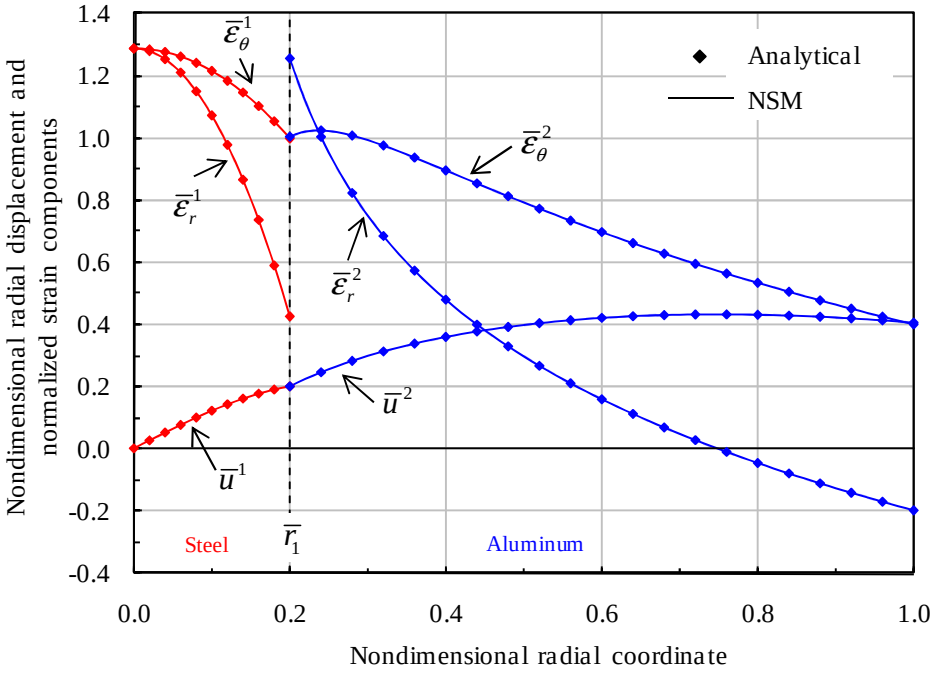

Figure 5.15: Variation of nondimensional radial displacement and normalized strain components with nondimensional radial coordinate in the two layered composite cylinder considered in Example 1.

Table 5.3: Comparison of the values of temperature and its gradient obtained from the analytical and numerical solutions of Example 1.

	Analytical	**Numerical**	**Analytical**	**Numerical**
r	Temperature [Celcius]		dT / dr	
0.0	2.66416836 8E+02	2.66416837 1E+02	0.000000000E+00	0.000000000E+00
0.1	2.29962520 6E+02	2.29962520 9E+02	-7.290863230E+02	-7.290863230E+02
0.2	1.20599572 2E+02	1.20599572 4E+02	-1.458172646E+03	-1.458172646E+03
0.2	1.20599572 2E+02	1.20599572 4E+02	-3.746636364E+02	-3.746636364E+02
0.3	9.02169658 0E+01	9.02169660 8E+01	-2.49775757 6E+02	-2.49775758 0E+02
0.4	6.86601635 2E+01	6.86601637 6E+01	-1.87331818 2E+02	-1.87331818 7E+02
0.5	5.19394086 5E+01	5.19394088 4E+01	-1.49865454 6E+02	-1.49865455 1E+02
0.6	3.82775571 5E+01	3.82775573 0E+01	-1.24887878 8E+02	-1.24887879 4E+02
0.7	2.67266263 0E+01	2.67266264 0E+01	-1.07046753 3E+02	-1.07046753 8E+02
0.8	1.67207548 8E+01	1.67207549 3E+01	-9.36659091 0E+01	-9.36659096 3E+01
0.9	7.89495078 6E+00	7.89495079 5E+00	-8.32585858 7E+01	-8.32585863 7E+01
1.0	0.000000000E+00	-3.711501906E-08	-7.49327272 8E+01	-7.49327277 5E+01

Table 5.4: Comparison of the values of stress components obtained from the analytical and numerical solutions of Example 1.

	Analytical	Numerical	Analytical	Numerical	Analytical	Numerical	Analytical	Numerical
r	$\bar{\sigma}_r$		$\bar{\sigma}_\theta$		$\bar{\sigma}_z$		Φ	
0.0	-3.721196071E-01	-3.721196167E-01	-3.721196071E-01	-3.721196167E-01	-1.372119607E+00	-1.372119614E+00	1.000000000E+00	9.999999973E-01
0.1	-3.165024513E-01	-3.165024532E-01	-2.052681398E-01	-2.052681416E-01	-1.149650984E+00	-1.149650986E+00	8.939710584E-01	8.939710588E-01
0.2	-1.496509840E-01	-1.496509858E-01	2.952862624E-01	2.952862606E-01	-4.822451145E-01	-4.822451168E-01	6.757007663E-01	6.757007666E-01
0.2	-1.496509840E-01	-1.496509858E-01	-2.133268601E-01	-2.133268620E-01	-4.637726351E-01	-4.637726371E-01	9.329413941E-01	9.329413947E-01
0.3	-1.469646779E-01	-1.469646797E-01	-8.661949581E-02	-8.661949755E-02	-3.343789648E-01	-3.343789667E-01	7.258505206E-01	7.258505212E-01
0.4	-1.227652280E-01	-1.227652297E-01	-1.901267555E-02	-1.901267715E-02	-2.425726946E-01	-2.425726964E-01	6.285409468E-01	6.285409473E-01
0.5	-9.720569597E-02	-9.720569766E-02	2.663826788E-02	2.663826642E-02	-1.713622192E-01	-1.713622208E-01	5.620096029E-01	5.620096034E-01
0.6	-7.357102507E-02	-7.357102669E-02	6.118679190E-02	6.118679059E-02	-1.131790242E-01	-1.131790256E-01	5.135442977E-01	5.135442982E-01
0.7	-5.226478449E-02	-5.226478604E-02	8.907374169E-02	8.907374054E-02	-6.398583388E-02	-6.398583506E-02	4.785981344E-01	4.785981350E-01
0.8	-3.309381129E-02	-3.309381276E-02	1.125158483E-01	1.125158472E-01	-2.137275410E-02	-2.137275508E-02	4.544933943E-01	4.544933950E-01
0.9	-1.576424868E-02	-1.576425008E-02	1.327736859E-01	1.327736850E-01	1.621464611E-02	1.621464533E-02	4.392271474E-01	4.392271484E-01
1.0	0.000000000E+00	-1.335284561E-09	1.506325124E-01	1.506325116E-01	4.983772134E-02	4.983772075E-02	4.311361257E-01	4.311361270E-01

Table 5.5: Comparison of the values of radial displacement and strain components obtained from the analytical and numerical solutions of Example 1.

	Analytical	Numerical	Analytical	Numerical	Analytical	Numerical	Numerical
r	$\bar{u}$		$\bar{\varepsilon}_r$		$\bar{\varepsilon}_\theta$		$\bar{\varepsilon}_z$
0.0	0.000000000E+00	0.000000000E+00	1.287806221E+00	1.287806217E+00	1.287806221E+00	1.287806217E+00	0.000000000E+00
0.1	1.216182102E-01	1.216182102E-01	1.072933863E+00	1.072933864E+00	1.216182102E+00	1.216182102E+00	-1.110223025E-16
0.2	2.002619488E-01	2.002619489E-01	4.283167903E-01	4.283167909E-01	1.001309744E+00	1.001309745E+00	0.000000000E+00
0.2	2.002619488E-01	2.002619489E-01	1.255892898E+00	1.255892898E+00	1.001309744E+00	1.001309745E+00	0.000000000E+00
0.3	2.971708791E-01	2.971708793E-01	7.493029244E-01	7.493029250E-01	9.905695970E-01	9.905695978E-01	0.000000000E+00
0.4	3.575270143E-01	3.575270146E-01	4.790034239E-01	4.790034241E-01	8.938175357E-01	8.938175365E-01	0.000000000E+00
0.5	3.958138583E-01	3.958138586E-01	2.964859329E-01	2.964859326E-01	7.916277165E-01	7.916277171E-01	-5.551115123E-17
0.6	4.182802222E-01	4.182802225E-01	1.583571354E-01	1.583571346E-01	6.971337037E-01	6.971337041E-01	0.000000000E+00
0.7	4.283643080E-01	4.283643081E-01	4.686204413E-02	4.686204267E-02	6.119490114E-01	6.119490115E-01	-2.775557562E-17
0.8	4.282410822E-01	4.282410821E-01	-4.686207535E-02	-4.686207729E-02	5.353013528E-01	5.353013526E-01	0.000000000E+00
0.9	4.194142705E-01	4.194142701E-01	-1.278551373E-01	-1.278551398E-01	4.660158561E-01	4.660158557E-01	0.000000000E+00
1.0	4.029886567E-01	4.029886560E-01	-1.992566894E-01	-1.992566923E-01	4.029886567E-01	4.029886560E-01	-9.053897019E-18

5.2.2 Example 2: Three Layered Composite Tube Having Temperature Independent Physical Properties

In this problem, we consider a three layered composite tube as shown in Figure 5.16. The first and third layers of the composite system are assumed to be made from steel alloy UNS G41300 whereas the second layer is made from aluminum alloy UNS A93550. It is also assumed that, uniform heat is generated only in the first layer, that is, $Q^1 \neq 0$, $Q^2 = 0$ and $Q^3 = 0$. The inner radius of the tube is $\overline{r}_0 = 0.4$; the radius of the first and second interfaces are, respectively, $\overline{r}_1 = 0.6$ and $\overline{r}_2 = 0.8$; and the outer radius is $\overline{r}_3 = 1.0$.

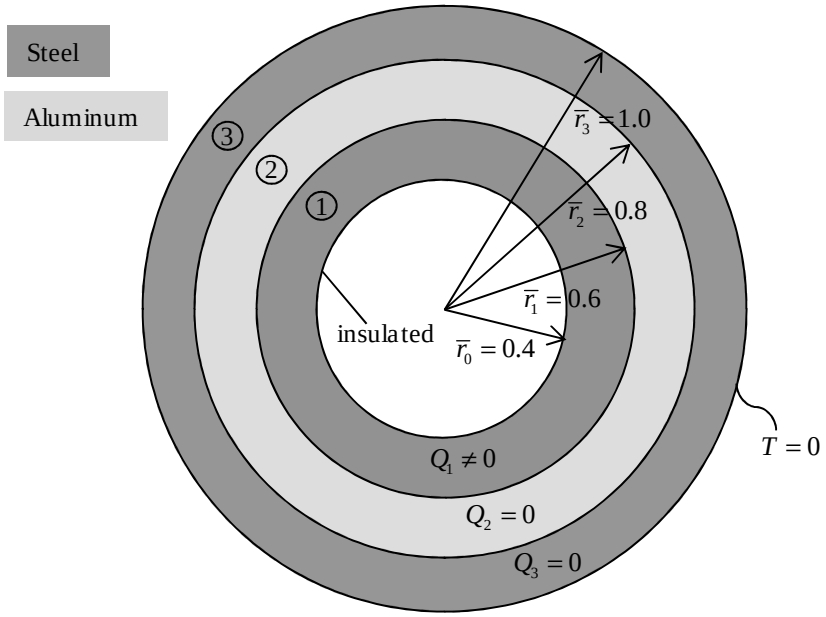

Figure 5.16: Three layered composite tube. First layer is made from UNS G41300, second layer is made from UNS A93550 and the third layer is made from UNS G41300. Uniform heat is generated in the first layer.

Figure 5.17 and 5.18 show the variation of temperature and its gradient at the elastic limit heat load $\left[\overline{Q}_{el}^1\right]_{CP} = 16.83533698$. The red, blue and green colors, respectively, are used to identify the results of first, second and third layers easily. The corresponding stress and radial displacement-strain variations are depicted in Figures 5.19 and 5.20, respectively. In the analytical solutions, the values of integration constants evaluated, respectively, for the thermal and mechanical problems are:

$C_1 = 309.8801899$, $C_2 = 621.9765001$, $C_3 = -99.52597100$, $C_4 = 64.22612895$, $C_5 = -387.3502373$, $C_6 = 0$, and, $\bar{D}_1 = 0.2912582110 \times 10^{-2}$, $\bar{D}_2 = 0.3040966526$, $\bar{D}_3 = 0.7141289669 \times 10^{-1}$, $\bar{D}_4 = 0.5460334489 \times 10^{-1}$, $\bar{D}_5 = 0.2487241314$, $\bar{D}_6 = 0.3422434349$. From Figure 5.19, it is seen that, the yielding starts at the first interface of the tube ($\Phi_Y^2(\bar{r}_1) = 1$) in the aluminum alloy. Tables 5.6 through 5.8 compare these results as in the previous example.

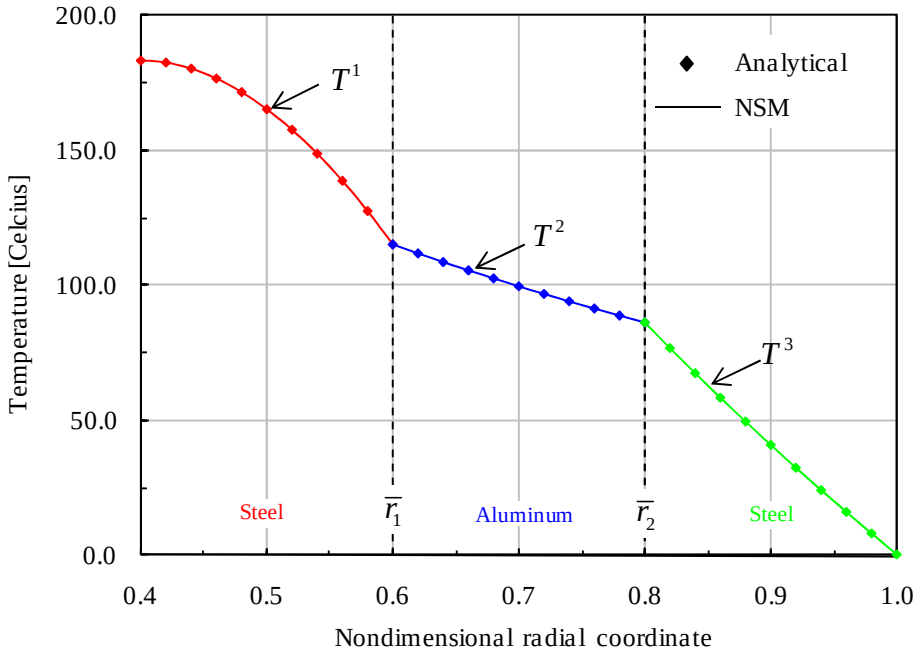

Figure 5.17: Variation of temperature with nondimensional radial coordinate in the three layered composite tube considered in Example 2.

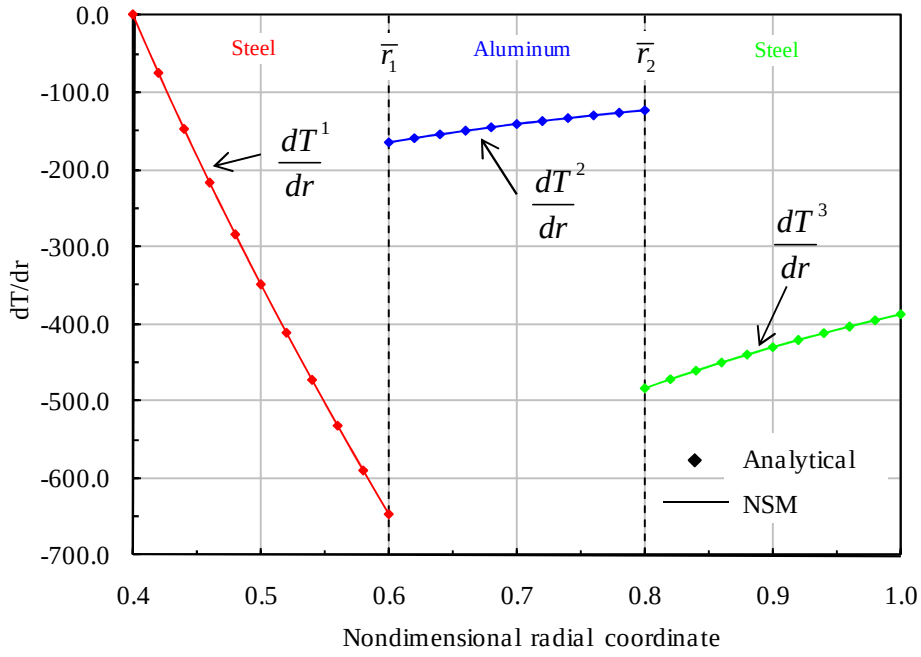

Figure 5.18: Variation of temperature gradient with nondimensional radial coordinate in the three layered composite tube considered in Example 2.

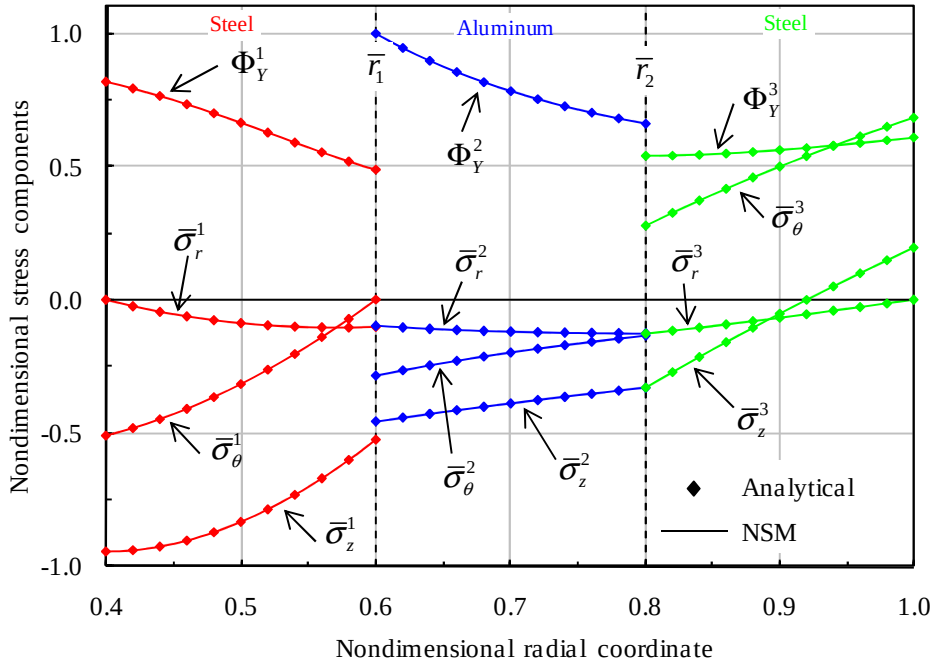

Figure 5.19: Variation of nondimensional stress components with nondimensional radial coordinate in the three layered composite tube considered in Example 2.

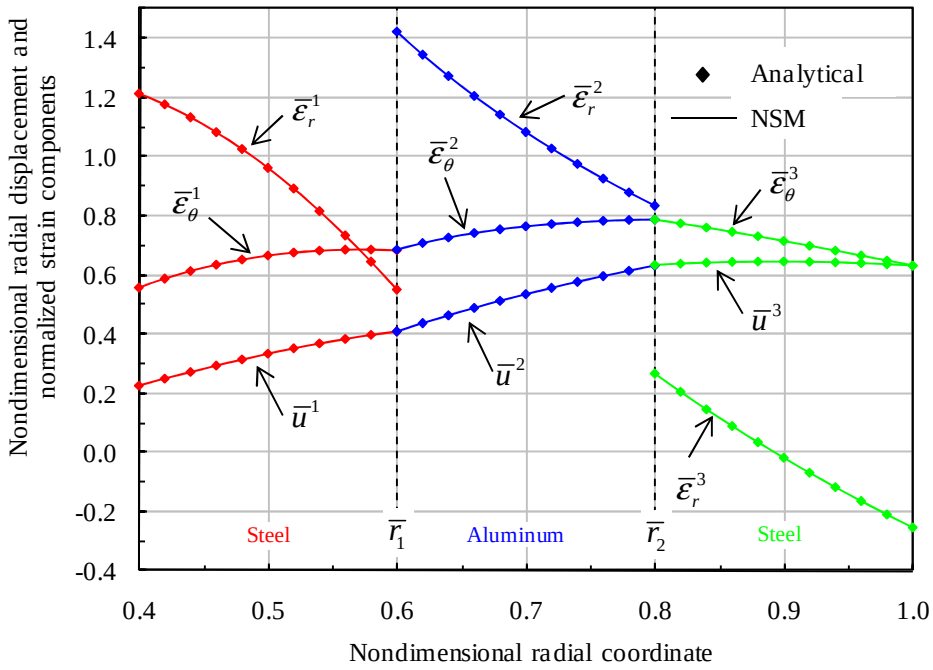

Figure 5.20: Variation of nondimensional radial displacement and normalized strain components with nondimensional radial coordinate in the three layered composite tube considered in Example 2.

Table 5.6: Comparison of the values of temperature and its gradient obtained from the analytical and numerical solutions of Example 2.

	Analytical	**Numerical**	**Analytical**	**Numerical**
r	Temperature [Celcius]		dT / dr	
0.4	1.830960591E+02	1.830960592E+02	0.000000000E+00	0.000000000E+00
0.5	1.650900218E+02	1.650900218E+02	-3.486152136E+02	-3.486152134E+02
0.6	1.150665452E+02	1.150665452E+02	-6.455837289E+02	-6.455837284E+02
0.6	1.150665452E+02	1.150665452E+02	-1.658766183E+02	-1.658766182E+02
0.7	9.972454907E+01	9.972454910E+01	-1.421799586E+02	-1.421799586E+02
0.8	8.643470756E+01	8.643470760E+01	-1.244074637E+02	-1.244074638E+02
0.8	8.643470756E+01	8.643470760E+01	-4.841877967E+02	-4.841877970E+02
0.9	4.081142075E+01	4.081142076E+01	-4.303891526E+02	-4.303891529E+02
1.0	0.000000000E+00	2.077686023E-09	-3.873502373E+02	-3.873502378E+02

Table 5.7: Comparison of the values of stress components obtained from the analytical and numerical solutions of Example 2.

	Analytical	Numerical	Analytical	Numerical	Analytical	Numerical	Analytical	Numerical
r	$\bar{\sigma}_r$		$\bar{\sigma}_\theta$		$\bar{\sigma}_z$		Φ	
0.4	0.000000000E+00	0.000000000E+00	-5.091813294E-01	-5.091813295E-01	-9.423328180E-01	-9.423328181E-01	8.169690870E-01	8.169690870E-01
0.5	-8.457856966E-02	-8.457856970E-02	-3.147178748E-01	-3.147178748E-01	-8.324479330E-01	-8.324479330E-01	6.634444579E-01	6.634444579E-01
0.6	-9.801611423E-02	-9.801611430E-02	3.996387306E-03	3.996387137E-03	-5.271712155E-01	-5.271712156E-01	4.882210942E-01	4.882210942E-01
0.6	-9.801611423E-02	-9.801611430E-02	-2.828234558E-01	-2.828234559E-01	-4.539145344E-01	-4.539145345E-01	1.000000000E+00	1.000000000E+00
0.7	-1.179753626E-01	-1.179753627E-01	-1.975256002E-01	-1.975256003E-01	-3.885759272E-01	-3.885759273E-01	7.813565573E-01	7.813565576E-01
0.8	-1.238338790E-01	-1.238338791E-01	-1.350682078E-01	-1.350682078E-01	-3.319770511E-01	-3.319770513E-01	6.576838475E-01	6.576838478E-01
0.8	-1.238338790E-01	-1.238338791E-01	2.808383429E-01	2.808383430E-01	-3.304828267E-01	-3.304828269E-01	5.385986294E-01	5.385986296E-01
0.9	-6.618659755E-02	-6.618659760E-02	5.016148772E-01	5.016148774E-01	-5.205901099E-02	-5.205901102E-02	5.608711429E-01	5.608711432E-01
1.0	0.000000000E+00	-1.775388061E-11	6.844868698E-01	6.844868702E-01	1.969995791E-01	1.969995792E-01	6.103175270E-01	6.103175274E-01

Table 5.8: Comparison of the values of radial displacement and strain components obtained from the analytical and numerical solutions of Example 2.

	Analytical	Numerical	Analytical	Numerical	Analytical	Numerical	Numerical
r	$\bar{u}$		$\bar{\varepsilon}_r$		$\bar{\varepsilon}_\theta$		$\bar{\varepsilon}_z$
0.4	2.231260726E-01	2.231260726E-01	1.213542065E+00	1.213542065E+00	5.578151814E-01	5.578151815E-01	0.000000000E+00
0.5	3.333679948E-01	3.333679948E-01	9.631108183E-01	9.631108183E-01	6.667359896E-01	6.667359896E-01	0.000000000E+00
0.6	4.104245658E-01	4.104245658E-01	5.526686090E-01	5.526686091E-01	6.840409431E-01	6.840409430E-01	0.000000000E+00
0.6	4.104245658E-01	4.104245658E-01	1.422921013E+00	1.422921014E+00	6.840409431E-01	6.840409430E-01	1.110223025E-16
0.7	5.346881487E-01	5.346881488E-01	1.081890809E+00	1.081890809E+00	7.638402125E-01	7.638402125E-01	0.000000000E+00
0.8	6.298105641E-01	6.298105643E-01	8.321792867E-01	8.321792870E-01	7.872632051E-01	7.872632054E-01	0.000000000E+00
0.8	6.298105641E-01	6.298105643E-01	2.661238004E-01	2.661238005E-01	7.872632051E-01	7.872632054E-01	0.000000000E+00
0.9	6.417222097E-01	6.417222100E-01	-1.819359386E-02	-1.819359388E-02	7.130246775E-01	7.130246778E-01	0.000000000E+00
1.0	6.277891654E-01	6.277891658E-01	-2.536972834E-01	-2.536972836E-01	6.277891654E-01	6.277891658E-01	-9.860799973E-18

5.2.3 Example 3: Three Layered Composite Cylinder Having Temperature Independent Physical Properties

Here, a three layered composite cylinder as shown in Figure 5.21 is considered. The first and second layers of the composite system are assumed to be made from steel alloy UNS G41300 whereas the third layer is made from aluminum alloy UNS A93550. In this problem, we assume that uniform heat is generated only in the second layer, that is, $Q^1 = 0$, $Q^2 \neq 0$ and $Q^3 = 0$. The radius of the first and second interfaces are, respectively, $\bar{r}_1 = 0.3$ and $\bar{r}_2 = 0.5$; and the outer radius is $\bar{r}_3 = 1.0$.

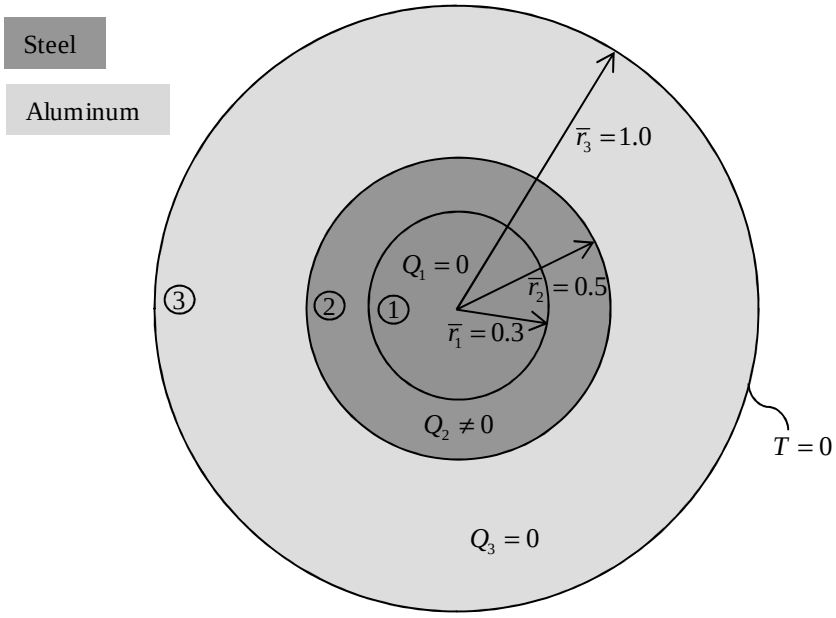

Figure 5.21: Three layered composite cylinder. First layer is made from UNS G41300, second layer is made from UNS G41300 and the third layer is made from UNS A93550. Uniform heat is generated in the second layer.

Figure 5.22 and 5.23 show the variation of temperature and its gradient at the elastic limit heat load $\left[\bar{Q}_{el}^2\right]_{CP} = 34.91449259$. The corresponding stress and radial displacement-strain variations are depicted in Figures 5.24 and 5.25, respectively. In the analytical solutions, the values of integration constants evaluated, respectively, for the thermal and mechanical problems are: $C_1 = 0$, $C_2 = 251.1226097$, $C_3 = 361.4933074$, $C_4 = 867.0973744$, $C_5 = -165.1240498$, $C_6 = 0$, and, $\bar{D}_1 = 0$, $\bar{D}_2 = 0.5507723292$, $\bar{D}_3 = -0.2481833229 \times 10^{-1}$, $\bar{D}_4 = 0.5507723292$,

$\bar{D}_5 = 0.4383325094\times10^{-1}$, $\bar{D}_6 = 0.1319746324$. From Figure 5.24, we observe that the first layer (steel alloy) starts to yield simultaneously as a whole ($\Phi_Y^1(\bar{r}^*)=1$ where $\bar{r}^*$ denotes values of $\bar{r}$ between 0 and $\bar{r}_1$) . As before, we compare the values of the results obtained from analytical and numerical solutions in Tables 5.9 through 5.11.

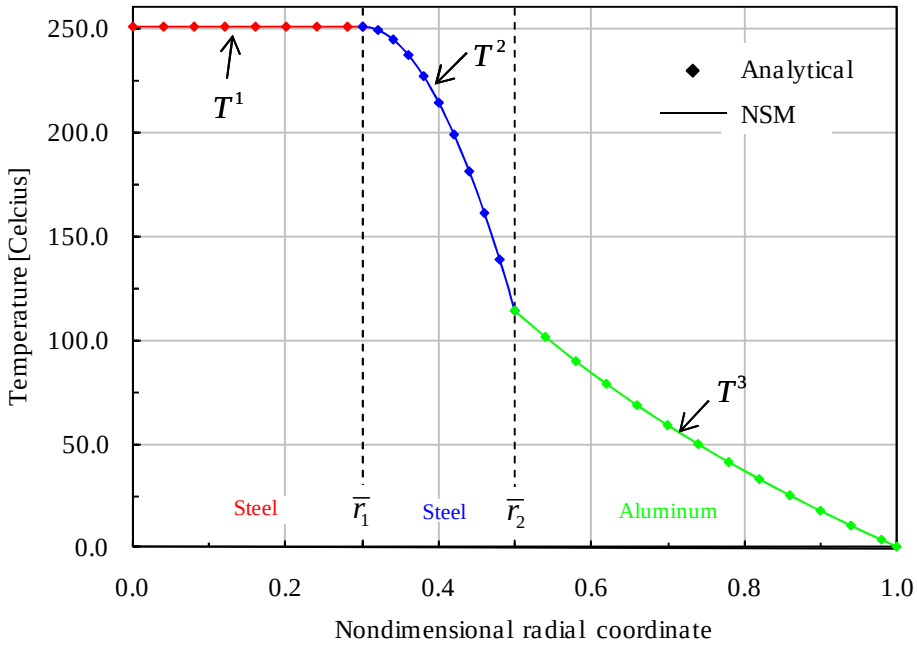

Figure 5.22: Variation of temperature with nondimensional radial coordinate in the three layered composite cylinder considered in Example 3.

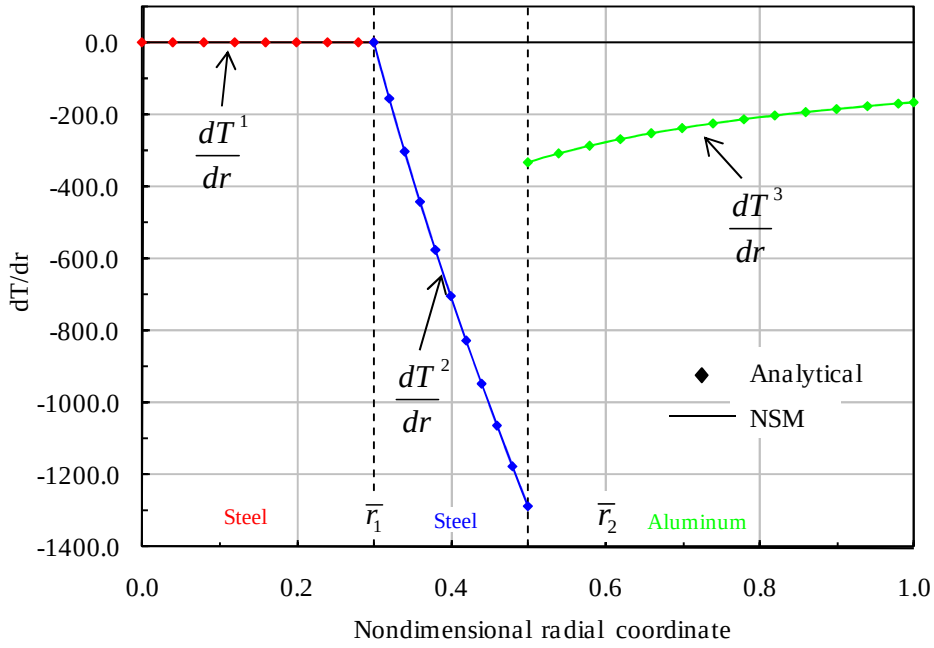

Figure 5.23: Variation of temperature gradient with nondimensional radial coordinate in the three layered composite cylinder considered in Example 3.

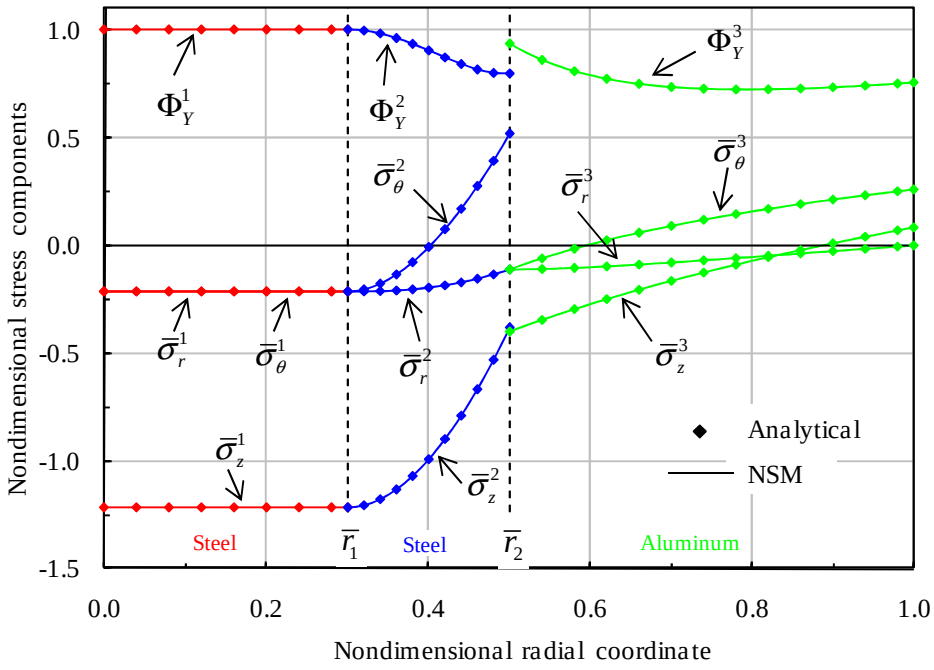

Figure 5.24: Variation of nondimensional stress components with nondimensional radial coordinate in the three layered composite cylinder considered in Example 3.

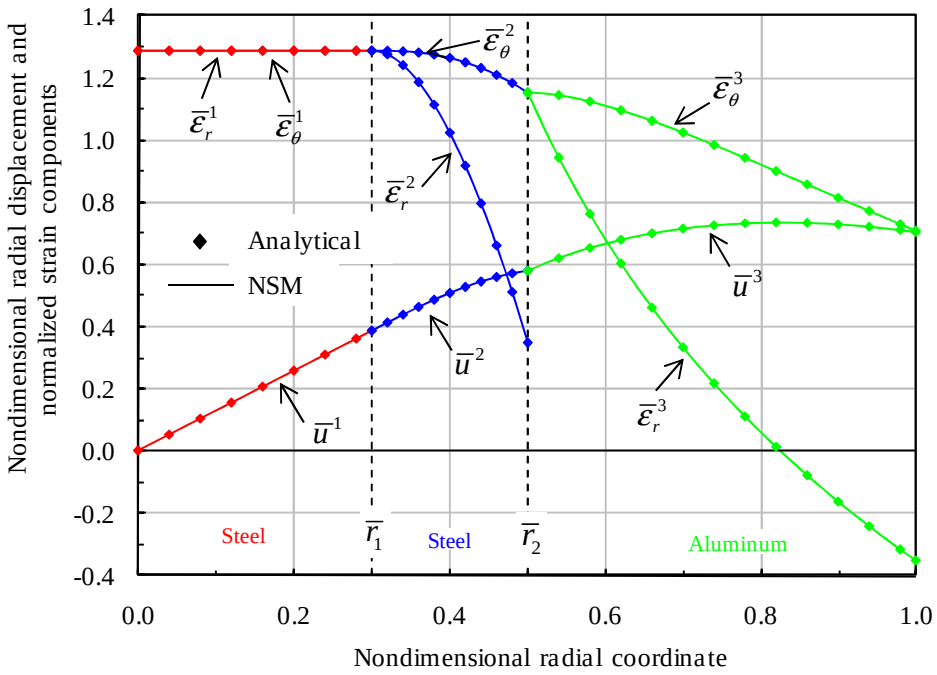

Figure 5.25: Variation of nondimensional radial displacement and normalized strain components with nondimensional radial coordinate in the three layered composite cylinder considered in Example 3.

Table 5.9: Comparison of the values of temperature and its gradient obtained from the analytical and numerical solutions of Example 3.

	Analytical	Numerical	Analytical	Numerical
r	Temperature [Celcius]		dT / dr	
0.0	2.511226097E+02	2.511226097E+02	0.000000000E+00	0.000000000E+00
0.1	2.511226097E+02	2.511226097E+02	0.000000000E+00	0.000000000E+00
0.2	2.511226097E+02	2.511226097E+02	0.000000000E+00	0.000000000E+00
0.3	2.511226097E+02	2.511226097E+02	0.000000000E+00	0.000000000E+00
0.3	2.511226097E+02	2.511226097E+02	0.000000000E+00	0.000000000E+00
0.4	2.145370229E+02	2.145370228E+02	-7.029036533E+02	-7.029036529E+02
0.5	1.144552695E+02	1.144552695E+02	-1.285309537E+03	-1.285309536E+03
0.5	1.144552695E+02	1.144552695E+02	-3.302480996E+02	-3.302480993E+02
0.6	8.434959573E+01	8.434959576E+01	-2.752067496E+02	-2.752067496E+02
0.7	5.889561120E+01	5.889561124E+01	-2.358914997E+02	-2.358914998E+02
0.8	3.684636688E+01	3.684636691E+01	-2.064050622E+02	-2.064050625E+02
0.9	1.739755503E+01	1.739755506E+01	-1.834711664E+02	-1.834711667E+02
1.0	0.000000000E+00	1.072881617E-09	-1.651240498E+02	-1.651240501E+02

Table 5.10: Comparison of the values of stress components obtained from the analytical and numerical solutions of Example 3.

	Analytical	Numerical	Analytical	Numerical	Analytical	Numerical	Analytical	Numerical
r	$\bar{\sigma}_r$		$\bar{\sigma}_\theta$		$\bar{\sigma}_z$		Φ	
0.0	-2.154867468E-01	-2.154867467E-01	-2.154867468E-01	-2.154867467E-01	-1.215486747E+00	-1.215486747E+00	1.000000000E+00	1.000000000E+00
0.1	-2.154867468E-01	-2.154867467E-01	-2.154867468E-01	-2.154867467E-01	-1.215486747E+00	-1.215486747E+00	1.000000000E+00	1.000000000E+00
0.2	-2.154867468E-01	-2.154867467E-01	-2.154867468E-01	-2.154867467E-01	-1.215486747E+00	-1.215486747E+00	1.000000000E+00	1.000000000E+00
0.3	-2.154867468E-01	-2.154867467E-01	-2.154867468E-01	-2.154867467E-01	-1.215486747E+00	-1.215486747E+00	1.000000000E+00	1.000000000E+00
0.3	-2.154867468E-01	-2.154867467E-01	-2.154867468E-01	-2.154867467E-01	-1.215486747E+00	-1.215486747E+00	1.000000000E+00	1.000000000E+00
0.4	-1.976866285E-01	-1.976866284E-01	-1.001714049E-02	-1.001714051E-02	-9.922170224E-01	-9.922170223E-01	9.031099024E-01	9.031099023E-01
0.5	-1.122217245E-01	-1.122217245E-01	5.152837637E-01	5.152837632E-01	-3.814512143E-01	-3.814512144E-01	7.969884806E-01	7.969884802E-01
0.5	-1.122217245E-01	-1.122217245E-01	-1.112719653E-01	-1.112719655E-01	-4.001136677E-01	-4.001136677E-01	9.353688071E-01	9.353688070E-01
0.6	-1.016885639E-01	-1.016885639E-01	6.409142021E-03	6.409141860E-03	-2.718993997E-01	-2.718993999E-01	7.882586283E-01	7.882586283E-01
0.7	-7.979017066E-02	-7.979017068E-02	9.291436773E-02	9.291436766E-02	-1.634957808E-01	-1.634957809E-01	7.346008636E-01	7.346008638E-01
0.8	-5.380458723E-02	-5.380458725E-02	1.608322703E-01	1.608322703E-01	-6.959229476E-02	-6.959229488E-02	7.231759457E-01	7.231759459E-01
0.9	-2.676454482E-02	-2.676454482E-02	2.166209727E-01	2.166209727E-01	1.323645001E-02	1.323644997E-02	7.332468613E-01	7.332468616E-01
1.0	0.000000000E+00	2.785907789E-11	2.639492648E-01	2.639492650E-01	8.732928700E-02	8.732928706E-02	7.554681364E-01	7.554681367E-01

Table 5.11: Comparison of the values of radial displacement and strain components obtained from the analytical and numerical solutions of Example 3.

	Analytical	Numerical	Analytical	Numerical	Analytical	Numerical	Numerical
r	$\bar{u}$		$\bar{\varepsilon}_r$		$\bar{\varepsilon}_\theta$		$\bar{\varepsilon}_z$
0.0	0.000000000E+00	0.000000000E+00	1.287806221E+00	1.287806221E+00	1.287806221E+00	1.287806221E+00	0.000000000E+00
0.1	1.287806221E-01	1.287806221E-01	1.287806221E+00	1.287806221E+00	1.287806221E+00	1.287806221E+00	0.000000000E+00
0.2	2.575612442E-01	2.575612442E-01	1.287806221E+00	1.287806221E+00	1.287806221E+00	1.287806221E+00	0.000000000E+00
0.3	3.863418663E-01	3.863418663E-01	1.287806221E+00	1.287806221E+00	1.287806221E+00	1.287806221E+00	0.000000000E+00
0.3	3.863418663E-01	3.863418663E-01	1.287806221E+00	1.287806221E+00	1.287806221E+00	1.287806221E+00	0.000000000E+00
0.4	5.059532472E-01	5.059532471E-01	1.023201184E+00	1.023201184E+00	1.264883118E+00	1.264883118E+00	0.000000000E+00
0.5	5.774104414E-01	5.774104412E-01	3.467154117E-01	3.467154119E-01	1.154820883E+00	1.154820882E+00	0.000000000E+00
0.5	5.774104414E-01	5.774104412E-01	1.151023641E+00	1.151023641E+00	1.154820883E+00	1.154820882E+00	0.000000000E+00
0.6	6.676248892E-01	6.676248892E-01	6.805216355E-01	6.805216361E-01	1.112708149E+00	1.112708149E+00	1.110223025E-16
0.7	7.176091754E-01	7.176091756E-01	3.346642323E-01	3.346642328E-01	1.025155965E+00	1.025155965E+00	0.000000000E+00
0.8	7.370101962E-01	7.370101966E-01	6.312099052E-02	6.312099090E-02	9.212627453E-01	9.212627457E-01	0.000000000E+00
0.9	7.318383145E-01	7.318383149E-01	-1.599283753E-01	-1.599283751E-01	8.131536828E-01	8.131536833E-01	0.000000000E+00
1.0	7.061460900E-01	7.061460903E-01	-3.491520909E-01	-3.491520910E-01	7.061460900E-01	7.061460903E-01	-2.493824638E-18

In the above benchmark examples, we observe that, the results of the analytical solutions and those obtained from NSM are in perfect agreement for both temperature and mechanical problems. In fact, for all quantities, analytical and numerical solutions agree up to 6 significant digits, which show the accuracy of NSM. This can also be identified from Tables 5.3 through 5.11. Finally, the last column in Tables 5.5, 5.8 and 5.11 give the values of axial strain $\bar{\varepsilon}_z$ obtained from the numerical solution. As we know, for our problem (plane strain problem) these values must be equal to zero. The axial strain values in these tables show also the accuracy and validity of our computations.

In the next three problems, the examples presented as benchmark problems are reconsidered. But for these problems, we obtain the solutions by assuming that the physical properties of the materials change with temperature according to the polynomials given in the beginning of this chapter.

5.2.4 Example 4: Two Layered Composite Cylinder Having Temperature Dependent Physical Properties

The definition of the problem is the same as in Example 1. On the other hand, the VP composite cylinder is considered here. The elastic limit heat load is calculated as $\left[\bar{Q}_{el}^{1}\right]_{VP} = 52.915900$. Figures 5.26 and 5.27 show the variations of temperature and its gradient obtained for $\left[\bar{Q}_{el}^{1}\right]_{VP}$ in which these results are denoted by solid lines. For comparison, these figures also contain the results of the CP composite system obtained for $\left[\bar{Q}_{el}^{1}\right]_{VP}$ and these results are denoted by dashed lines with diamonds. Again different colors are used to identity the results that belong to different layers. The corresponding stress and radial displacement-strain variations obtained for $\left[\bar{Q}_{el}^{1}\right]_{VP}$ are depicted in Figures 5.28 and 5.29, respectively. From Figure 5.28, it is seen that, the yielding starts at the axis of the cylinder ($\left[\Phi_{Y}^{1}(0)\right]_{VP} = 1$) in the steel alloy for VP system as in CP system. The elastic limit heat load of VP composite cylinder is about 17% lower than the problem considered in Example 1 ($\left[\bar{Q}_{el}^{1}\right]_{VP} < \left[\bar{Q}_{el}^{1}\right]_{CP}$).

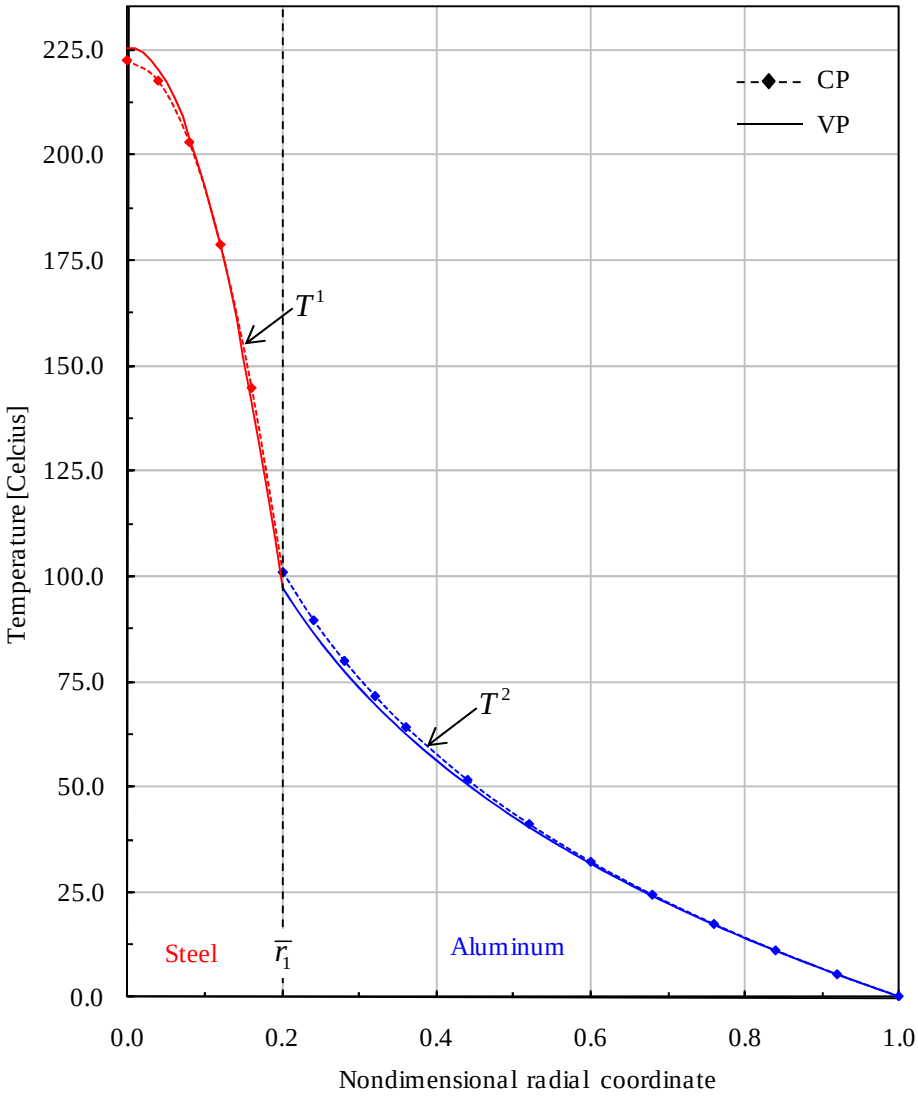

Figure 5.26: Variation of temperature with nondimensional radial coordinate in the two layered composite cylinder considered in Example 4.

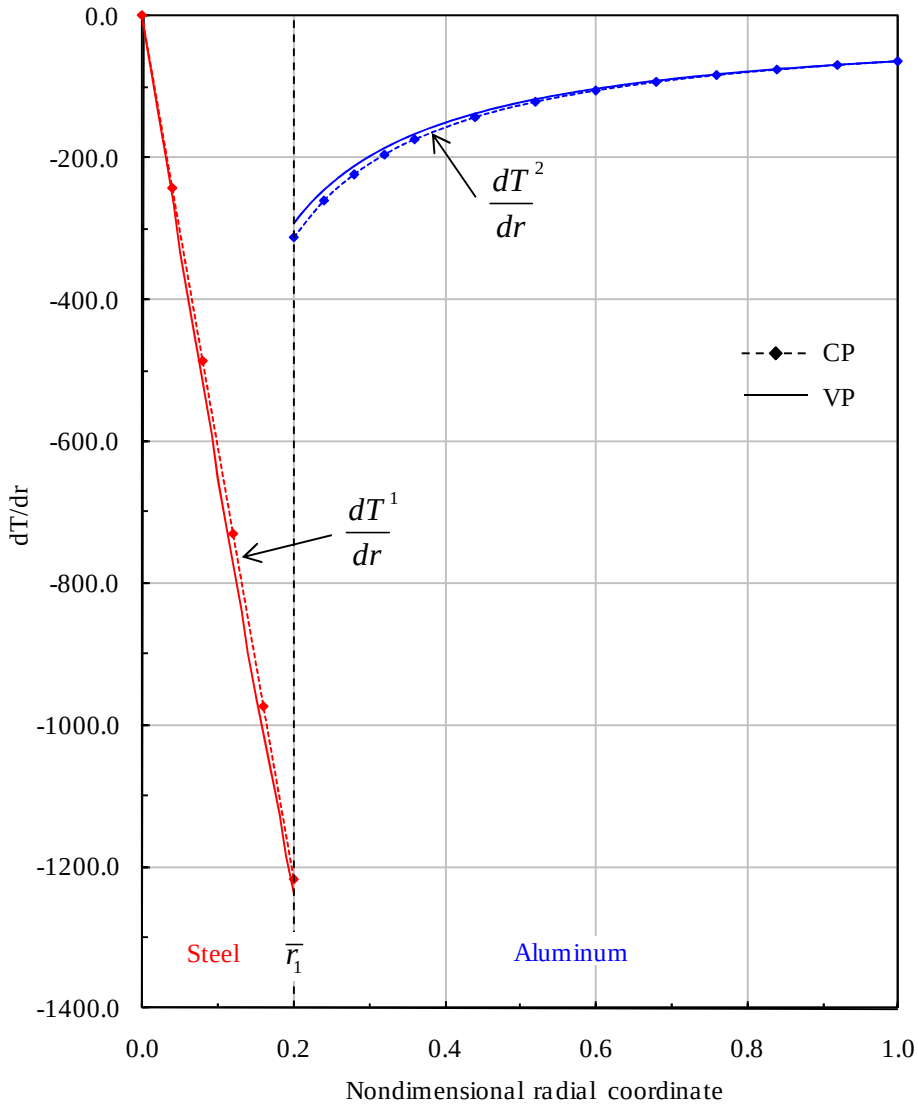

Figure 5.27: Variation of temperature gradient with nondimensional radial coordinate in the two layered composite cylinder considered in Example 4.

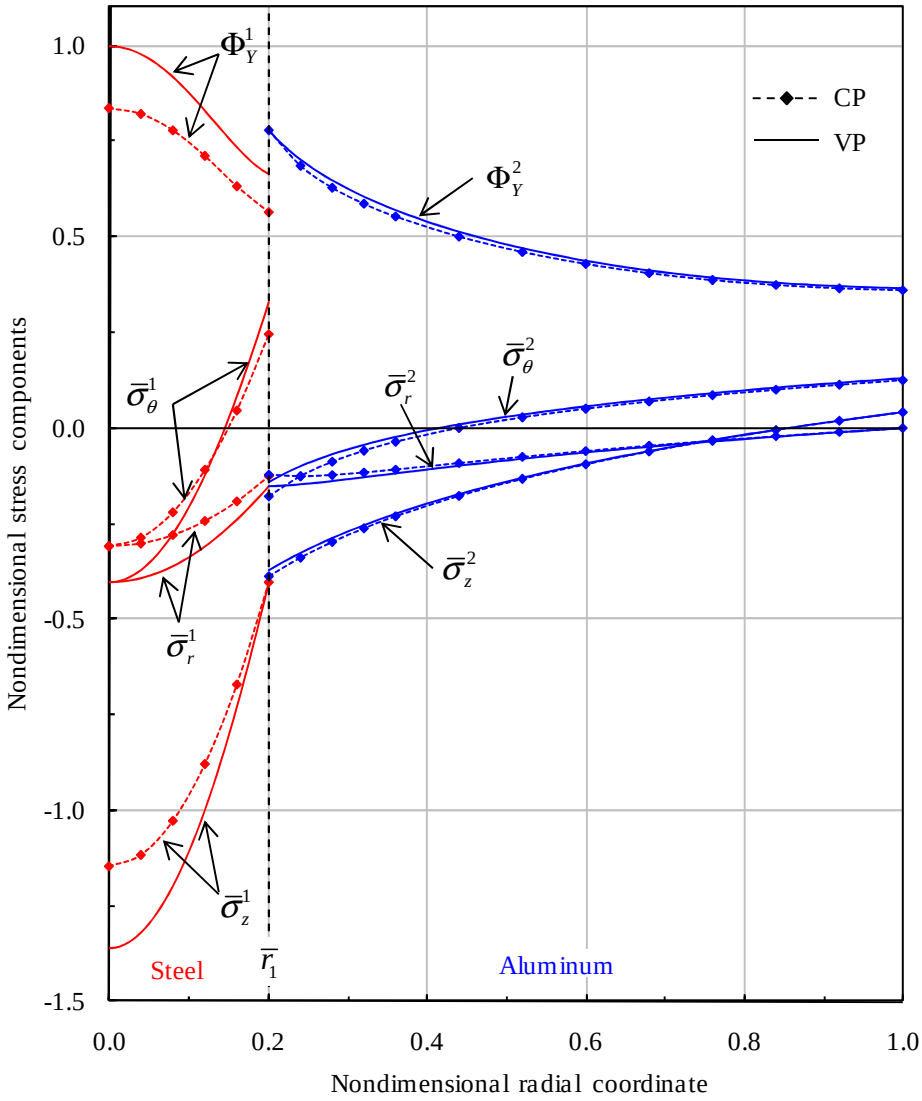

Figure 5.28: Variation of nondimensional stress components with nondimensional radial coordinate in the two layered composite cylinder considered in Example 4.

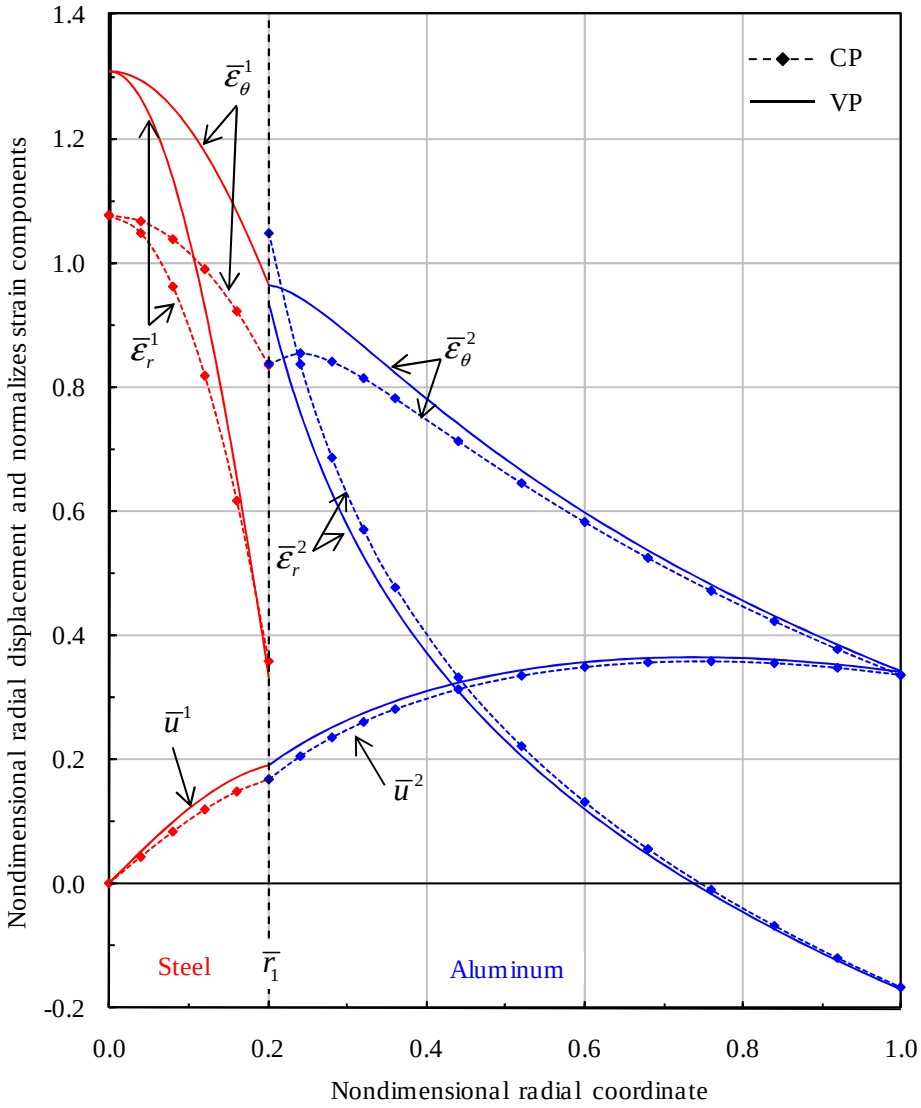

Figure 5.29: Variation of nondimensional radial displacement and normalized strain components with nondimensional radial coordinate in the two layered composite cylinder considered in Example 4.

5.2.5 Example 5: Three layered composite tube having temperature dependent properties

The definition of the problem is the same as in Example 2. The elastic limit heat load is calculated as $\left[\bar{Q}_{el}^{1}\right]_{VP} = 16.6089190$. In that problem, we observe that there is not much difference between the elastic limit heat loads of this problem and the one considered in Example 2. The temperature and its gradient obtained for $\left[\bar{Q}_{el}^{1}\right]_{VP}$ are depicted in Figures 5.30 and 5.31 whereas the corresponding stresses and radial displacement-strains are shown in Figures 5.32 and 5.33, respectively. As before, these figures also contain the results of the CP composite system obtained for $\left[\bar{Q}_{el}^{1}\right]_{VP}$. From Figure 5.32, it is seen that, the yielding starts at the first interface of the tube ($\left[\Phi_{Y}^{2}(\bar{r}_1)\right]_{VP} = 1$) in the aluminum alloy for the VP system as in CP system.

5.2.6 Example 6: Three layered composite cylinder having temperature dependent properties

The definition of the problem is the same as in Example 3. The elastic limit heat load is calculated as $\left[\bar{Q}_{el}^{1}\right]_{VP} = 29.2917849$. The elastic limit heat load of VP composite cylinder is about 16% lower than the problem considered in Example 3 ($\left[\bar{Q}_{el}^{1}\right]_{VP} < \left[\bar{Q}_{el}^{1}\right]_{CP}$). The temperature and its gradient obtained for $\left[\bar{Q}_{el}^{1}\right]_{VP}$ are depicted in Figures 5.34 and 5.35 whereas the corresponding stresses and radial displacement-strains are shown in Figures 5.36 and 5.37, respectively. Again, these figures also contain the results of the CP composite system obtained for $\left[\bar{Q}_{el}^{1}\right]_{VP}$. As in Example 3, we observe that the first layer (steel alloy) starts to yield simultaneously as a whole ($\left[\Phi_{Y}^{1}(\bar{r}^{*})\right]_{VP} = 1$ where $\bar{r}^{*}$ denotes values of $\bar{r}$ between 0 and $\bar{r}_1$)

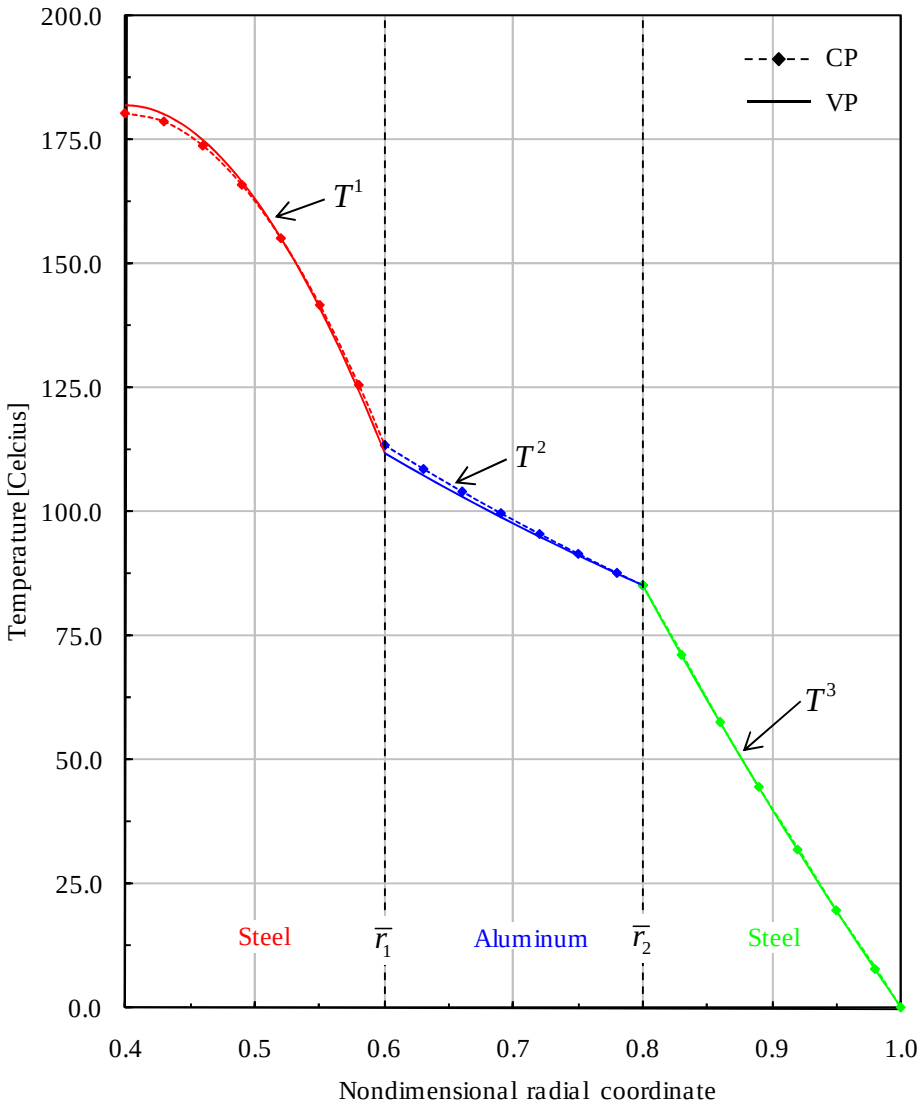

Figure 5.30: Variation of temperature with nondimensional radial coordinate in the three layered composite tube considered in Example 5.

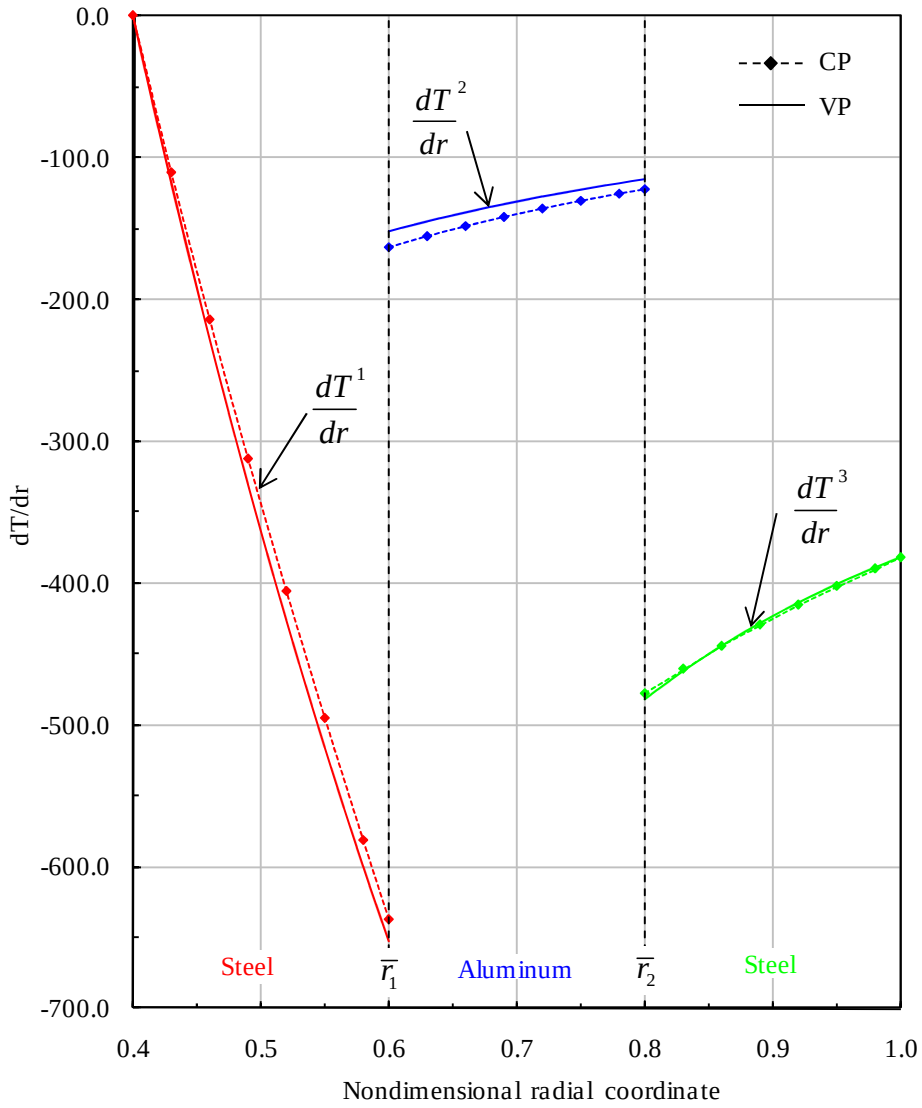

Figure 5.31: Variation of temperature gradient with nondimensional radial coordinate in the three layered composite tube considered in Example 5.

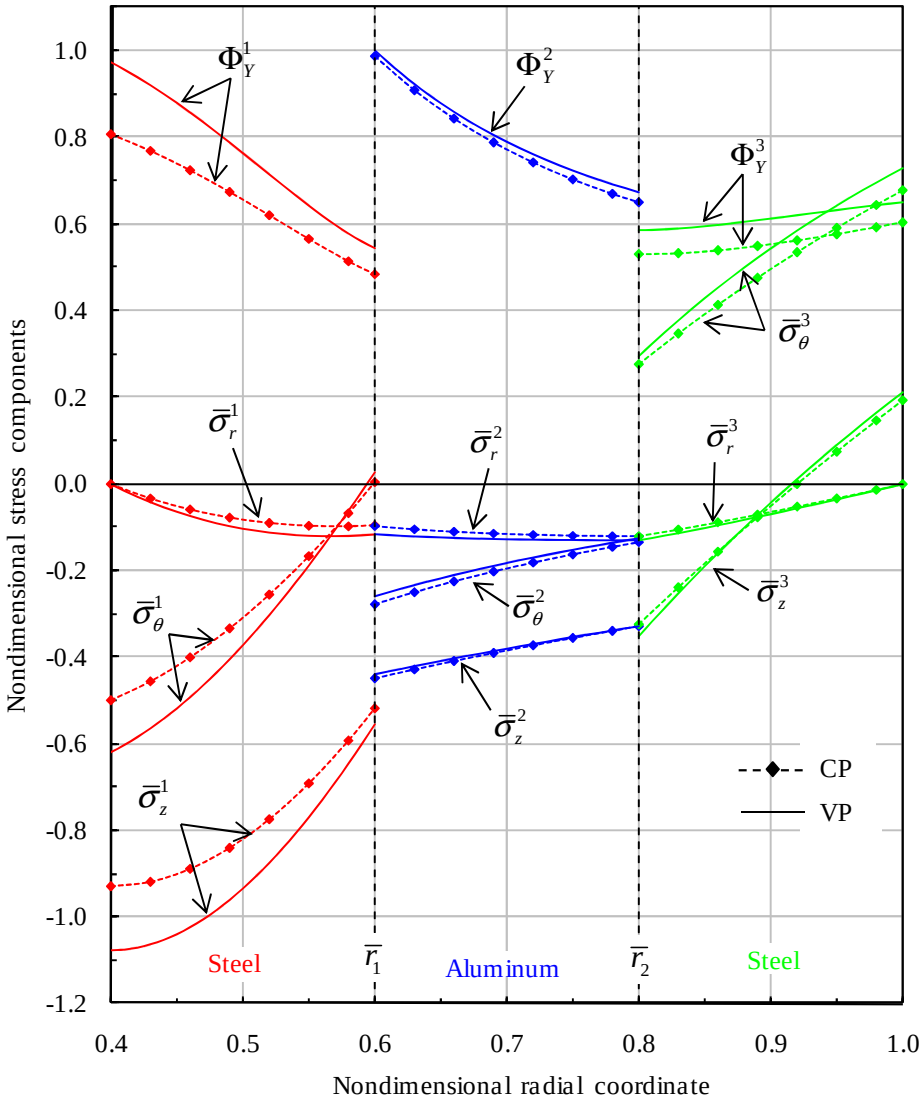

Figure 5.32: Variation of nondimensional stress components with nondimensional radial coordinate in the three layered composite tube considered in Example 5.

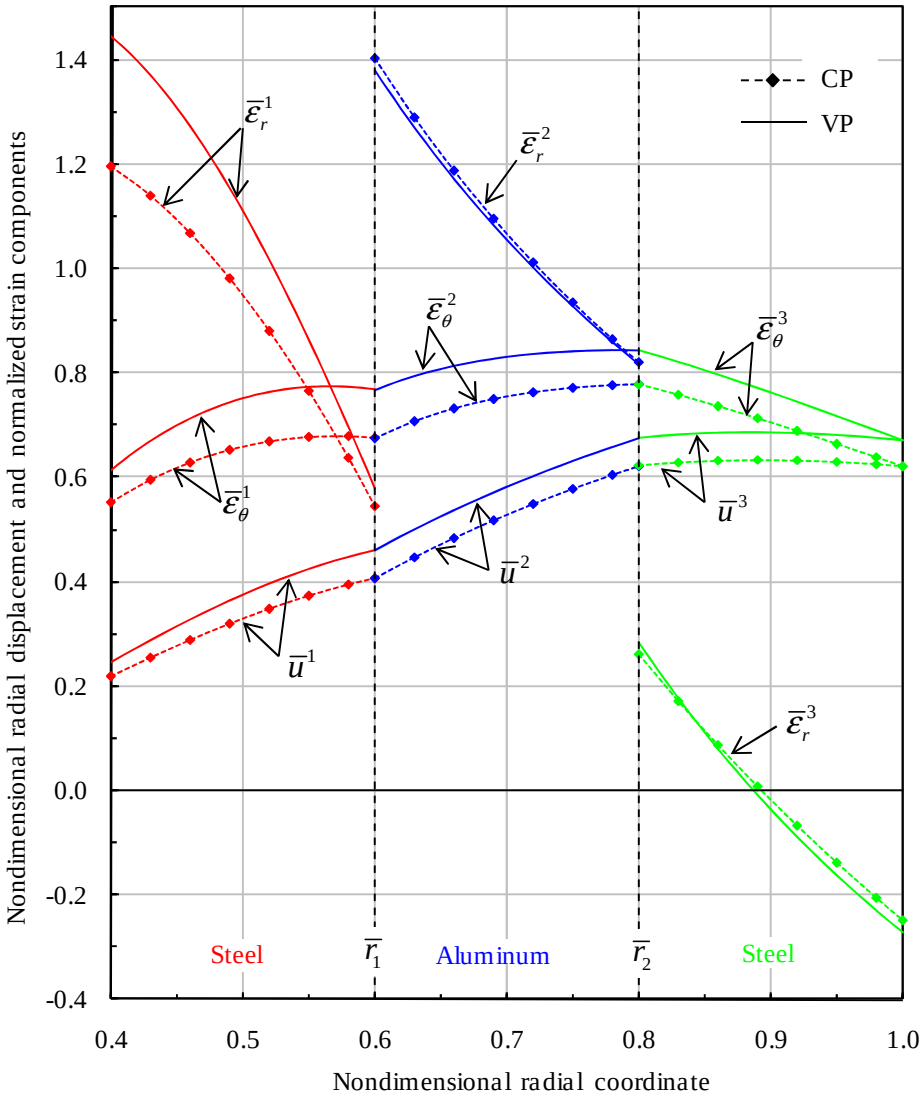

Figure 5.33: Variation of nondimensional radial displacement and normalized strain components with nondimensional radial coordinate in the three layered composite tube considered in Example 5.

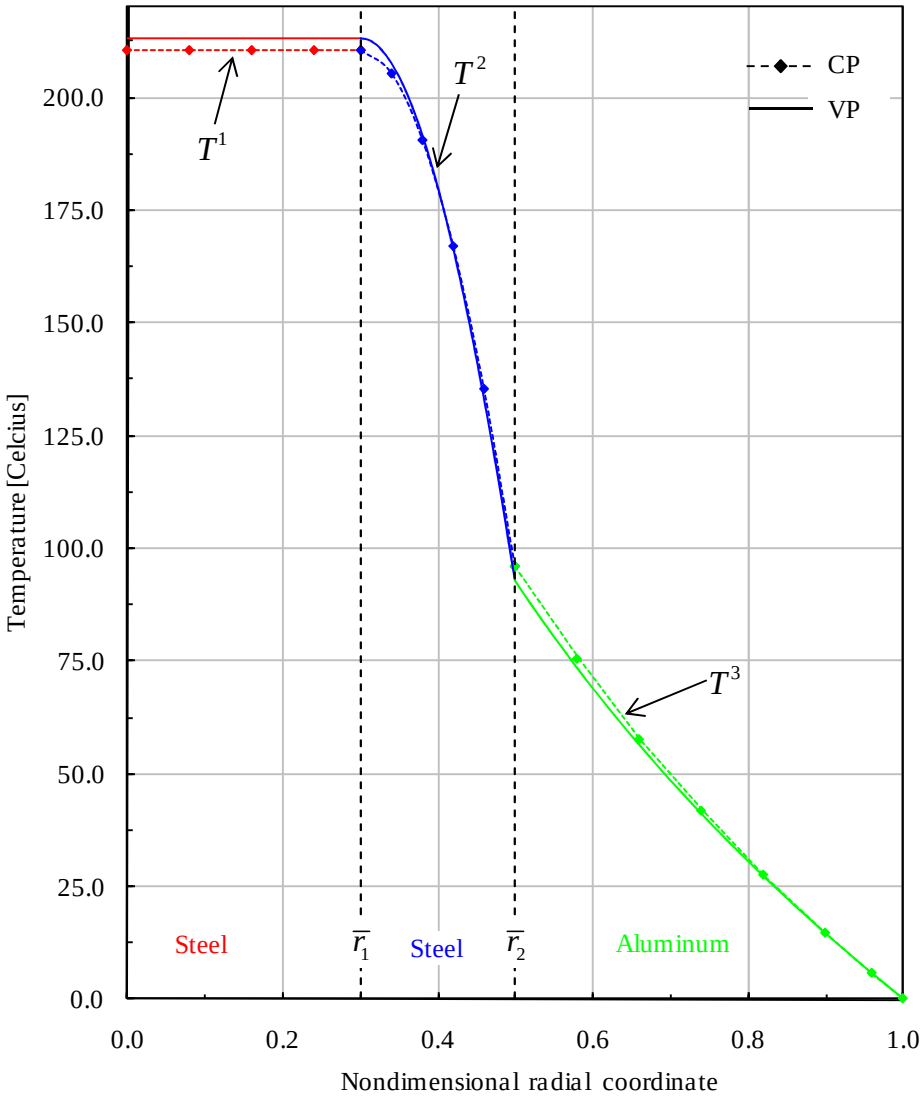

Figure 5.34: Variation of temperature with nondimensional radial coordinate in the three layered composite cylinder considered in Example 6.

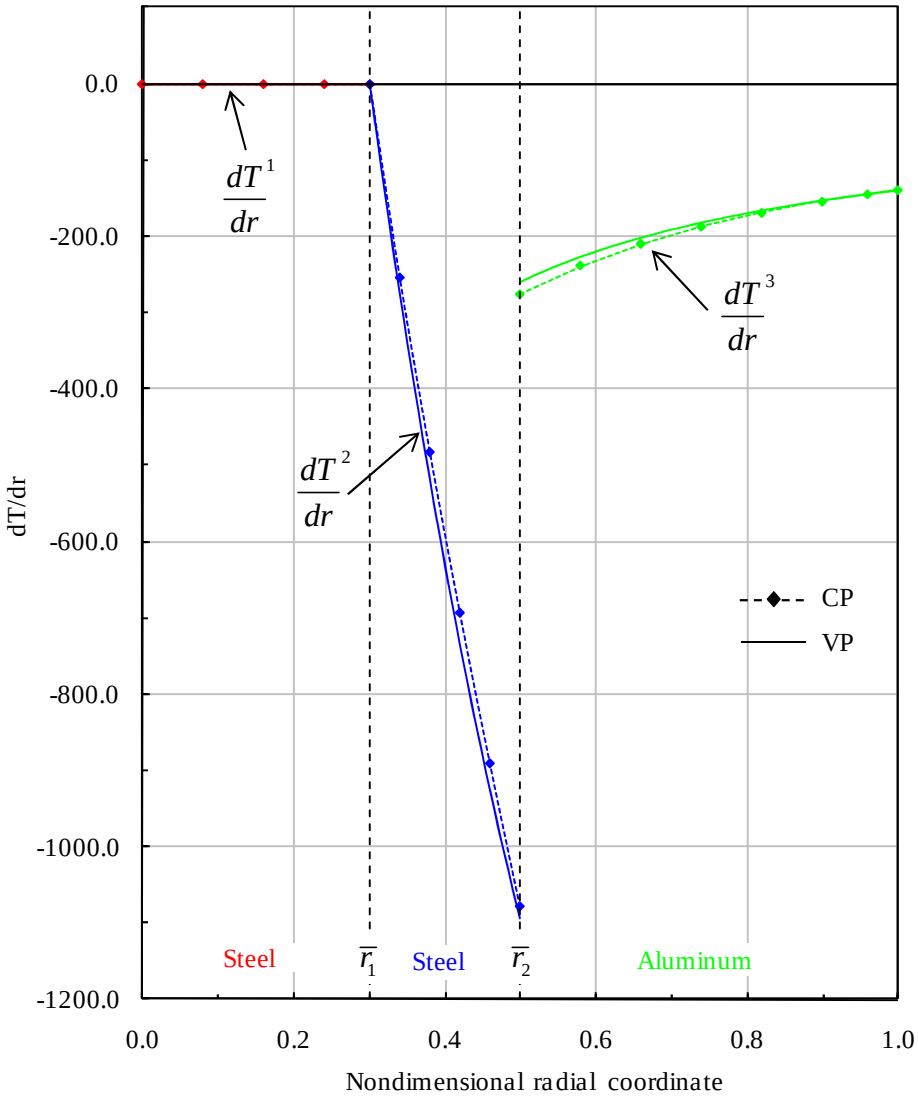

Figure 5.35: Variation of temperature gradient with nondimensional radial coordinate in the three layered composite cylinder considered in Example 6.

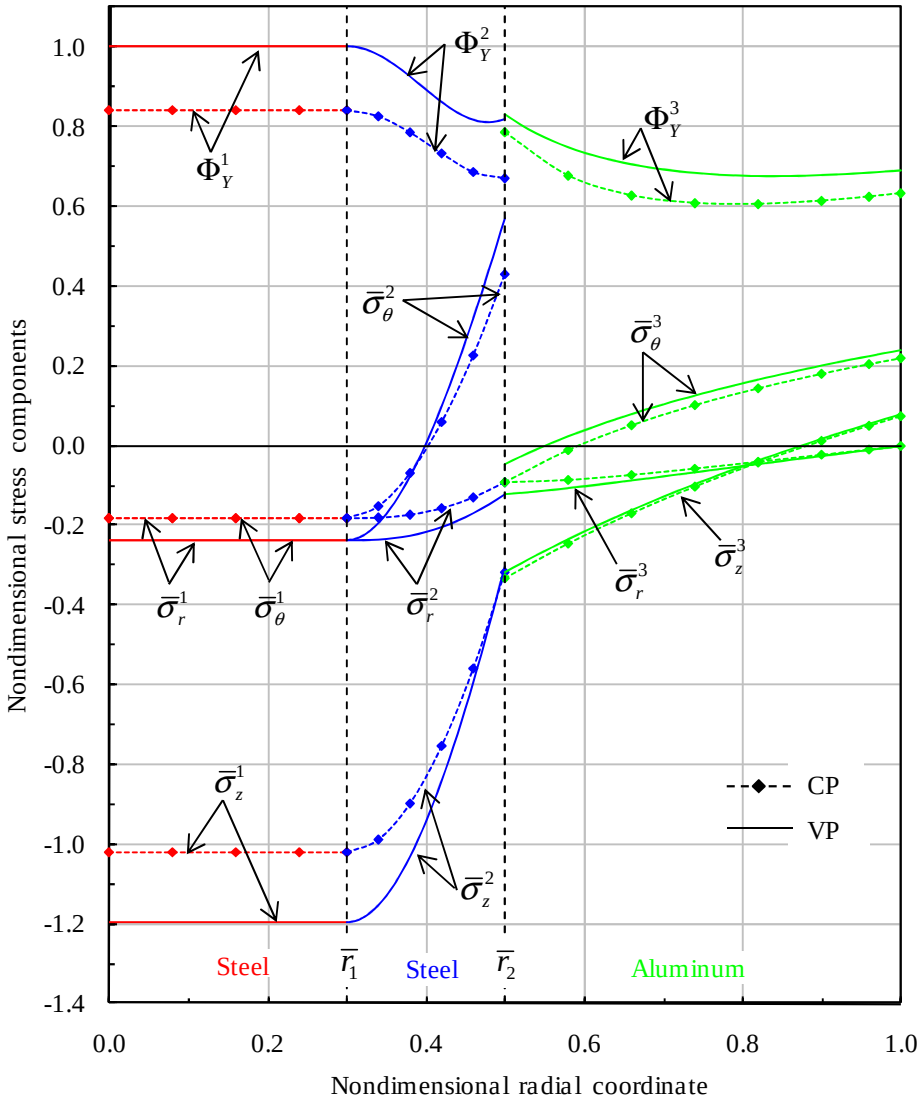

Figure 5.36: Variation of nondimensional stress components with nondimensional radial coordinate in the three layered composite cylinder considered in Example 6.

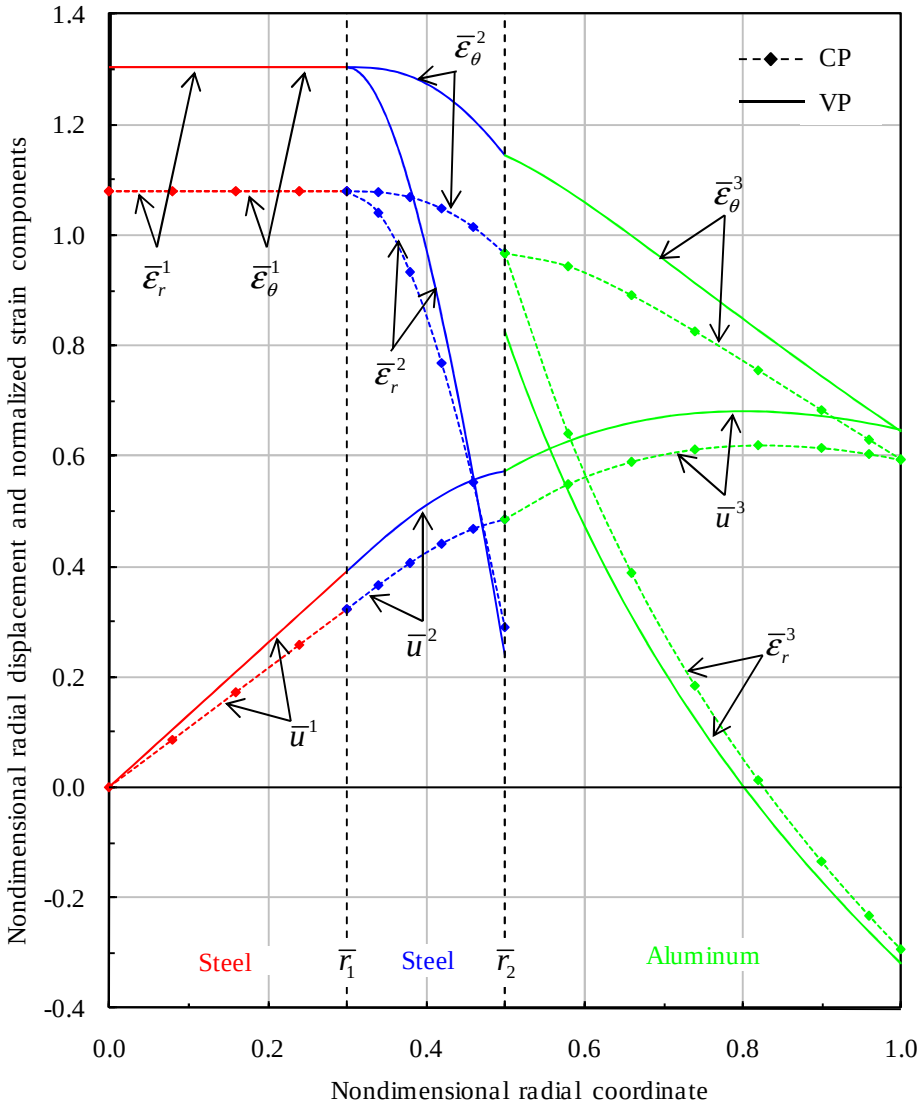

Figure 5.37: Variation of nondimensional radial displacement and normalized strain components with nondimensional radial coordinate in the three layered composite cylinder considered in Example 6.

Common observations that can be made from the results of Examples 4, 5 and 6 are as follows:

1) Comparing the variations of temperature and its gradient for VP and CP solutions, it is seen that they are very close to each other. This can be seen from Figures 5.26, 5.27 and 5.30, 5.31 and 5.34, 5.35. The only property that effects the temperature problem is the thermal conductivity. The values of thermal conductivities for both type of materials change about 10% with respect to the value at 0 degree Celcius within the temperature range for the selected problems (see Figures 5.2 and 5.7). For the selected example problems, it seems that, the variation of thermal conductivities do not effect the distrubution of thermal variables significantly.
2) Comparing the variations of stresses and strains for VP and CP solutions, we observe that, in the regions where there are high values temperature some of the stress and strain components differ significantly. This behaviour is observed even in Example 5 where the elastic limit heat loads for CP and VP systems are very close to each other.

CHAPTER 6

CONCLUSIONS

In this study, a computational method is developed for the thermoelastic analysis of internally heat generating infinitely long multi-layered composite cylinders and tubes with fixed ends. In the formulation the following assumptions are made: Deformations are small. The physical properties of the materials that form the layers of the composite assembly are varying with temperature. The layers of the composite assembly are perfectly bonded with each other. Each layer is made from an isotropic linear elastic material. The thermal problem is steady state. The thermal and mechanical problems are uncoupled.

The proposed computational method is based on nonlinear shooting algorithm. In order to apply this algorithm, the boundary value problem that defines our problem is converted to system of initial value problems. For an n layered composite assembly, we have n number of system of initial value problems. These initial value problems are solved consecutively starting from the one corresponding to the first layer up to the one corresponding to the final layer. The solution of each system of initial value problem provides the initial conditions of the next one. On the other hand, one of the initial conditions of the system of initial value problem that corresponds to the first layer is unknown both for thermal and mechanical problems. Therefore, we use nonlinear shooting algorithm which is based on Newton's iterations and try to satisfy the outer boundary conditions. The solutions of initial value problems are obtained by using the state of art program LSODE. Since thermal and mechanical problems are uncoupled, the method is first used to determine the solution of thermal problem. Next, using of the solutions obtained from thermal problem, the mechanical problem is solved again via the nonlinear shooting algorithm.

In the sample problems two different material properties are used. These are: Steel alloy UNS G41300 and aluminum alloy UNS A93550. In the first three problems (benchmark problems) that are covered in Chapter 5, we have verified our computational method. For these problems, we consider temperature independent physical properties. The closed form solutions of benchmark problems are obtained with the use MATHEMATICA 7.0, and these solutions are compared with those obtained from our computational method. From these comparisons, it is observed that, our computational method gives very accurate results. In fact, the results of analytical and numerical solutions agree at least six significant digits both for thermal and mechanical problems in the distributions of all the field variables. In the following three problems in Chapter 5, we reconsider the first three problems. But this time, the solutions are obtained by taking into account of temperature dependency of physical properties. The distributions of the stress, strain components and radial displacement for the composite assemblies having temperature dependent and independent physical properties are also compared. In all the example problems, the analyses are carried out up to elastic limit heat loads, that is, until the yielding commences. As expected, the elastic limit heat loads for temperature dependent solutions are determined lower than with those obtained from temperature independent solutions. In the examples two different material properties are used.

The results of the last three problems show that, for thermal problem, temperature dependent and independent solutions give nearly the same distributions for thermal variables. On the other hand, when the distributions of stress, strain and radial distributions are examined, at the regions having high temperature values a significant difference between the values these field variables exist. This shows, the importance of taking into account of temperature dependency of physical properties in the thermoelastic analysis.

REFERENCES

[1] B. A. Boley, J.Fr. Weiner, *Theory of Thermal Stresses*, NewYork, Wiley, 1960.

[2] W. Nowacki, *Thermoelasticity*, London, Addison-Wesley, 1962.

[3] S. Timoshenko, J.N. Goodier, *Theory of Elasticity*, 3rd ed., NewYork, McGraw-Hill, 1970.

[4] N. Noda, R.B, Hetnarski, Y. Tanigawa, Thermal Stresses, 2nd ed., NewYork, 2003,

[5] U. Güven, O. Altay, Linear Hardening Solid Disk with Rigid Casing Subjected to a Uniform Heat Source, *Mechanics Research Communications*, vol. 25, pp. 679–684, 1998.

[6] U. Güven, O. Altay, Elastic–Plastic Solid Disk with Nonuniform Heat Source Subjected to External Pressure, *International Journal of Mechanical Sciences*, vol. 42, pp. 831–842, 2000.

[7] Y. Orcan, Thermal Stresses in a Heat Generating Elastic-Plastic Cylinder with Free Ends, *International Journal of Engineering Science*, vol. 32, pp. 883–898, 1994.

[8] Y. Orcan, Residual Stresses and Secondary Plastic Flow in a Heat Generating Elastic-Plastic Cylinder with Free Ends, *International Journal of Engineering Science*, vol. 33, pp. 1689–1698, 1995.

[9] M. Gulgec, Y. Orcan, Elastic–Plastic Deformation of a Heat Generating Tube with Temperature-Dependent Yield Stress, *International Journal of Engineering Science* vol. 38, pp. 89–106, 2000.

[10] Y. Orcan, M. Gulgec, Influence of the Temperature Dependence of the Yield Stress on the Stress Distribution in a Heat-Generating Tube with Free Ends, *Journal of Thermal Stresses*, vol. 23, pp. 529–547, 2000.

[11] Y. Orcan, M. Gulgec, Elastic–Plastic Deformation of a Tube with Free Ends Subjected to Internal Heat Generation, *Turkish Journal of Engineering and Environmental Science* vol. 25, pp. 1–10, 2001.

[12] Y. Orcan, A. N. Eraslan, Thermal Stresses in Elastic–plastic Tubes with Temperature Dependent Mechanical and Thermal Properties, *Journal of Thermal Stresses* vol. 24, pp. 1097–1113, 2001.

[13] A.N. Eraslan, Y. Orcan, Computation of Transient Thermal Stresses in Elastic–Plastic Tubes: Effect of Coupling and Temperature Dependent Physical Properties, *Journal of Thermal Stresses* vol. 25, pp. 559–572, 2002.

[14] A.N. Eraslan, Y. Orcan, Thermoplastic Response of a Linearly Hardening Cylinder Subjected to Nonuniform Heat Source and Convective Boundary Condition, *Mechanics Based Design of Structures and Machines*, vol. 32, pp. 133-164, 2004.

[15] A.N. Eraslan, H. Argeso, On the Application of von Mises' Yield Criterion to a Class of Plane Strain Thermal Stress Problems, *Turkish Journal of Engineering and Environmental Sciences*, vol. 29, pp. 113–128, 2005.

[16] A.N. Eraslan, H. Argeso, Computer Solutions of Plane Strain Axisymmetric Thermomechanical Problems, *Turkish Journal of Engineering and Environmental Sciences*, vol. 29, pp. 369–381, 2005.

[17] A.N. Eraslan, H. Argeso, A Nonlinear Shooting Method Applied to Solid Mechanics: Part 2. Numerical Solution of a Plane Strain Model, *International Journal of Nonlinear Analysis and Phenomena* vol. 2, pp. 31–42, 2005.

[18] H. Argeso, A.N. Eraslan, A Simple Computational Model for Unified Treatment of a Class of Plane Strain Thermoplastic Stress Problems, in: *Proceedings of the 6th International Congress on Thermal Stresses, TS2005*, vol. 1, pp. 203–206, 2005.

[19] H. Argeso, A.N. Eraslan, On the use of temperature-dependent physical properties in thermomechanical calculations for solid and hollow cylinders, *International Journal of Thermal Sciences*, vol. 47 ,pp. 136-146, 2008.

[20] A.N. Eraslan, Thermally Induced Deformations of Composite Tubes Subjected to a Nonuniform Heat Source, *Journal of Thermal Stresses*, vol. 26, pp. 167–193, 2003.

[21] A.N. Eraslan, E. Sener, H. Argeso, Stress Distributions in Energy Generating Two-Layer Tubes Subjected to Free and Radially Constrained Boundary Conditions, *International Journal of Mechanical Sciences*, vol. 45, pp. 469– 496, 2003.

[22] N. Noda, Thermal Stresses in Materials with Temperature-Dependent Properties, in: R.B. Hetnarsky (Ed.), *Thermal Stresses I*, Elsevier Science, North-Holland, Amsterdam, pp. 391–483, 1986.

[23] A.C. Hindmarsh, ODEPACK. A systematized collection of ODE solvers, in: R.S. Stepleman (Ed.), *Scientific computing*, North Holland, Amsterdam, 1983.

[24] P.N. Brown, A.C. Hindmarsh, Reduced storage matrix methods in stiff ODE systems, *Applied Mathematics and Computation* vol. 31, pp. 40–91, 1989.

[25] Material Property Database: MPDB Software, JAHM Software, Inc., 29 Valley Rd., North Reading, MA, 01864-1740 (http://www.jahm.com).